NASA Contractor Report 204134

Coordinates for a High Performance 4:1 Pressure Ratio Centrifugal Compressor

Ted F. McKain and Greg J. Holbrook
Detroit Diesel Allison
Indianapolis, Indiana

July 1997

Prepared for
Lewis Research Center
Under Contract NAS3-23268

National Aeronautics and
Space Administration

National Aeronautics and
Space Administration

Coordinates for a High Performance 4:1 Pressure Ratio Centrifugal Compressor

Final Report

by

Ted F. McKain

Greg J. Holbrook

Detroit Diesel Allison
Division of General Motors Corporation

February 1982

Prepared for
National Aeronautics and Space Administration
NASA Lewis Research Center
Contract NAS 3-23268

TABLE OF CONTENTS

SECTION	TITLE	PAGE
I	SUMMARY	1
II	AERODYNAMIC DESIGN AND ANALYSIS	2
III	STRUCTURAL ANALYSIS	22
IV	MANUFACTURING DEFINITION OF SCALED IMPELLER	66
V	APPENDICIES	72

LIST OF ILLUSTRATIONS

FIGURE	TITLE	PAGE
1	Meridional Flowpath for Scaled Impeller	3
2	Impeller Hub Relative Velocity	8
3	Impeller Mean Relative Velocity	9
4	Impeller Tip Relative Velocity	10
5	Impeller Hub Blade Loading	11
6	Impeller Mean Blade Loading	12
7	Impeller Tip Blade Loading	13
8	Vane Diffuser Entrance Region	14
9	Diffuser Cross-Section	15
10	Leading Edge Region of Vane Diffuser	16
11	90° Annular Bend	17
12	Area Distribution for 90° Annular Bend	18
13	Estimated Performance Map for Scaled Compressor	20
14	404-III "Hot" and "Cold" Clearance Distributions	21
15	Temperature Distributions for Scaled Impeller	23
16	Axisymmetric Stress Model for Scaled Impeller	25
17	Impeller Equivalent Stresses	26
18	Impeller Axial Stresses	27
19	Impeller Radial Stresses	28
20	Impeller Tangential Stresses	29
21	Impeller Equivalent Stress with 10,000 lbf Axial Load	30
22	Low Cycle Fatigue and Burst Analysis	31
23	Low Cycle Fatigue Material Properties for Ti 6Al4V	32
24	Triangular Plate Model for Scaled Impeller Full Blade	33
25	Pressure Surface - Maximum Principal Stress	34
26	Pressure Surface - Equivalent Stress	35
27	Suction Surface - Maximum Principal Stress	36
28	Suction Surface - Equivalent Stress	37
29	Triangular Plate Model for Scaled Impeller Splitter Blade	38

FIGURE	TITLE	PAGE
30	Pressure Surface - Maximum Principal Stress	39
31	Pressure Surface - Equivalent Stress	40
32	Suction Surface - Maximum Principal Stress	41
33	Suction Surface - Equivalent Stress	42
34	Triangular Plate Model for Impeller Back Plate	43
35	Maximum Principal Stress - Backface Surface	44
36	Equivalent Stress - Backface Surface	45
37	Maximum Principal Stress - Flowpath Hub Surface	46
38	Equivalent Stress - Flowpath Hub Surface	47
39	Summary of High Cycle Fatigue Analysis	49
40	Goodman Diagram for Ti 6Al-4V Material	50
41	Scaled Impeller Deflection Summary	51
42	Full Blade - 1st Natural Frequency	52
43	Full Blade - 2nd Natural Frequency	53
44	Full Blade - 3rd Natural Frequency	54
45	Full Blade - 4th Natural Frequency	55
46	Full Blade - 5th Natural Frequency	56
47	Full Blade - 6th Natural Frequency	57
48	Full Blade - 7th Natural Frequency	58
49	Full Blade - 8th Natural Frequency	59
50	Splitter Blade - 1st Natural Frequency	60
51	Splitter Blade - 2nd Natural Frequency	61
52	Splitter Blade - 3rd Natural Frequdncy	62
53	Frequency - Speed Diagram for Full Blade of Scaled Impeller	63
54	Frequency - Speed Diagram for Splitter Blade of Scaled Impeller	64
55	DDA Procedure for Clearance Allowance	67
56	Scaled Impeller Clearance Change from "Cold Build" to "Hot Running" Condition	68

LIST OF TABLES

TABLE	TITLE	PAGE
I	Inlet Bell and Spinner Contour Coordinates	4
II	Scaled 404-III Full Blade Coordinates - Hot Blade	5
III	Scaled 404-III Splitter Coordinates - Hot Blade	6
IV	Annular Bend Contour Coordinates	19
V	Scaled 404-III Full Blade Coordinates - Cold Blade	70
VI	Scaled 404-III Splitter Coordinates - Cold Blade	71

I. SUMMARY

The objective of the work conducted in this program was to define both aerodynamic and manufacturing design details for an advanced 4:1 pressure ratio single stage centrifugal compressor at a 10 lbm/sec flow size. The approach selected was to perform an exact aerodynamic scale of DDA's 404-III compressor from its design flow of 3.655 lbm/sec to the required 10 lbm/sec flow size.

Design tasks performed during this program included:

- o Aerodynamic design and analysis
- o Thermal analysis of the scaled impeller
- o Structural analysis of the scaled impeller including both static stress and vibration analyses.

The results of these tasks are reviewed in Sections II and III. Section IV presents a detailed manufacturing definition of the impeller blading and wheel geometry. The manufacturing definition includes a detail drawing of the impeller geometry and punched card description of both "hot" and "cold" impeller geometry.

II. AERODYNAMIC DESIGN AND ANALYSIS

The 4:1 Rc, 404-III single stage centrifugal compressor was designed in 1975 for use in an advanced regenerative gas turbine engine for truck/bus and power generation applications. The impeller design combined advanced aerodynamic features such as high back curvature (50°) and low blade loading with geometry completely compatible with production casting techniques. Goal compressor performance was achieved on the inital build and efficiency goals were exceeded by over 1% after one rematch. The design point total to static efficiency was 83.3% at a point with 8% minimum surge margin. This efficiency level is still the best total to static efficiency demonstrated in its flow class.

The flow size of the 404-III compressor is 3.655 lbm/sec at a mechanical speed of 36015 rpm. To scale the compressor to 10 lbm/sec, a 1.6529 scale factor must be applied to all linear dimensions. A true scale of this compressor would result in a diffuser exit radius of 16.306 inches. This radius exceeded current NASA rig constraints and, therefore, had to be reduced to 14.3 inches. A 90° annular bend was designed to direct the flow from the radial to the axial direction.

A complete meridional elevation of the scaled compressor is shown in Figure 1. The defined geometry is for the "hot running" conditon with no impeller to shroud clearance adjustment. The original 404-III compressor was tested with a smooth approach inlet bell and rotating spinner. These contours are shown in Figure 1 and specifically defined in Table I.

The impeller consists of 15 full blades and 15 splitters. "Hot" flow path contours, tangential thickness distributions and polar coordinate definition of the blade meanline are presented for the hub and shroud contours in Tables II and III. Table II presents full blade definition while Table III gives the splitter geometry. The blade surface elements are constructed linear from hub to shroud along the defined quasi-normals. The coordinates given in Tables II

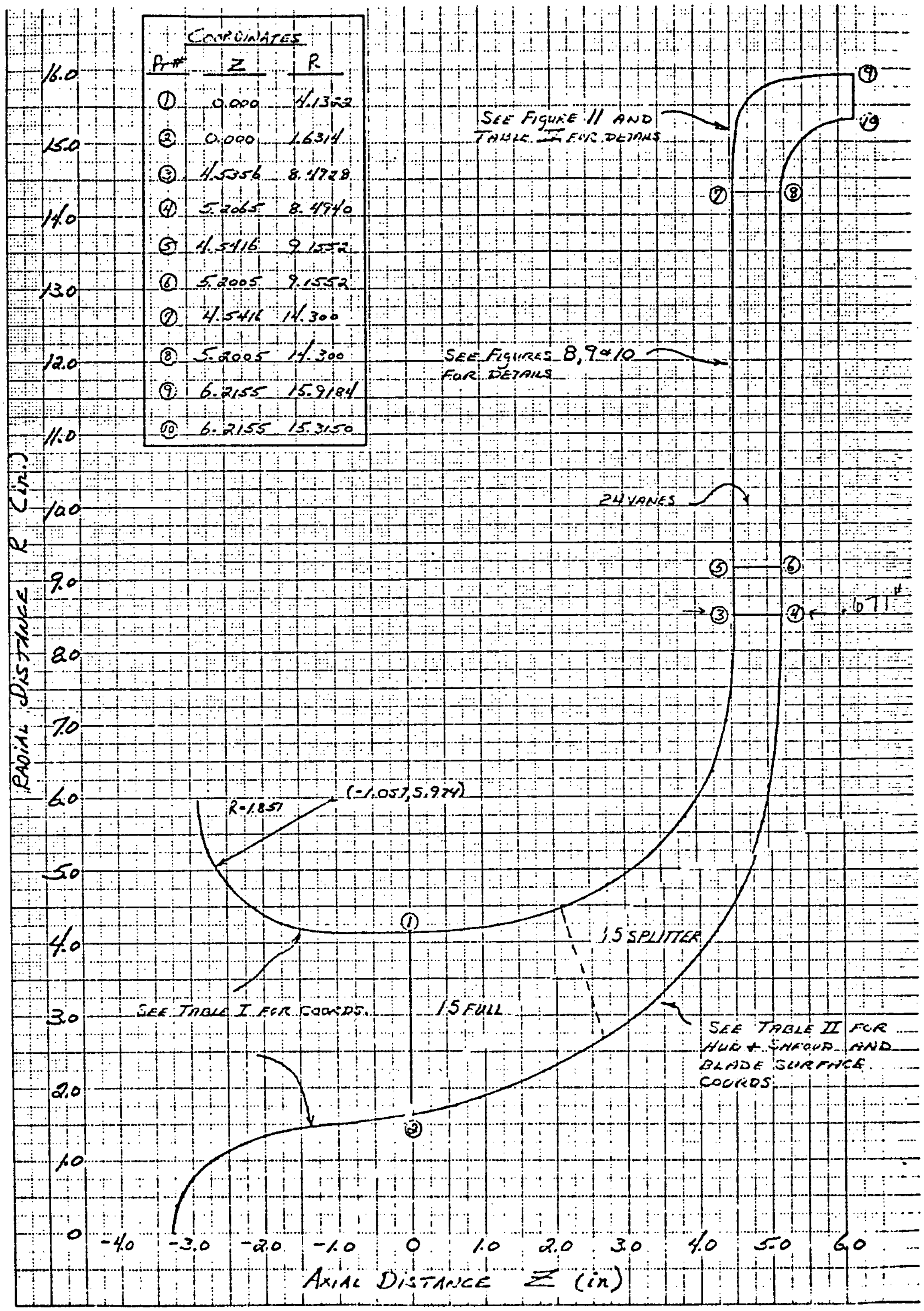

Figure 1. Meridional Flowpath for Scaled Impeller.

TABLE I. INLET BELL AND SPINNER CONTOUR COORDINATES.

INLET BELL: CIRCULAR ARC WITH CENTER AT (-1.057,5.974)

COORDINATES:

AXIAL LOCATION	RADIAL LOCATION
-2.908	5.974
-2.850	5.513
-2.750	5.225
-2.500	4.814
-2.250	4.558
-2.000	4.381
-1.750	4.257
-1.500	4.177
-1.057	4.123
-0.050	4.128
0.000	4.132

INLET SPINNER:

COORDINATES:

AXIAL LOCATION	RADIAL LOCATION
-3.3276	0.0000
-3.3111	0.1750
-3.2450	0.3886
-3.1623	0.5446
-2.9970	0.7564
-2.8317	0.9091
-2.6665	1.0293
-2.3359	1.2093
-2.0053	1.3344
-1.6747	1.4192
-1.3441	1.4711
-1.3000	1.4757
-1.0000	1.5000
-0.5000	1.5600
0.0000	1.6314

and III are for the impeller in the "hot and running" condition. A detailed description of the manufacturing or "cold" geometry is presented in Section IV.

Using data from the BU257 rig test of the 404-III compressor as a guide to impeller blockage and efficiency levels, a streamline curvature intrablade aerodynamic analysis was performed for the defined scaled compressor geometry. The aerodynamic analysis was conducted at design speed with the following input variables:

TABLE II. SCALED 404-III IMPELLER COORDINATES - HOT BLADE.

MEAN BLADE DEFINITION - FULL BLADE.

%M/MO	R HUB	Z HUB	R SHROUD	Z SHROUD	TTAN HUB	TTAN SHROUD	THETA HUB	THETA SHROUD
0.0	1.6314	0.0003	4.1322	0.0	0.1328	0.0755	1.6331	0.0040
2.5000	1.6765	0.2352	4.1400	0.1795	0.1940	0.0930	7.0300	3.5643
5.0000	1.7309	0.4678	4.1486	0.3593	0.2174	0.1050	11.4915	6.8815
7.5000	1.7953	0.6982	4.1552	0.5396	0.2323	0.1136	15.2587	9.9100
10.0000	1.8673	0.9261	4.1679	0.7194	0.2413	0.1207	18.5542	12.7871
12.5000	1.9475	1.1516	4.1872	0.8988	0.2490	0.1243	21.6394	15.5122
15.0000	2.0339	1.3745	4.2114	1.0772	0.2541	0.1262	24.3302	18.0871
17.5000	2.1264	1.5951	4.2400	1.2544	0.2593	0.1256	26.6931	20.5041
20.0000	2.2250	1.8129	4.2744	1.4308	0.2642	0.1249	28.8285	22.7880
22.5000	2.3287	2.0287	4.3126	1.6083	0.2691	0.1230	30.7135	24.9620
25.0000	2.4402	2.2402	4.3610	1.7809	0.2733	0.1213	32.4163	27.0020
27.5000	2.5605	2.4469	4.4222	1.9456	0.2762	0.1199	33.9167	28.8420
30.0000	2.6860	2.6504	4.4881	2.1113	0.2794	0.1187	35.2751	30.6249
32.5000	2.8149	2.8521	4.5590	2.2805	0.2829	0.1177	36.4730	32.2831
35.0000	2.9519	3.0479	4.6342	2.4457	0.2861	0.1166	37.5653	33.8532
37.5000	3.0972	3.2383	4.7123	2.6062	0.2890	0.1153	38.5328	35.3323
40.0000	3.2504	3.4217	4.7972	2.7637	0.2917	0.1142	39.4325	36.7284
42.5000	3.4114	3.5991	4.8883	2.9186	0.2942	0.1136	40.2456	38.0392
45.0000	3.5808	3.7675	4.9875	3.0695	0.2966	0.1126	41.0284	39.2710
47.5000	3.7592	3.9272	5.0971	3.2170	0.2984	0.1108	41.7665	40.4073
50.0000	3.9451	4.0770	5.2104	3.3590	0.3016	0.1092	42.5027	41.4968
52.5000	4.1397	4.2164	5.3250	3.4958	0.3034	0.1073	43.2269	42.5366
55.0000	4.3397	4.3471	5.4478	3.6265	0.3057	0.1060	43.9687	43.5349
57.5000	4.5456	4.4694	5.5808	3.7523	0.3069	0.1054	44.7215	44.4739
60.0000	4.7562	4.5823	5.7178	3.8693	0.3086	0.1050	45.5049	45.4073
62.5000	4.9721	4.6858	5.8558	3.9783	0.3107	0.1054	46.3135	46.3430
65.0000	5.1918	4.7797	6.0039	4.0770	0.3132	0.1053	47.1628	47.2569
67.5000	5.4154	4.8657	6.1641	4.1653	0.3161	0.1041	48.0518	48.1387
70.0000	5.6427	4.9390	6.3302	4.2434	0.3195	0.1033	48.9831	49.0192
72.5000	5.8742	4.9999	6.5051	4.3077	0.3231	0.1027	49.9448	49.8786
75.0000	6.1082	5.0477	6.6804	4.3610	0.3283	0.1028	50.9720	50.7763
77.5000	6.3458	5.0775	6.8553	4.4013	0.3359	0.1042	52.0642	51.7155
80.0000	6.5837	5.1041	7.0323	4.4350	0.3436	0.1049	53.2221	52.6866
82.5000	6.8217	5.1279	7.2114	4.4613	0.3501	0.1047	54.4460	53.6902
85.0000	7.0600	5.1476	7.3922	4.4828	0.3589	0.1047	55.7350	54.7242
87.5000	7.2987	5.1632	7.5755	4.4988	0.3698	0.1049	57.0767	55.7732
90.0000	7.5375	5.1749	7.7590	4.5117	0.3828	0.1056	58.5077	56.8829
92.5000	7.7766	5.1800	7.9427	4.5212	0.3970	0.1068	60.0166	58.0385
95.0000	8.0157	5.1870	8.1263	4.5284	0.4150	0.1089	61.6370	59.2839
97.5000	8.2548	5.1958	8.3096	4.5332	0.4370	0.1115	63.3685	60.6189
100.0000	8.4940	5.2065	8.4928	4.5356	0.4629	0.1150	65.2113	62.0437

TABLE III. SCALED 404-III IMPELLER COORDINATES - HOT BLADE.

MEAN BLADE DEFINITION - SPLITTER.

%M/MO	R HUB	Z HUB	R SHROUD	Z SHROUD	TTAN HUB	TTAN SHROUD	THETA HUB	THETA SHROUD
30.0000	2.6861	2.6506	4.4881	2.1113	0.1118	0.0559	34.3684	30.0904
31.7500	2.7755	2.7922	4.5375	2.2303	0.1401	0.0661	35.8399	31.3564
33.5000	2.8688	2.9311	4.5886	2.3471	0.1634	0.0746	36.7345	32.5645
35.2500	2.9659	3.0672	4.6408	2.4612	0.1802	0.0808	37.5435	33.7100
37.0000	3.0672	3.2003	4.6959	2.5739	0.1949	0.0863	38.2932	34.8066
38.7500	3.1728	3.3309	4.7537	2.6853	0.2068	0.0907	38.9734	35.8539
40.5000	3.2820	3.4579	4.8148	2.7950	0.2178	0.0948	39.6146	36.8528
42.2500	3.3945	3.5814	4.8783	2.9030	0.2280	0.0991	40.2088	37.7998
44.0000	3.5114	3.7007	4.9465	3.0092	0.2372	0.1023	40.7798	38.7051
45.7500	3.6330	3.8160	5.0206	3.1141	0.2452	0.1040	41.3225	39.5660
47.5000	3.7587	3.9267	5.0968	3.2156	0.2527	0.1052	41.8520	40.3902
49.2500	3.8887	4.0327	5.1749	3.3170	0.2597	0.1057	42.3604	41.1749
51.0000	4.0222	4.1339	5.2553	3.4145	0.2662	0.1060	42.8711	41.9288
52.7500	4.1594	4.2299	5.3367	3.5091	0.2721	0.1064	43.3815	42.6468
54.5000	4.2992	4.3217	5.4226	3.6009	0.2777	0.1063	43.8991	43.3441
56.2500	4.4416	4.4093	5.5142	3.6904	0.2829	0.1055	44.4210	44.0152
58.0000	4.5867	4.4924	5.6075	3.7750	0.2880	0.1050	44.9559	44.6767
59.7500	4.7346	4.5711	5.7015	3.8581	0.2928	0.1050	45.5017	45.3269
61.5000	4.8847	4.6452	5.7990	3.9356	0.2974	0.1050	46.0650	45.9707
63.2500	5.0374	4.7146	5.8989	4.0088	0.3019	0.1051	46.6448	46.6076
65.0000	5.1918	4.7797	6.0039	4.0770	0.3062	0.1050	47.2437	47.2391
66.7500	5.3472	4.8420	6.1147	4.1407	0.3105	0.1042	47.8614	47.8626
68.5000	5.5050	4.8970	6.2293	4.1984	0.3144	0.1036	48.4987	48.4860
70.2500	5.6656	4.9440	6.3488	4.2498	0.3178	0.1032	49.1526	49.1059
72.0000	5.8278	4.9850	6.4696	4.2955	0.3215	0.1030	49.8315	49.7321
73.7500	5.9919	5.0196	6.5923	4.3352	0.3256	0.1028	50.5335	50.3616
75.5000	6.1567	5.0491	6.7152	4.3696	0.3298	0.1029	51.2637	51.0029
77.2500	6.3225	5.0722	6.8377	4.3976	0.3337	0.1033	52.0213	51.6544
79.0000	6.4886	5.0931	6.9613	4.4223	0.3382	0.1037	52.8077	52.3204
80.7500	6.6551	5.1116	7.0858	4.4431	0.3432	0.1041	53.6197	52.9998
82.5000	6.8217	5.1280	7.2114	4.4613	0.3489	0.1043	54.4666	53.6955
84.2500	6.9885	5.1422	7.3381	4.4765	0.3557	0.1045	55.3461	54.4054
86.0000	7.1554	5.1544	7.4655	4.4895	0.3631	0.1047	56.2650	55.1356
87.7500	7.3225	5.1649	7.5938	4.5002	0.3712	0.1045	57.2224	55.8819
89.5000	7.4898	5.1729	7.7223	4.5093	0.3801	0.1053	58.2212	56.6569
91.2500	7.6572	5.1764	7.8507	4.5157	0.3896	0.1078	59.2581	57.4572
93.0000	7.8245	5.1812	7.9795	4.5229	0.4007	0.1099	60.3432	58.2926
94.7500	7.9917	5.1883	8.1093	4.5276	0.4129	0.1112	61.4709	59.1551
96.5000	8.1590	5.1949	8.2379	4.5313	0.4274	0.1125	62.5578	60.0683
98.2500	8.3266	5.2010	8.3654	4.5340	0.4440	0.1137	63.9039	61.0318
100.0000	8.4943	5.2066	8.4918	4.5356	0.4628	0.1150	55.2093	62.0458

- o Corrected flow = 10 lbm/sec
- o Corrected speed = 21789 rpm
- o Inlet pressure = 14.7 psia
- o Inlet temperature = 518.7°R

The resulting distributions of impeller relative velocity and blade loading distributions are shown plotted as a function of percent meridional distance in Figures 2 through 7.

The vane diffuser consists of 24 modified, two-dimensional wedge vanes with the leading edge located at a radius ratio of 1.0778 relative to the impeller exit. The diffuser entrance region is shown in Figure 8 and is centered on the impeller exit. The diffuser has an overall area ratio of 2.754 with a total divergence angle of 7.791°. The vane passage cross-section is presented in Figure 9 with an enlarged view of the leading edge shown in Figure 10. The individual vanes are constructed from straight line segments between points 1 and 2, Figure 9, for the pressure surface and between points 4 and 5 for a portion of the suction surface. The leading edge portion of the suction surface is formed by an arc as shown in Figure 10. The suction surface arc has a radius of curvature of 45.233 inches and is tangent to the leading edge circle at points 3 and to the straight line between points 4 and 5 at point 4. The diffuser exit radius is 14.30 inches and dumps directly into a 90° annular bend.

The annular bend is shown in Figure 11 with detailed coordinates presented in Table IV. Primary considerations in the design of the annular bend were:

- o Minimize static pressure gradients at the diffuser exit plane
- o Maintain maximum flowpath radius at 16.0 inches

To avoid large static pressure gradients at the diffuser exit, the annular bend was designed with a generous radius of curvature to gap ratio of 2.0. The area distribution shown in Figure 12 was selected to reduce velocity levels around the bend and, thereby, reduce total pressure losses.

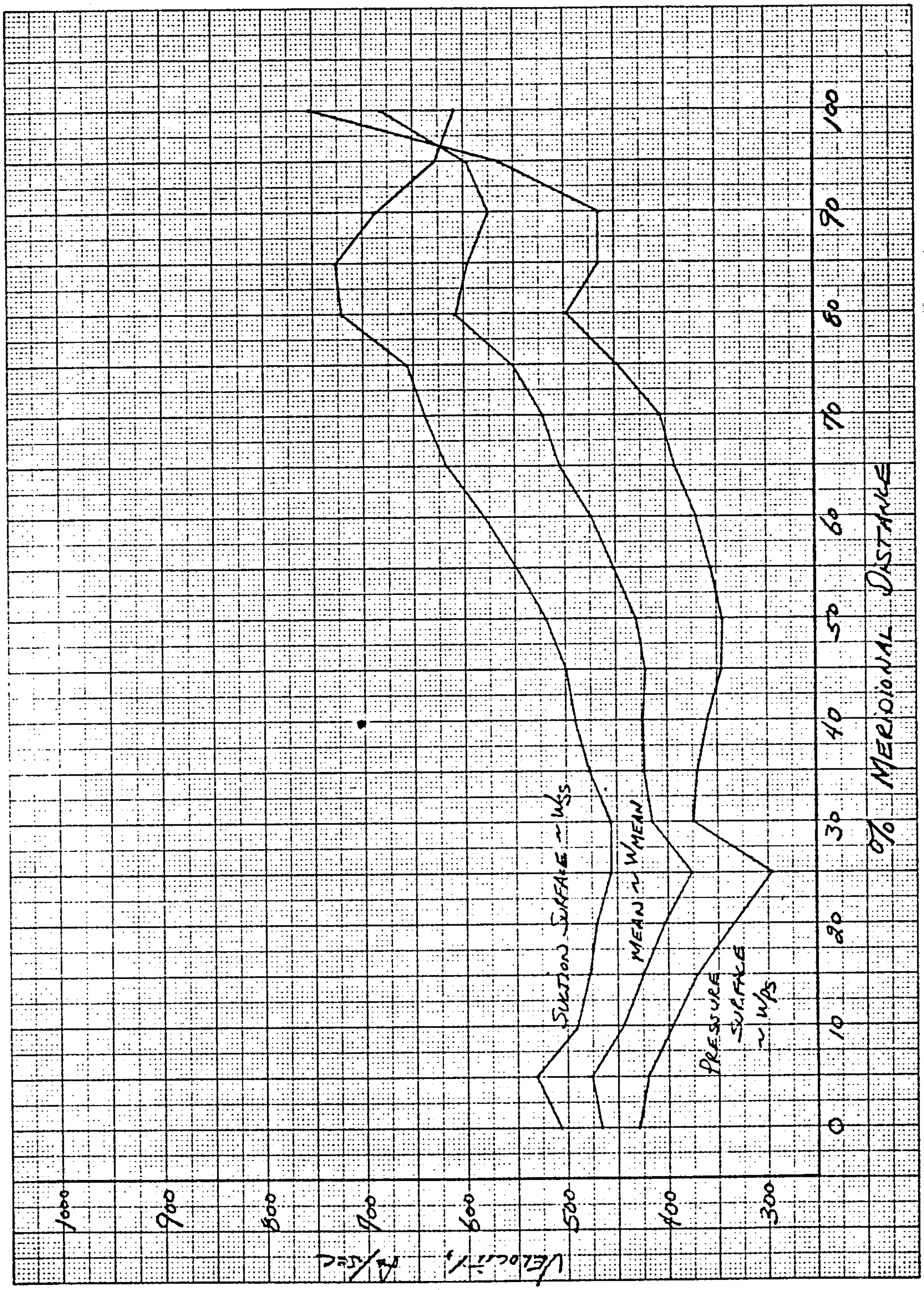

Figure 2. Impeller Hub Relative Velocity.

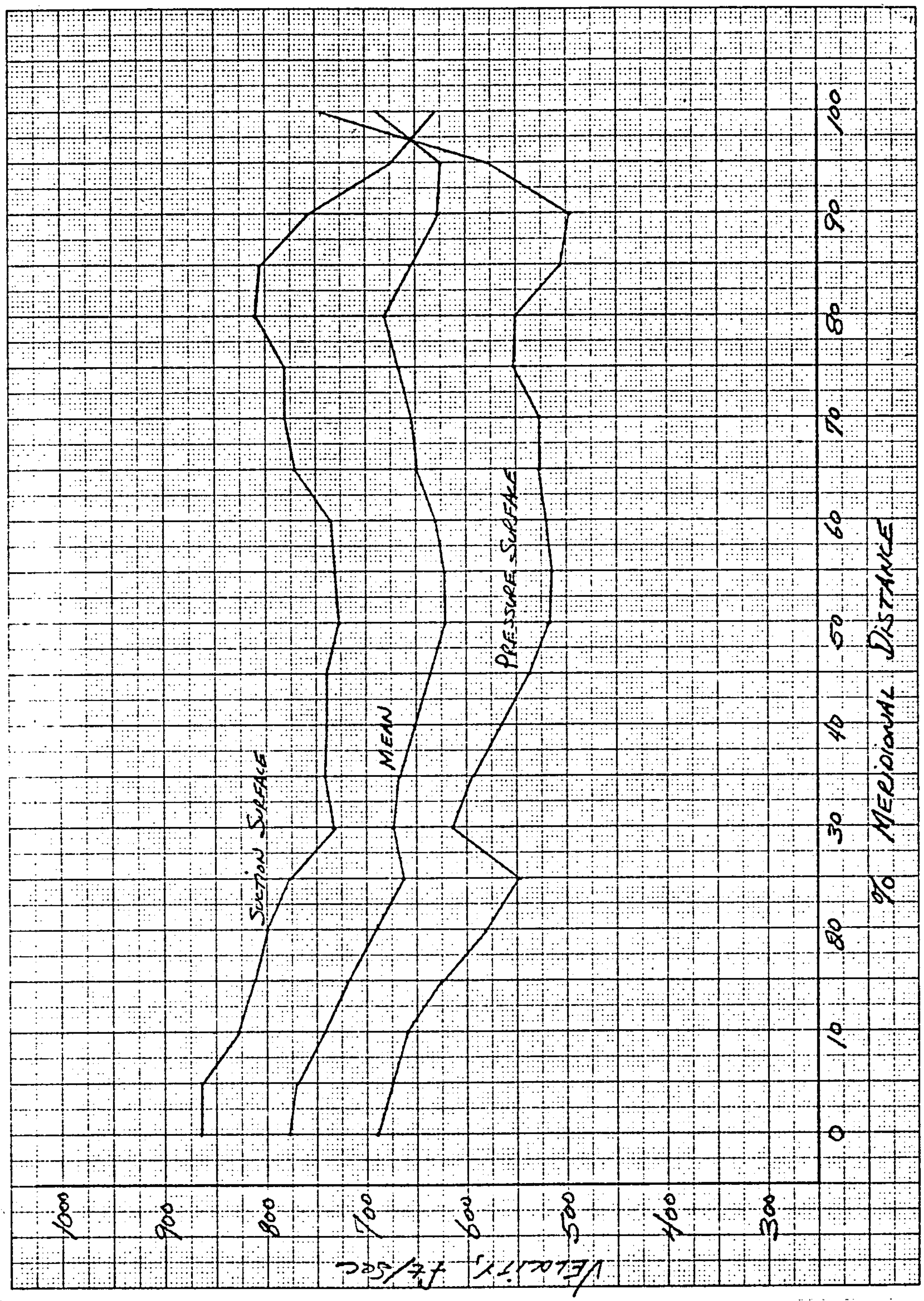

Figure 3. Impeller Mean Relative Velocity.

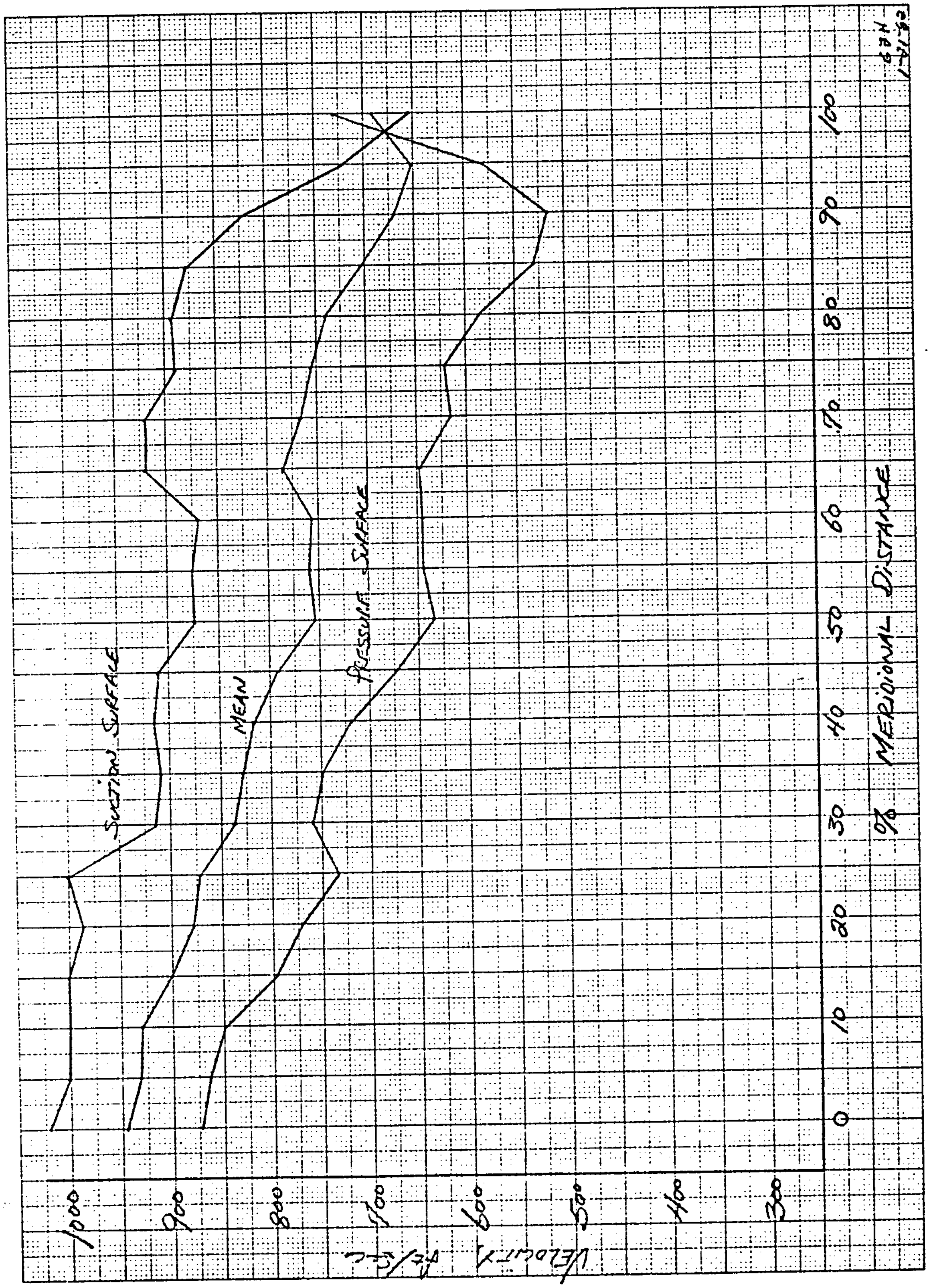

Figure 4. Impeller Tip Relative Velocity.

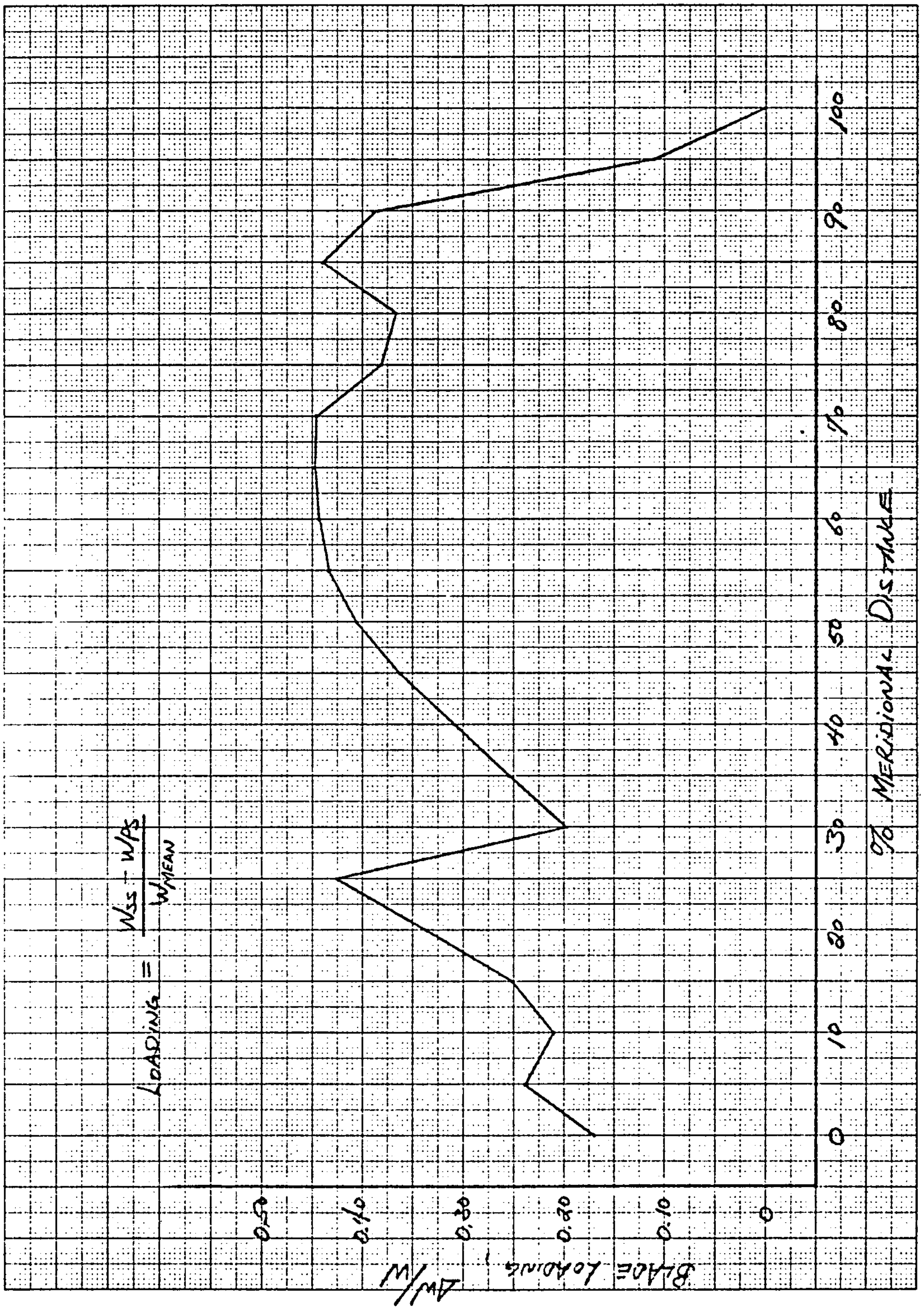

Figure 5. Impeller Hub Blade Loading.

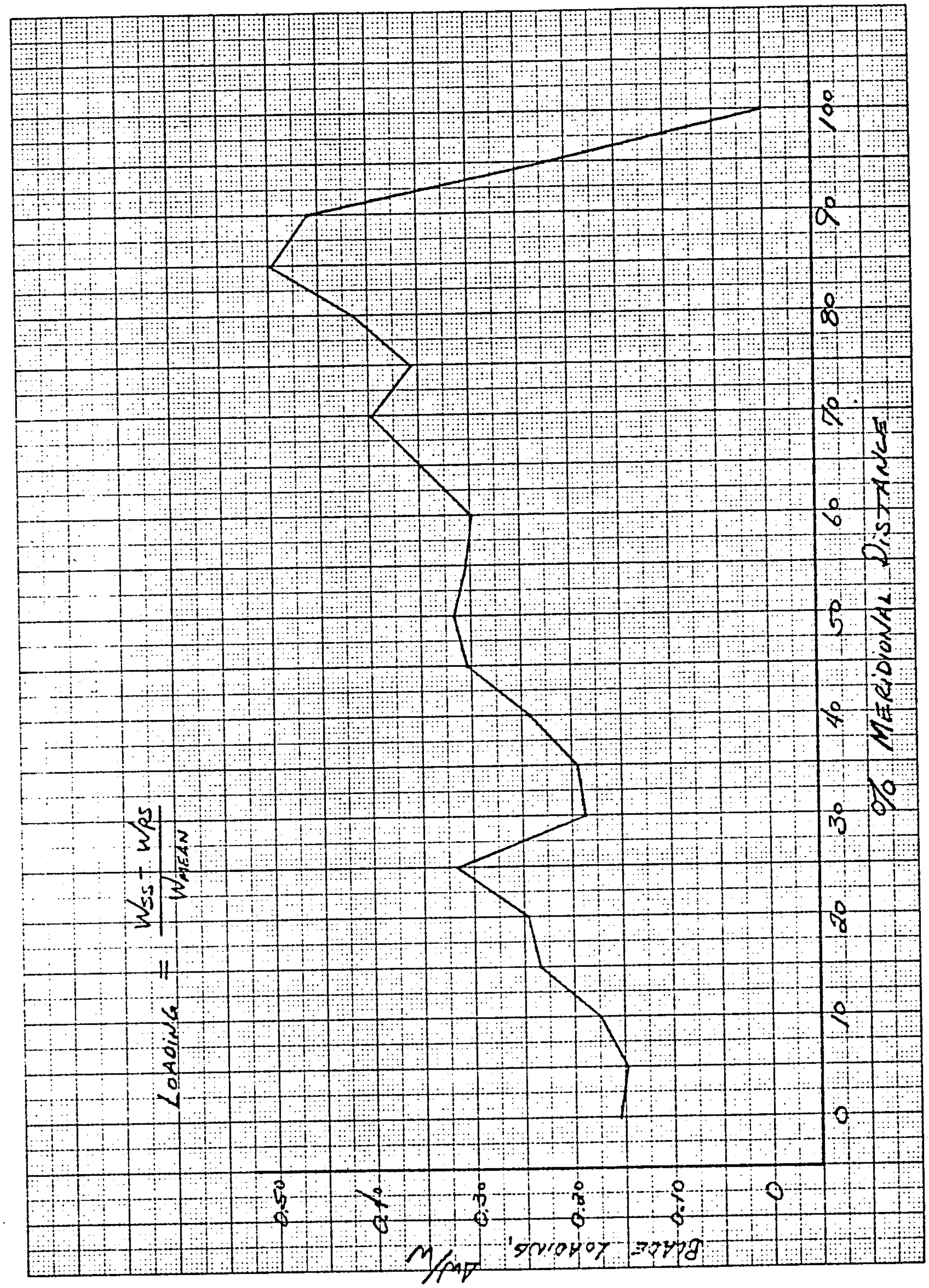

Figure 6. Impeller Mean Blade Loading.

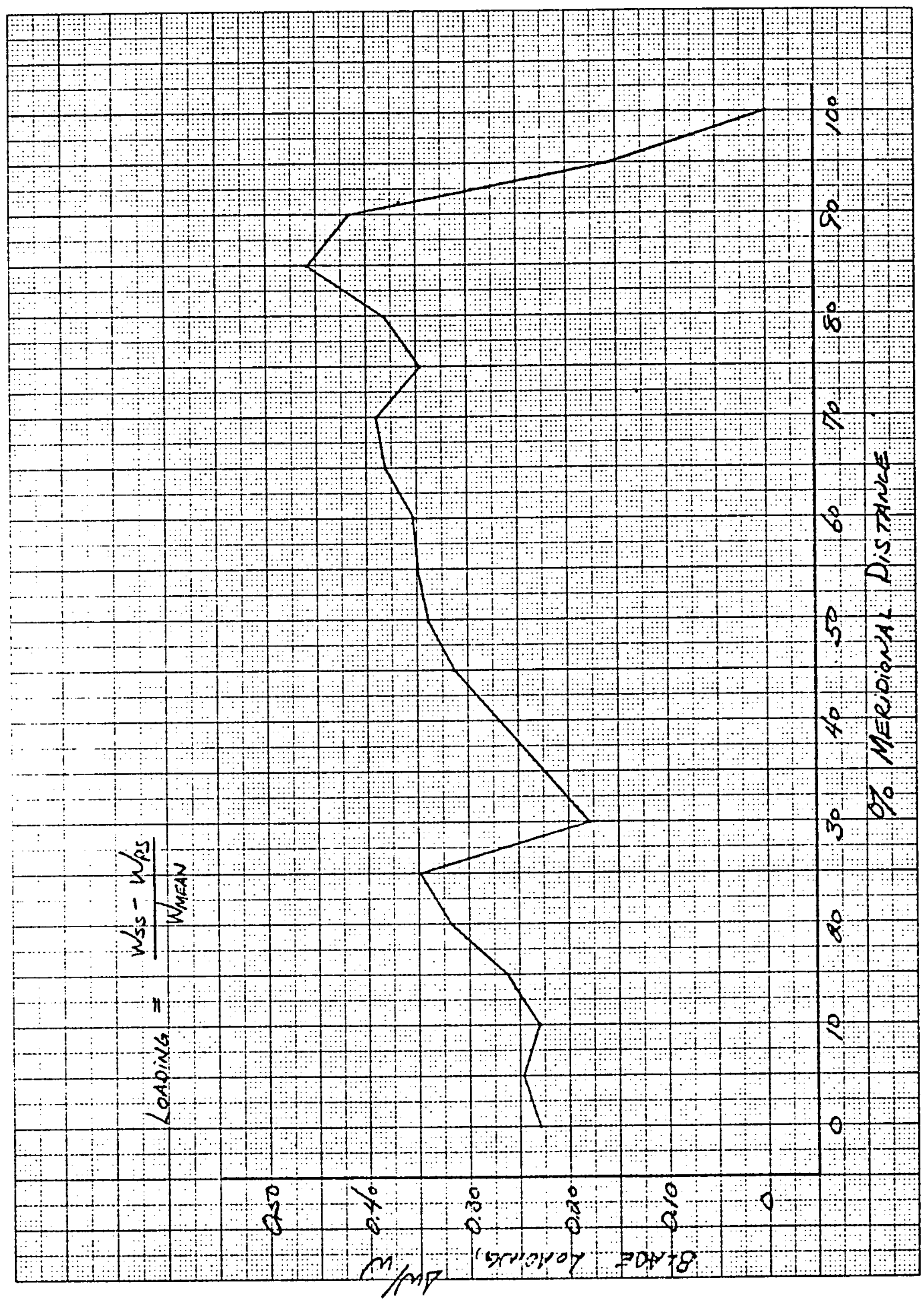

Figure 7. Impeller Tip Blade Loading.

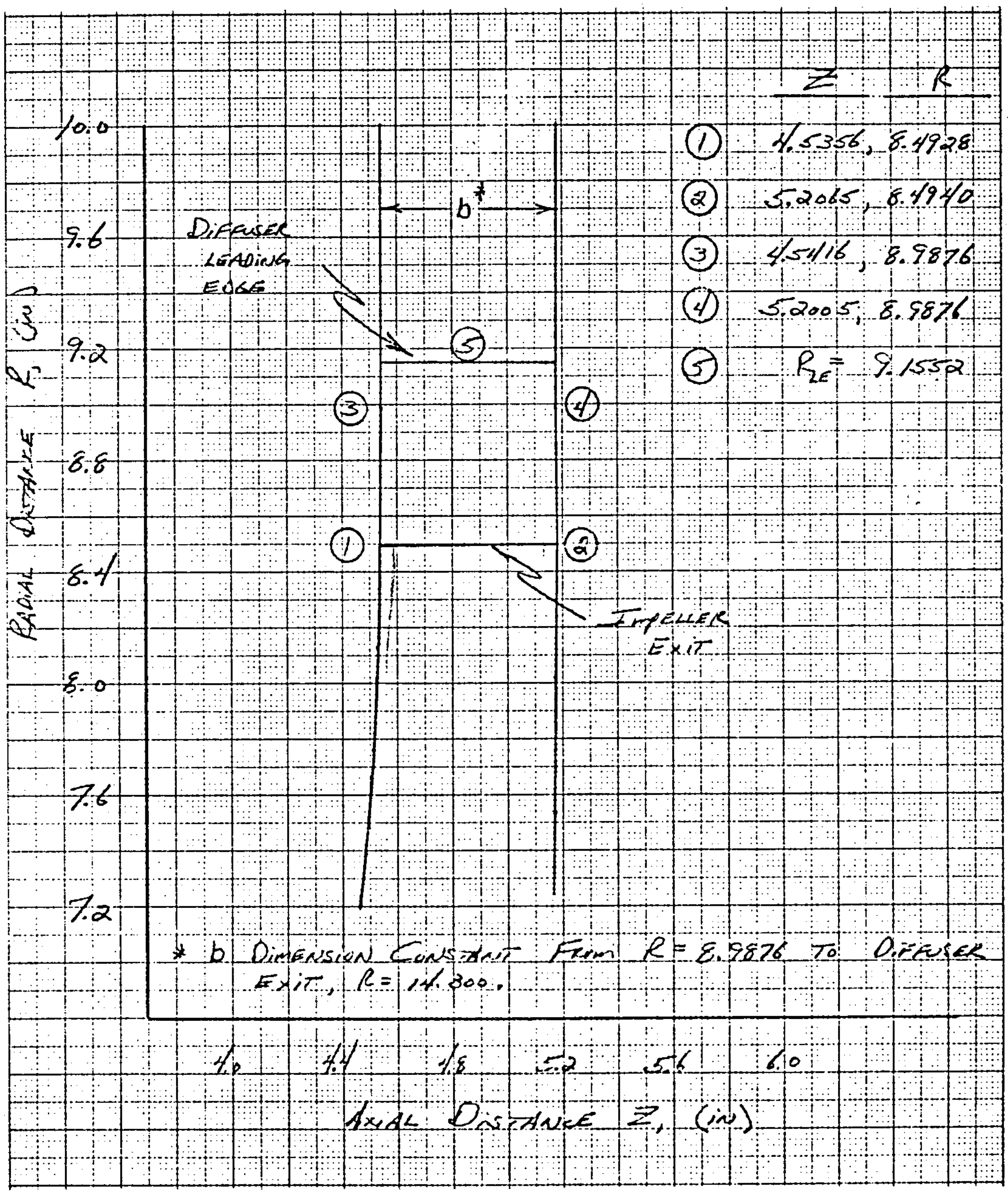

Figure 8. Vane Diffuser Entrance Region.

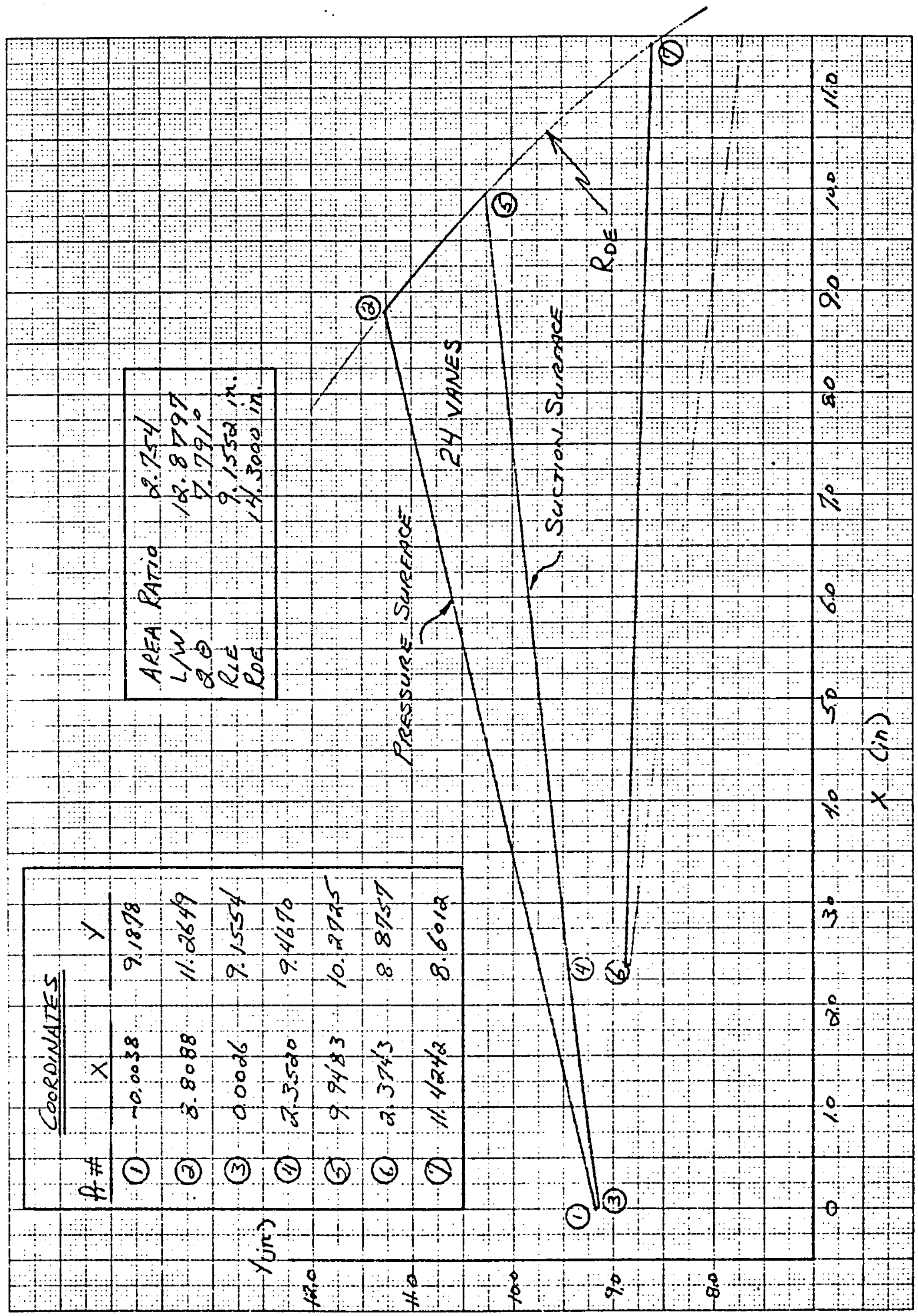

Figure 9. Diffuser Cross-section.

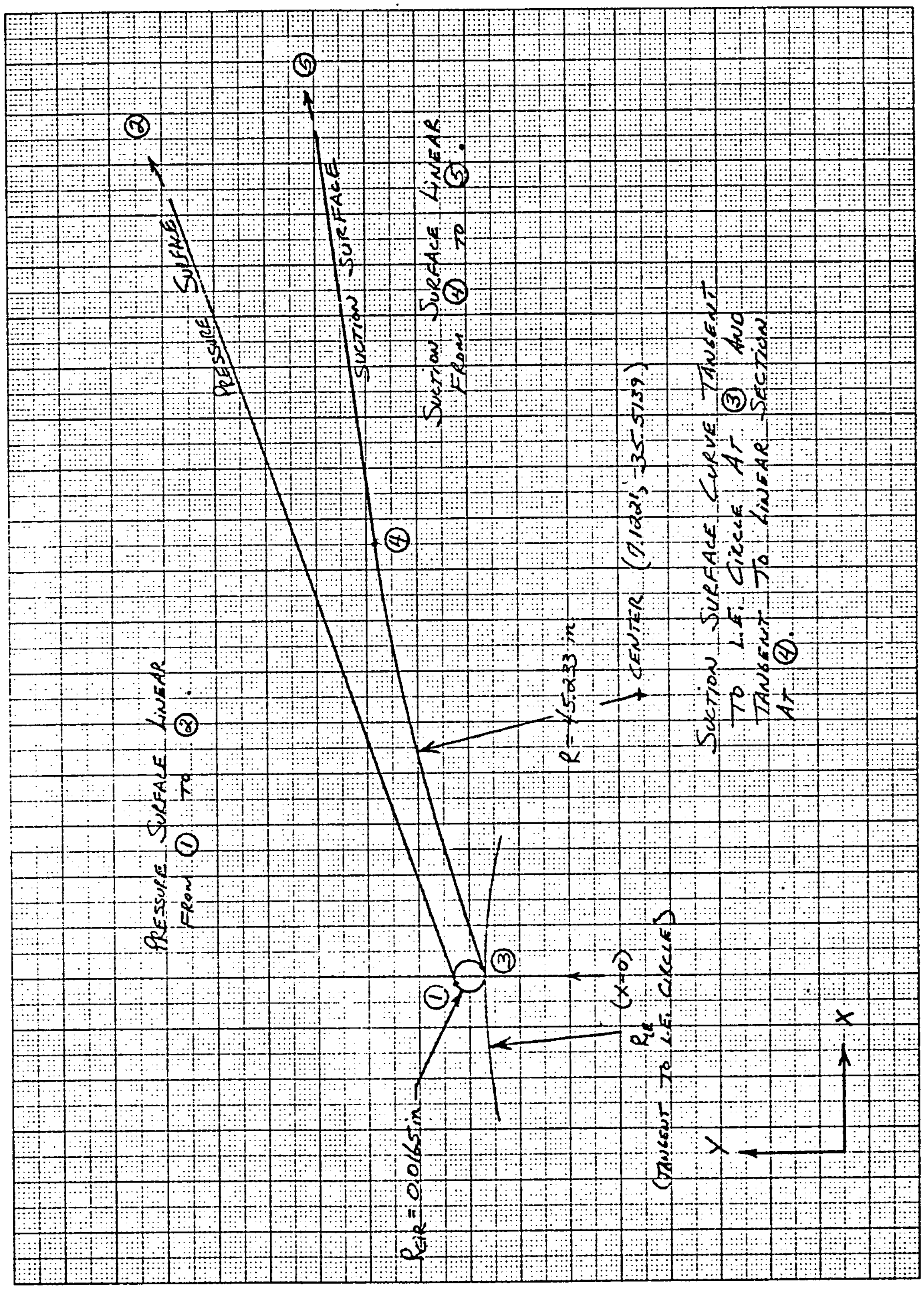

Figure 10. Leading Edge Region of Vane Diffuser.

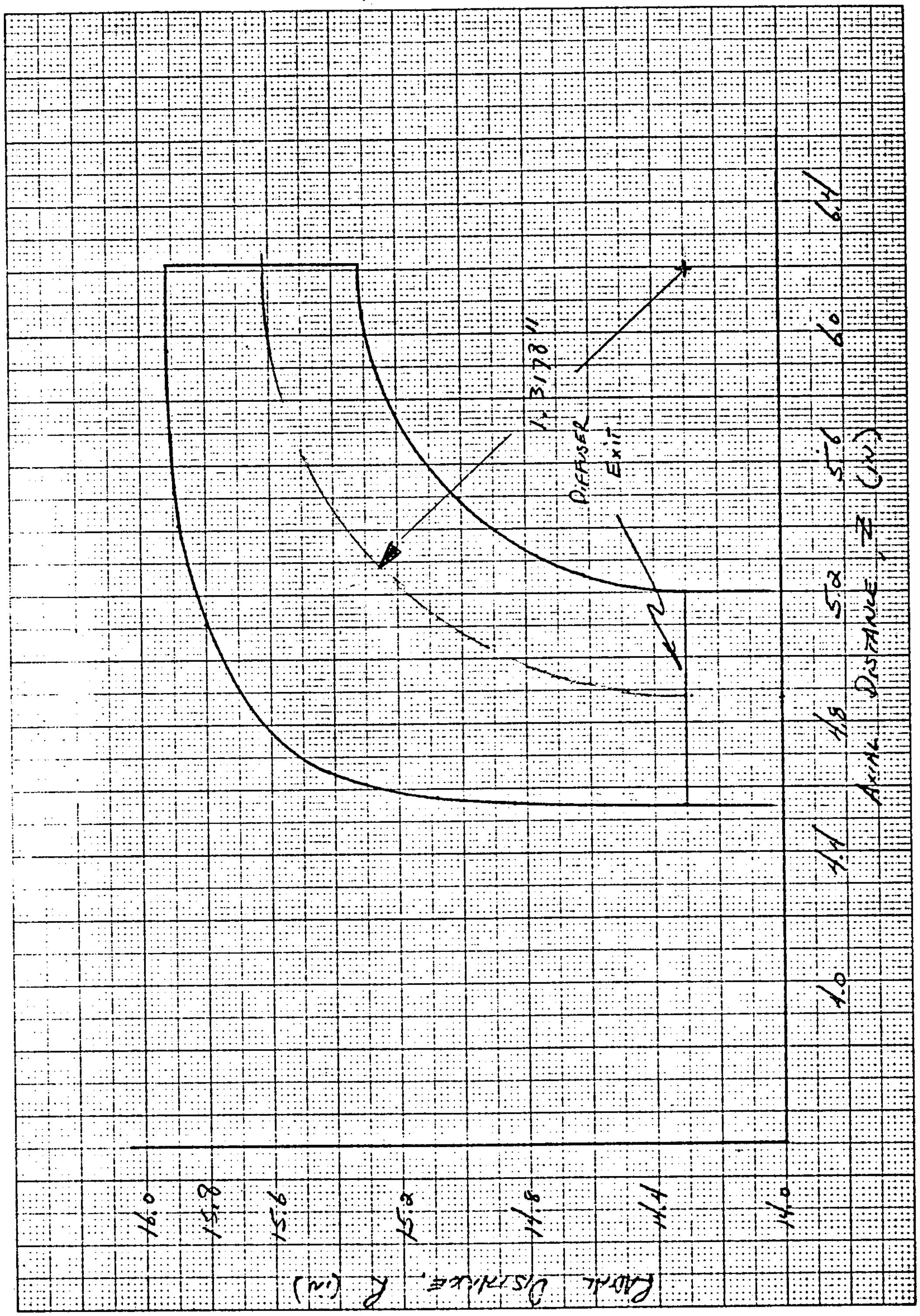

Figure 11. 90° Annular Bend.

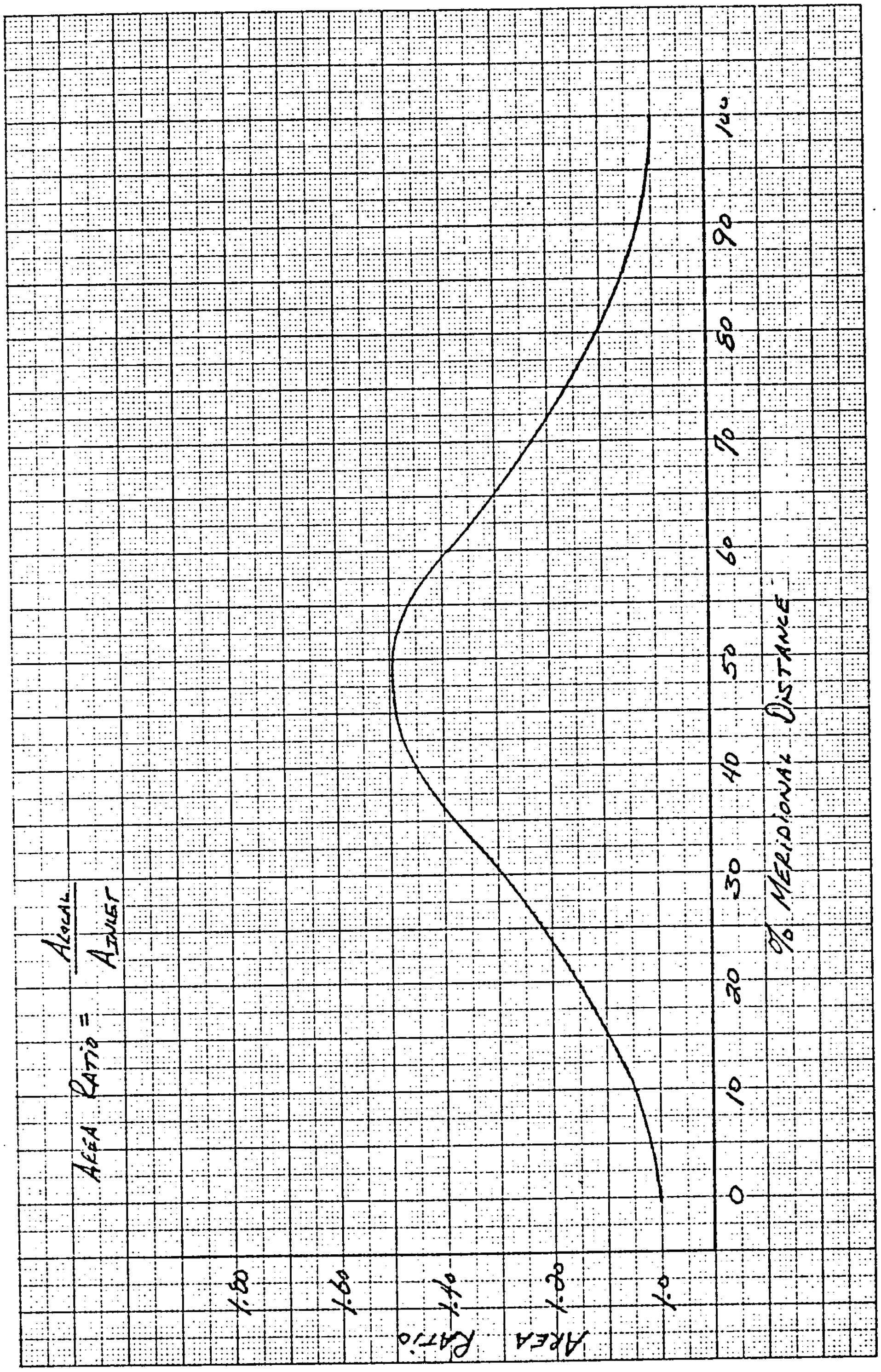

Figure 12. Area Distribution for 90° Annular Bend.

TABLE IV. ANNULAR BEND CONTOUR COORDINATES.

%M/MO	R HUB	Z HUB	R SHROUD	Z SHROUD	AREA /AREA1
0	14.3000	5.2005	14.3000	4.5416	1.0000
10	14.4588	5.2130	14.5600	4.5450	1.0404
20	14.6137	5.2502	14.8400	4.5500	1.1501
30	14.7608	5.3111	15.0840	4.5720	1.2776
40	14.8966	5.3943	15.4190	4.6580	1.4524
50	15.0177	5.4978	15.6670	4.8520	1.4911
60	15.1211	5.6189	15.8000	5.1150	1.3872
70	15.2044	5.7547	15.8680	5.4160	1.2285
80	15.2653	5.9018	15.9020	5.6930	1.1082
90	15.3025	6.0567	15.9150	5.9580	1.0277
100	15.3150	6.2155	15.9184	6.2155	1.0001

An estimated performance map was prepared for the scaled compressor stage and is given in Figure 13. Flow-speed and efficiency lapse rates were maintained similar to BU 257 data. However, allowance was made to overall efficiency levels to account for the geometrical changes, i.e. reduced area ratio diffuser and the 90° annular bend. In addition, Reynold's number effects were estimated from internal DDA procedures.

Impeller to shroud clearance distributions for both "build" and "hot running" conditions are presented for the 404-III impeller in Figure 14. Build clearances were deduced from design contours for the "cold" impeller and shroud in conjunction with "build" wax check measurements. "Hot running" clearances were developed from predicted design speed contours for the impeller and shroud and post test rub pin measurements. Scaled values of these clearances were assumed in the estimated map shown in Figure 13.

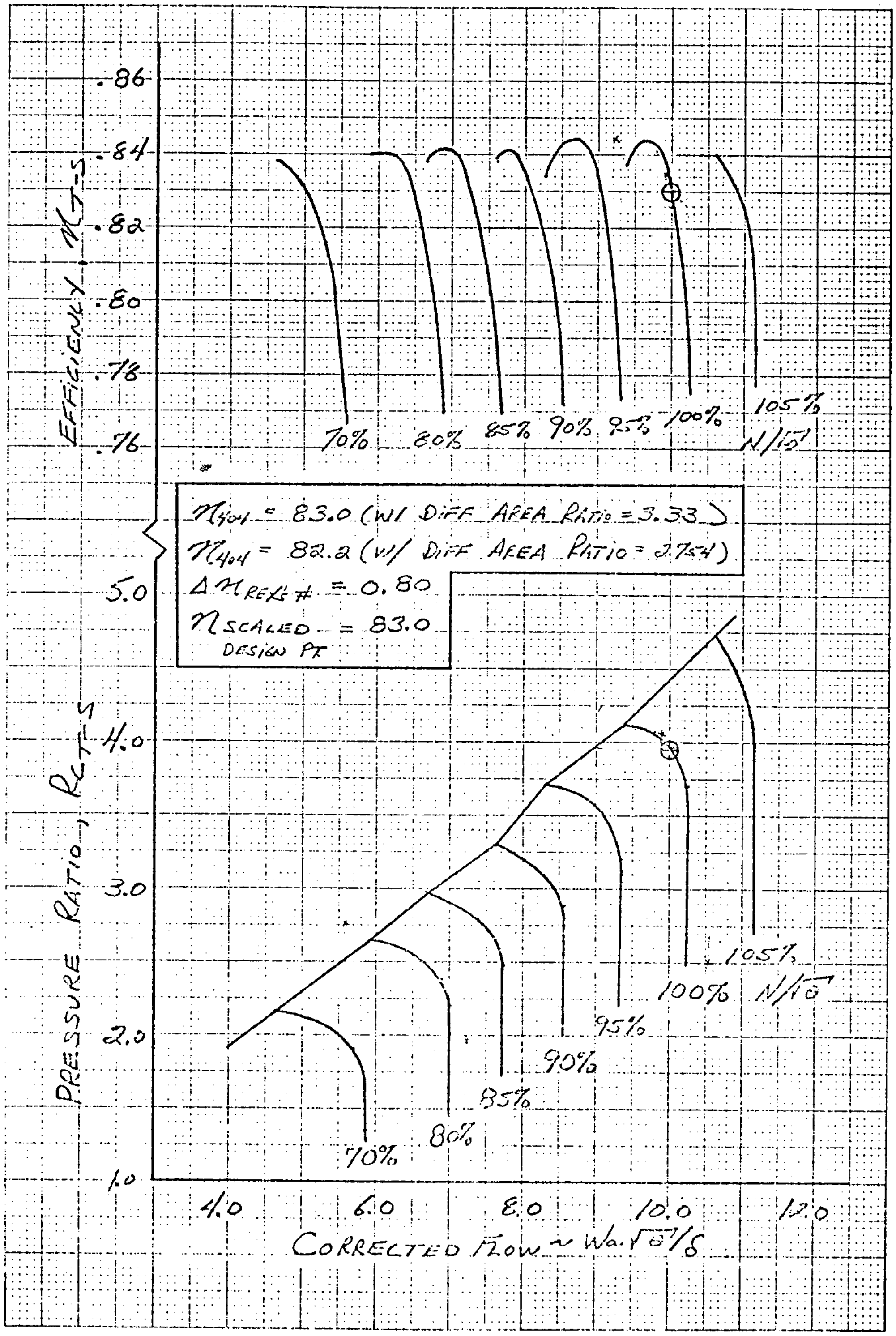

Figure 13. Estimated Performance Map for Scaled Compressor.

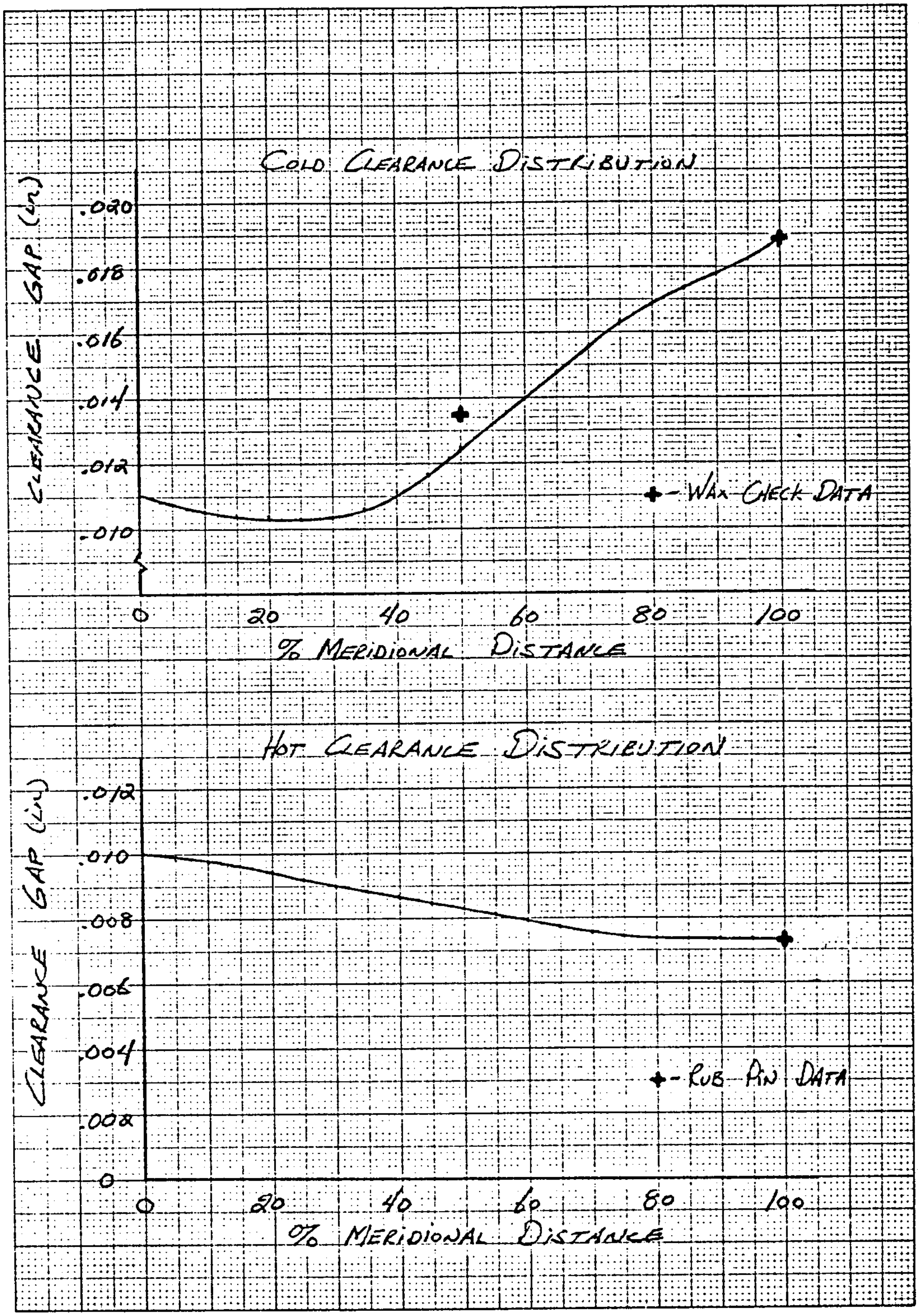

Figure 14. 404-III "hot" and "cold" Clearance Distributions.

III. STRUCTURAL ANALYSIS

A complete structural analysis was performed for the scaled impeller. The overall analysis was conducted for the defined aerodynamic geometry at a design speed of 21789 rpm and with standard day inlet conditions of 14.7 psia pressure and 518.7°R inlet temperature. The material properties were assumed to be those of Titanium 6AL4V. The overall structural analysis consisted of several individual but complementary tasks, namely:

- o Heat transfer
- o Static stress, and
- o Vibrational analyses.

The heat transfer analysis was required to provide temperature distributions for accurate determination of thermally induced stresses and deflections. Boundary conditions consisting of anticipated rig oil temperatures and back face seal leakage were obtained from NASA personnel and were included in the axisymmetric heat transfer analysis. Results of the heat transfer analysis are presented as isotherm lines on the defined scale compressor impeller geometry in Figure 15.

The static stress analysis consisted of several tasks:

- o Axisymmetric modeling of the complete wheel geometry
- o Evaluation of stresses from axisymmetric model in terms of low cycle fatigue and burst margins
- o Triangular plate modeling of the full blade, splitter and backplate
- o Evaluation of triangular plate results in terms of peak stress levels, high cycle fatigue and detailed deflection characteristics.

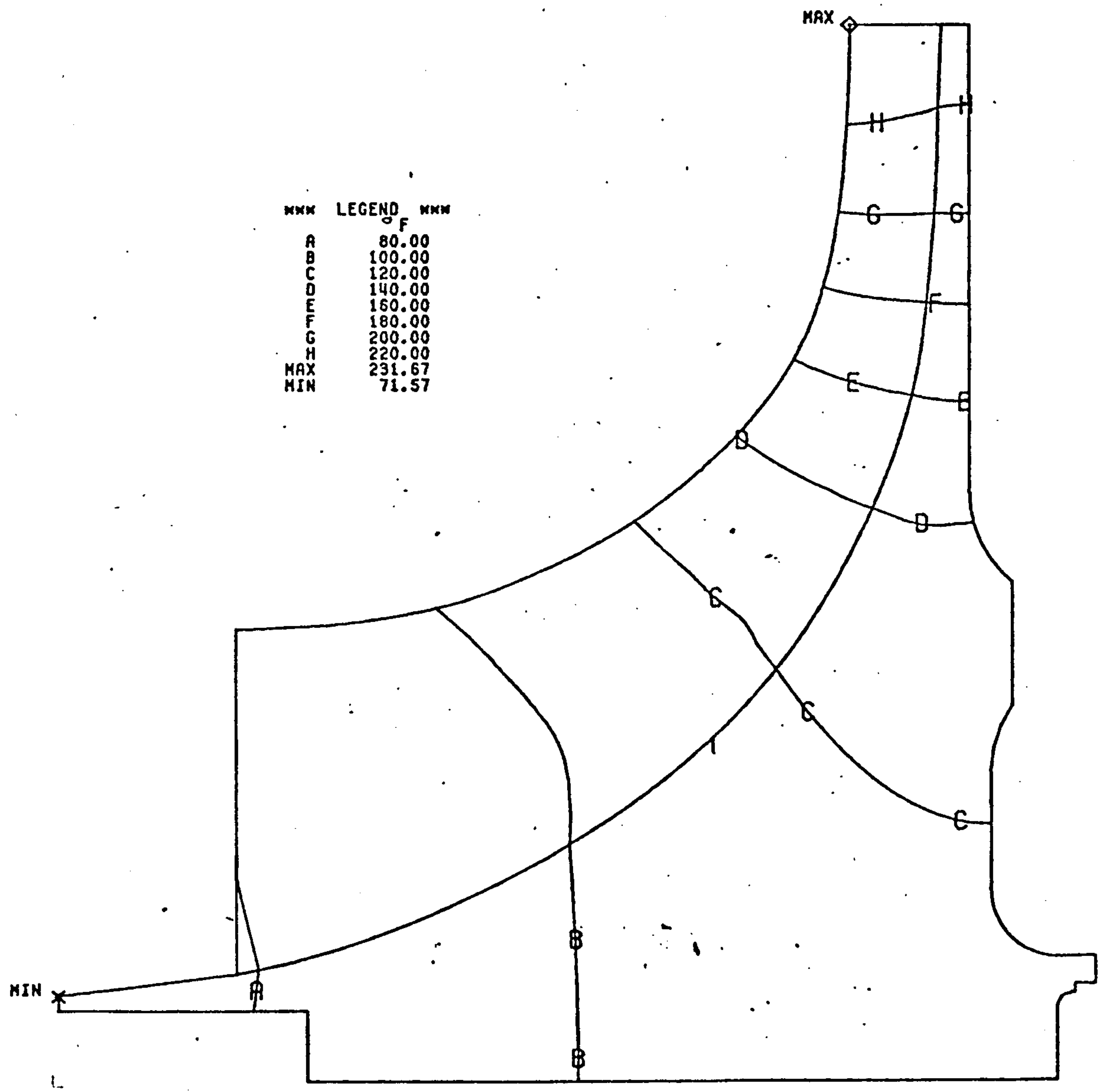

Figure 15. Temperature Distributions for Scaled Impeller.

Initially, the entire wheel was described with an axisymmetric finite element model. This model incorporated the isotherms from the heat transfer analysis, the desired wheel geometry (back face contouring and bore diameters) and flat radial plates to simulate the weight and approximate stiffness of the impeller blading.

The axisymmetric finite element model for the scaled impeller geometry is shown in Figure 16. Resulting distributions of design speed equivalent, axial, radial and tangential stresses are presented in Figures 17, 18, 19 and 20. The analysis did not include an axial clamp load which would result from tie bolt stretching. In order to evalaute the possible effects of a given axial load on stress levels and distribution, an arbitrarily assumed 10,000 lb load (typical of 404-III loads) was then applied at the curvic coupling location. The effects of this load are minimal as shown in Figure 21.

The locations of peak stress were identified and used in a low cycle fatigue and burst speed analysis. The results of these analyses are summarized in Figure 22 with the highest stresses occurring in the bore. Material properties used in the low cycle fatigue analysis are given in Figure 23. As evident from the peak stresses of Figure 22 and the properties of Figure 23, stress levels were such that lives well in excess of 10^6 cycles are projected. Burst speeds were calculated to be 182% of design speed based on an average radial stress and 199% speed based on average tangential stress.

Using deflections from the axisymmetric wheel analysis as boundary conditions, a triangular plate model was constructed for the full blade, splitter and backplate. The full blade model is shown in Figure 24. Figures 25, 26, 27 and 28 present the results for maximum principal and Von Mises equivalent stresses for the full blade pressure and suction surfaces. The same data is provided for the splitter in Figures 29 through 33. A segment of the backplate was analyzed to evaluate blade/backplate interaction effects. The backplate model is presented in Figure 34 with maximum principal and Von Mises equivalent stresses given in Figures 35 through 38.

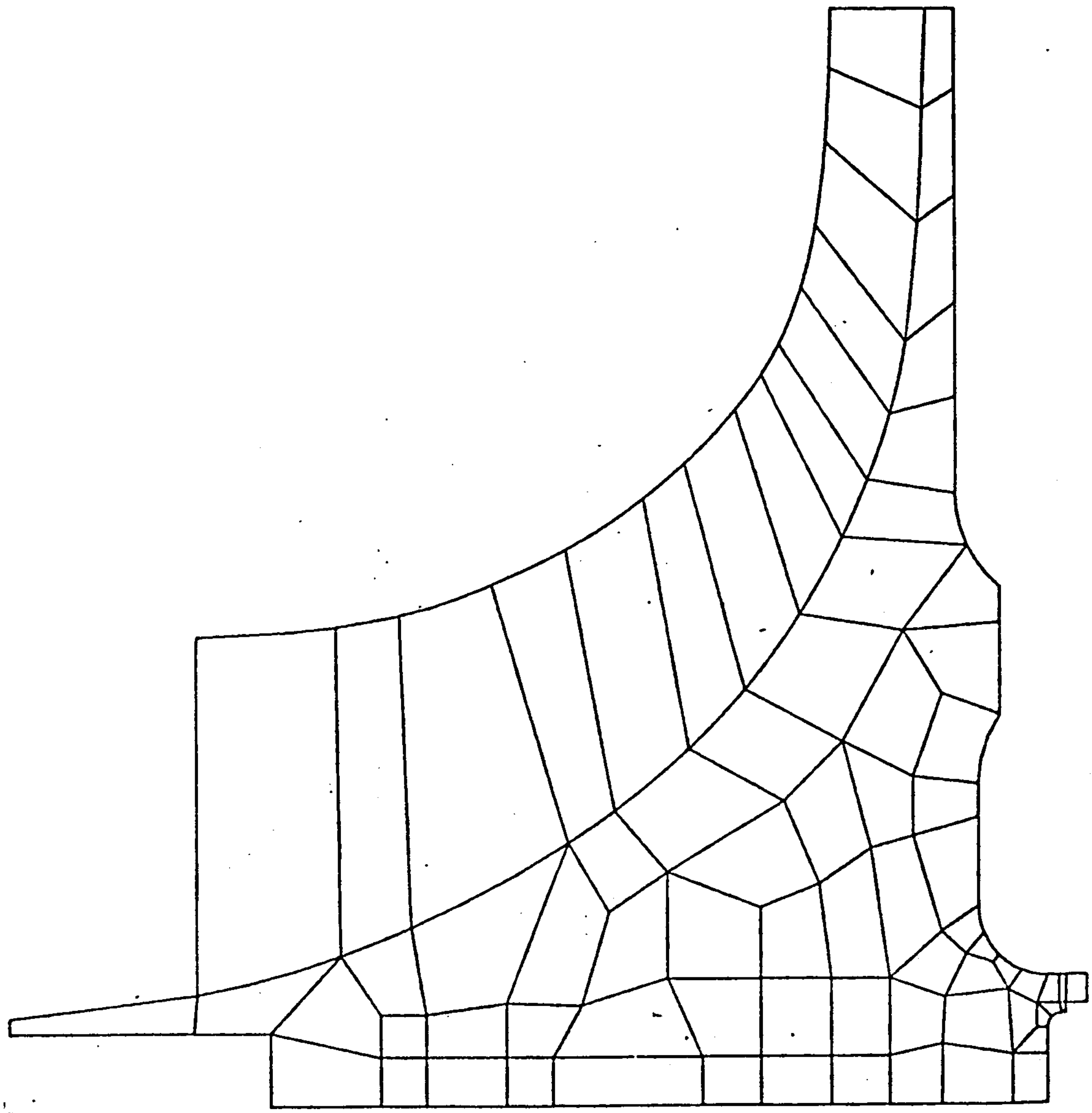

Figure 16. Axisymmetric Stress Model for Scaled Impeller.

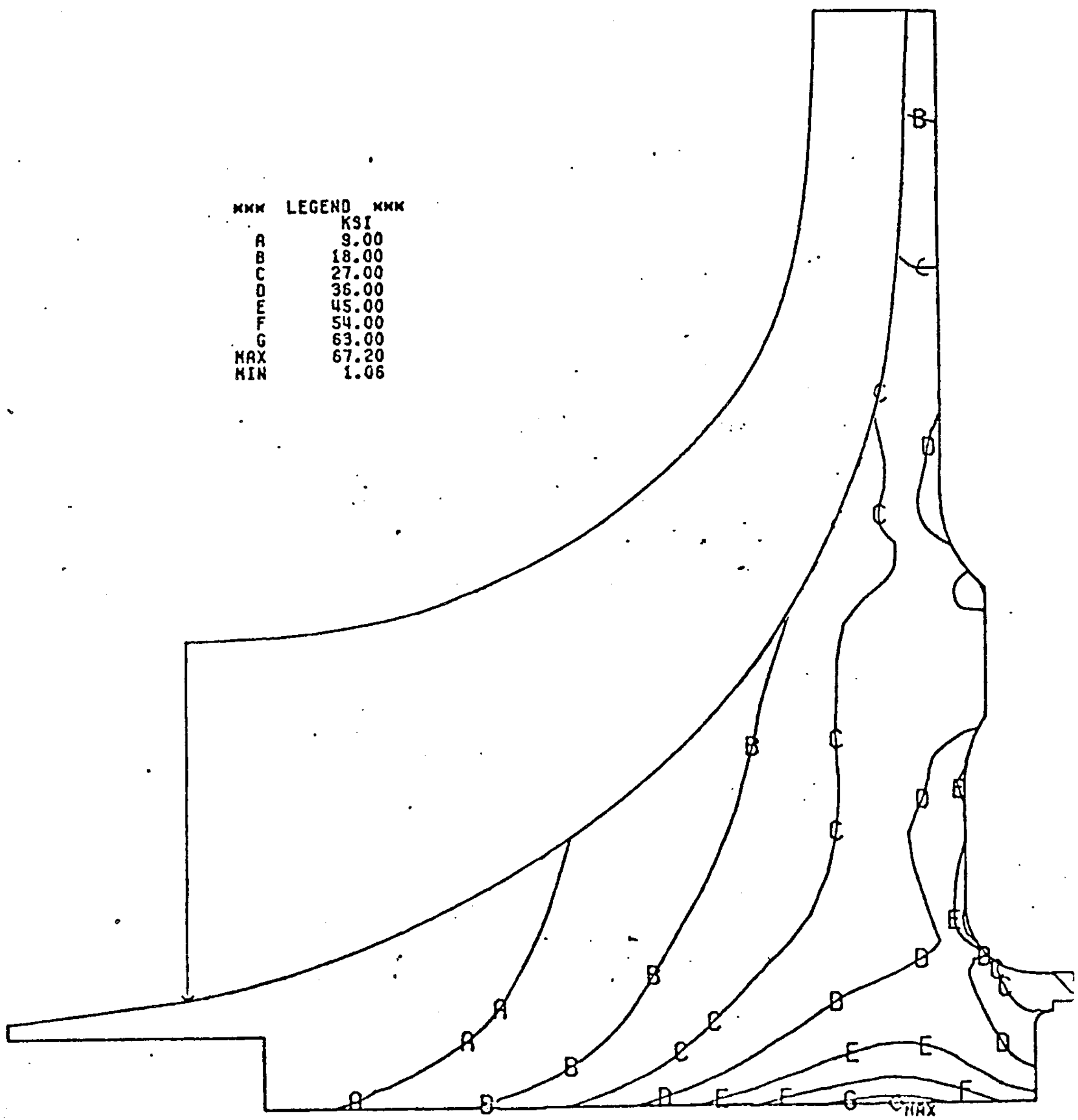

Figure 17. Impeller Equivalent Stresses.

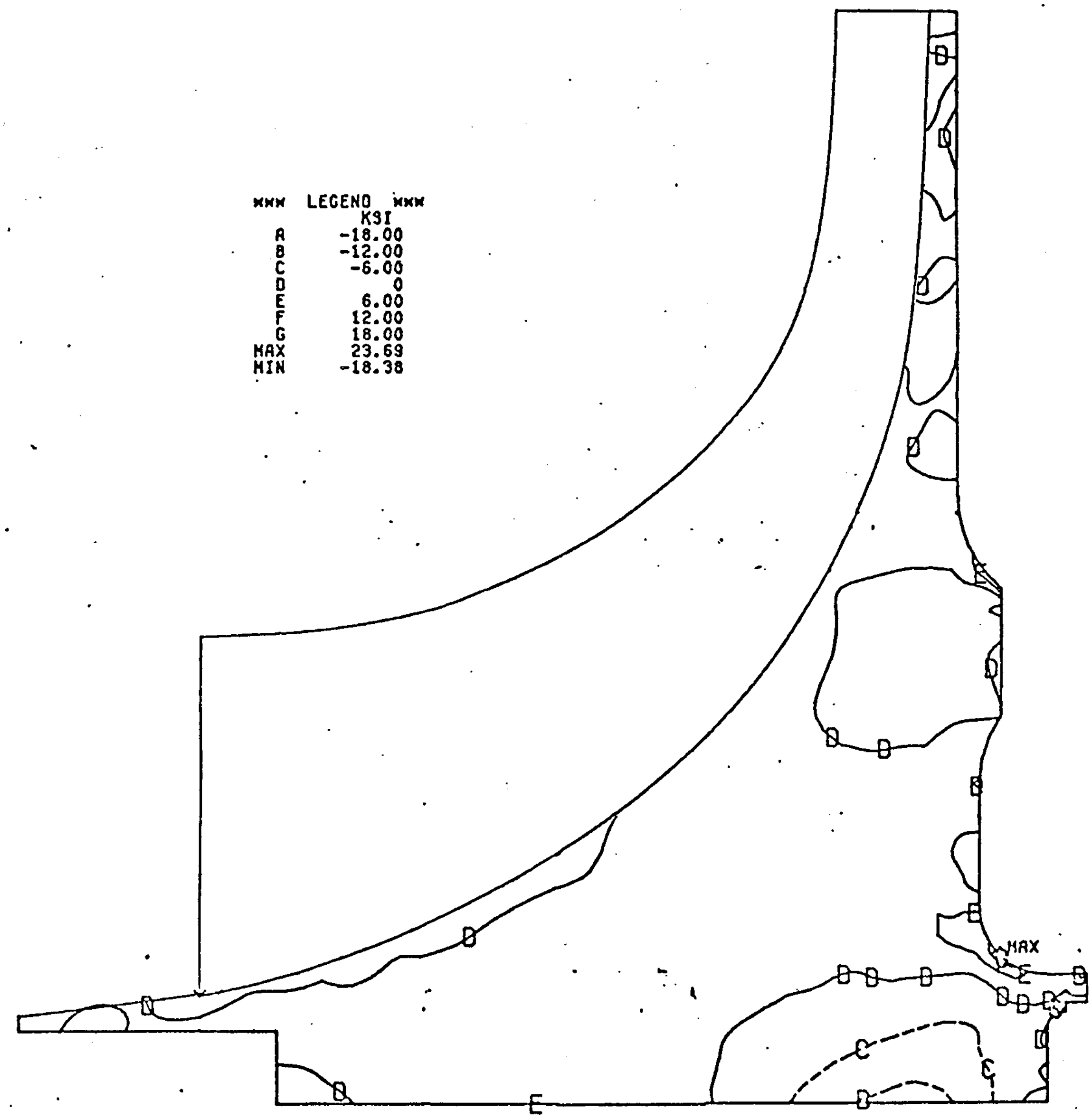

Figure 18. Impeller Axial Stresses.

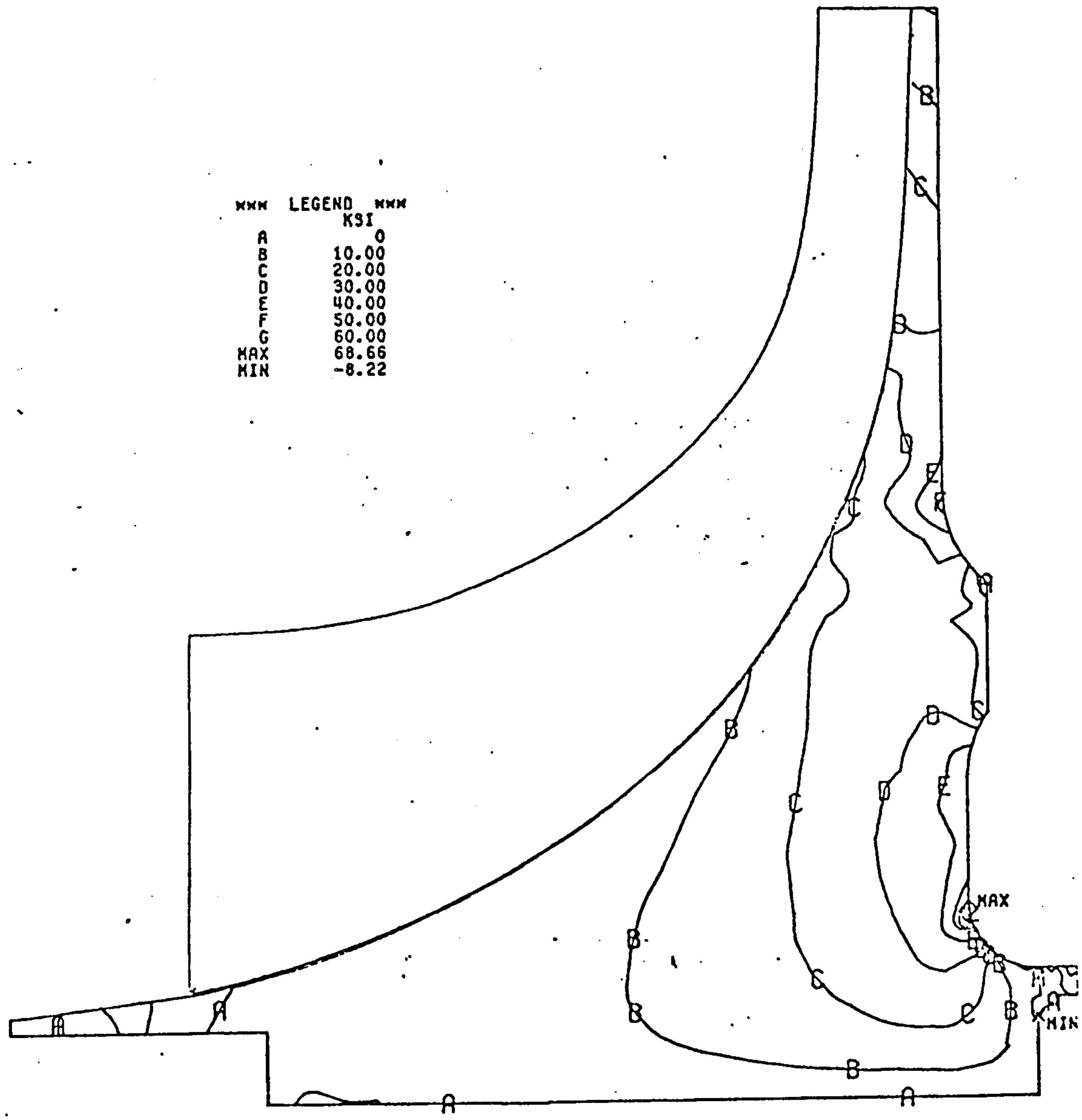

Figure 19. Impeller Radial Stresses.

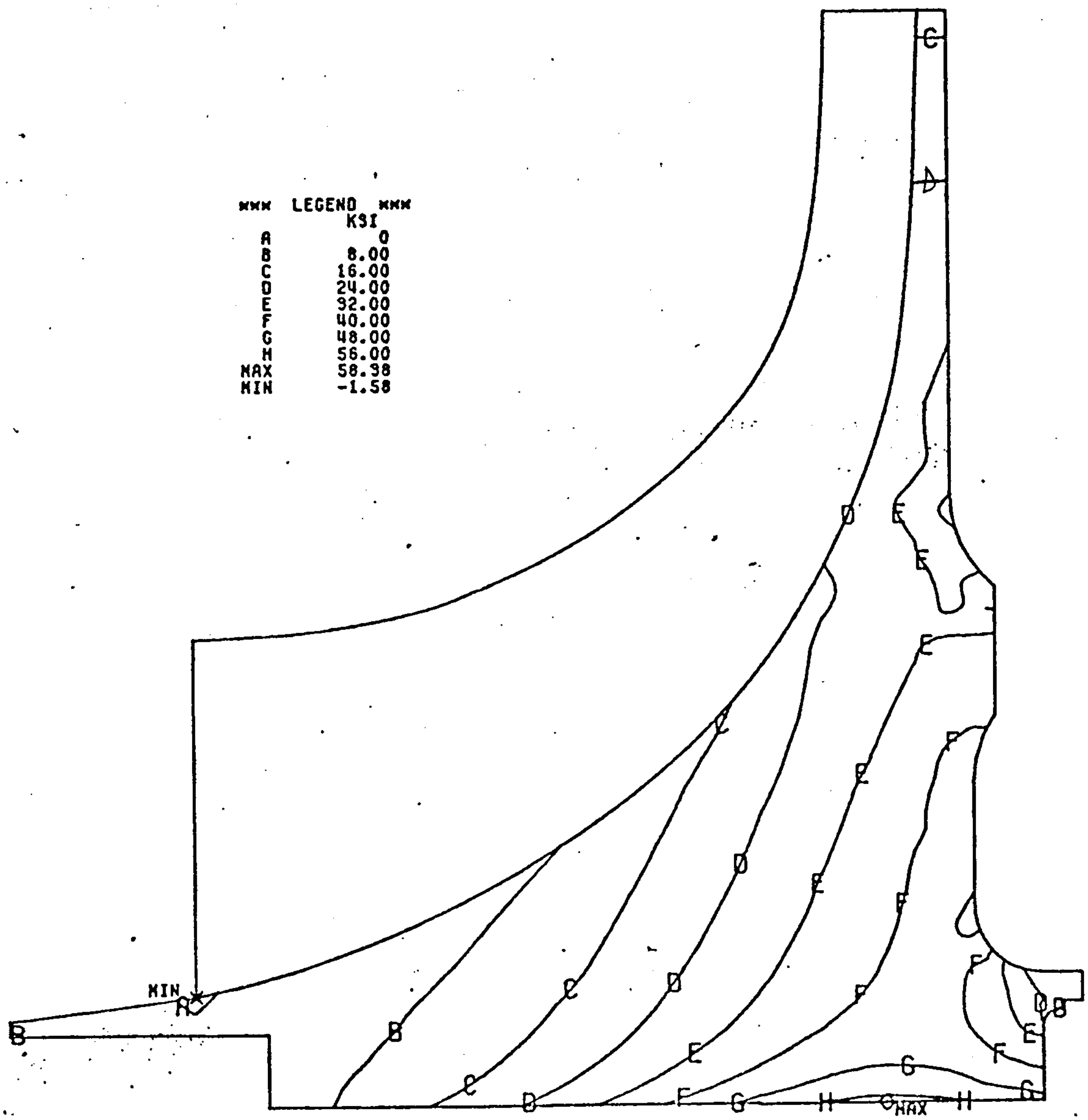

Figure 20. Impeller Tangential Stresses.

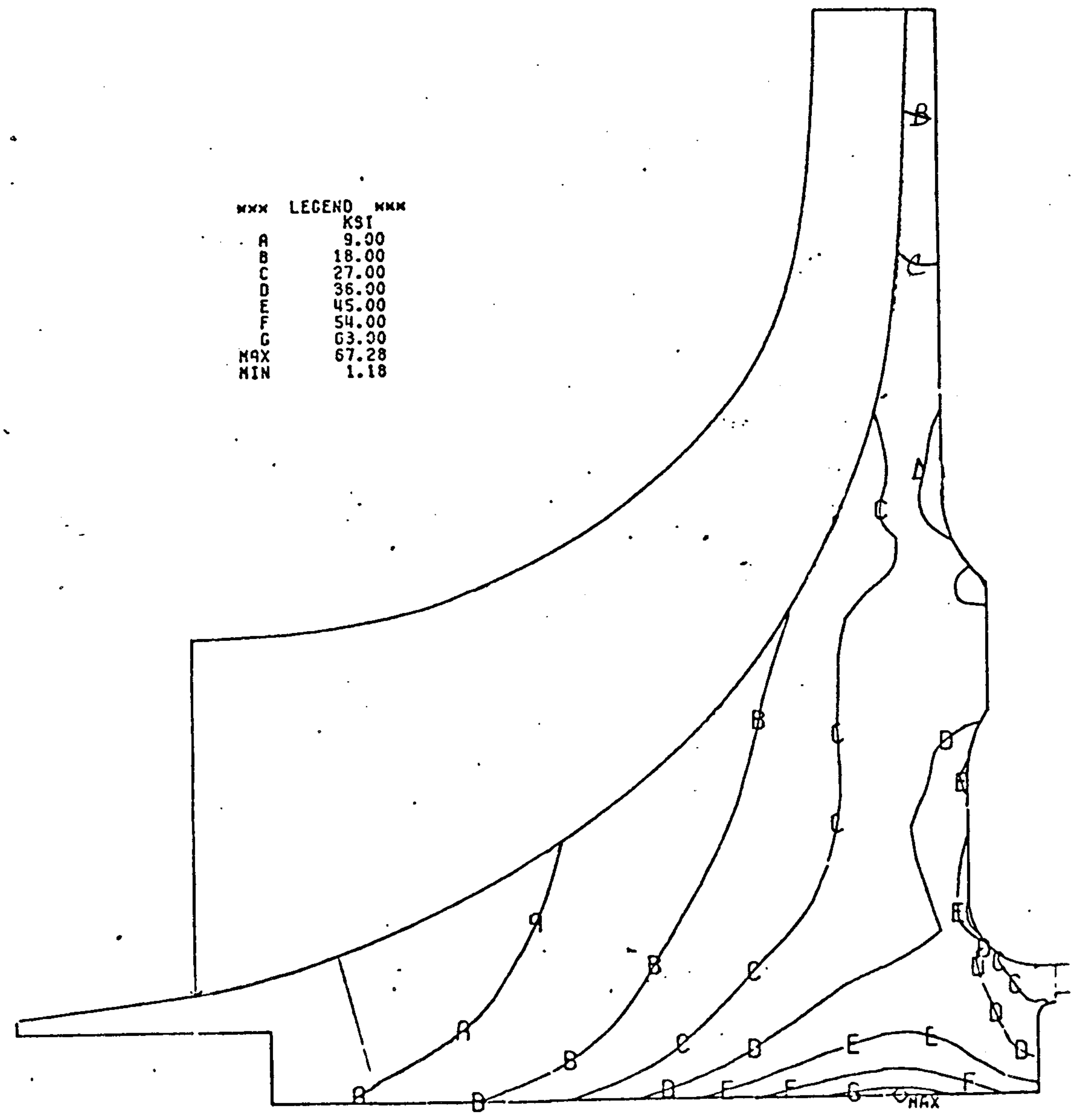

Figure 21. Impeller Equivalent Stress with 10,000 lbf Axial Load.

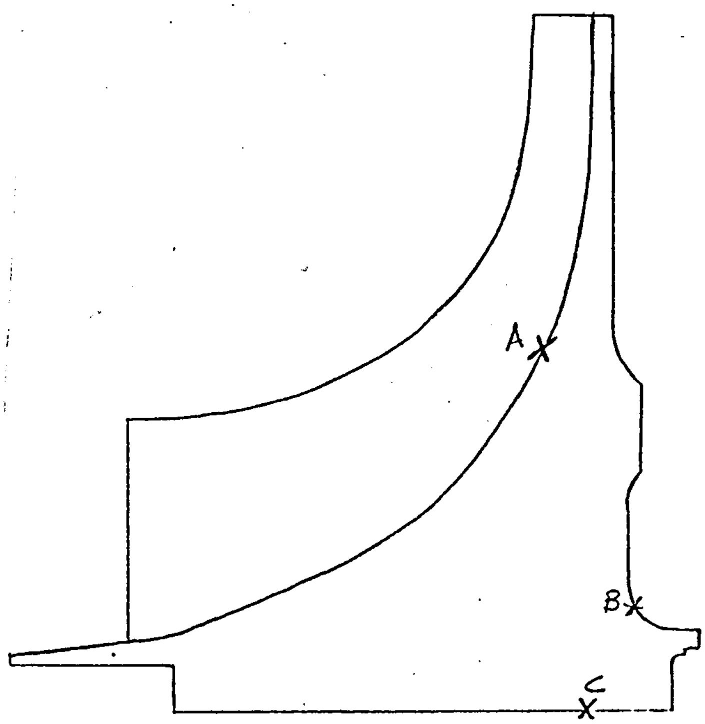

Location	σ_{MAX}(KSI)	K_t	R_{RATIO}	Life (cycles) Mean	Temp(°F)	-3σ Yield Strength (KSI)
A *	58.5	1.35	0.0	$> 10^6$	140	106
B	61.66	1.0	0.0	$> 10^6$	116	110
C	67.2	1.0	0.0	$> 10^6$	114	110

* Max. Stress in the Backplate (From Triangular Plate Model)

-3σ Burst Speed

Avg. Tang. = 199% N_D
Avg. Radial = 182% N_D

Figure 22. Low Cycle Fatigue and Burst Analysis

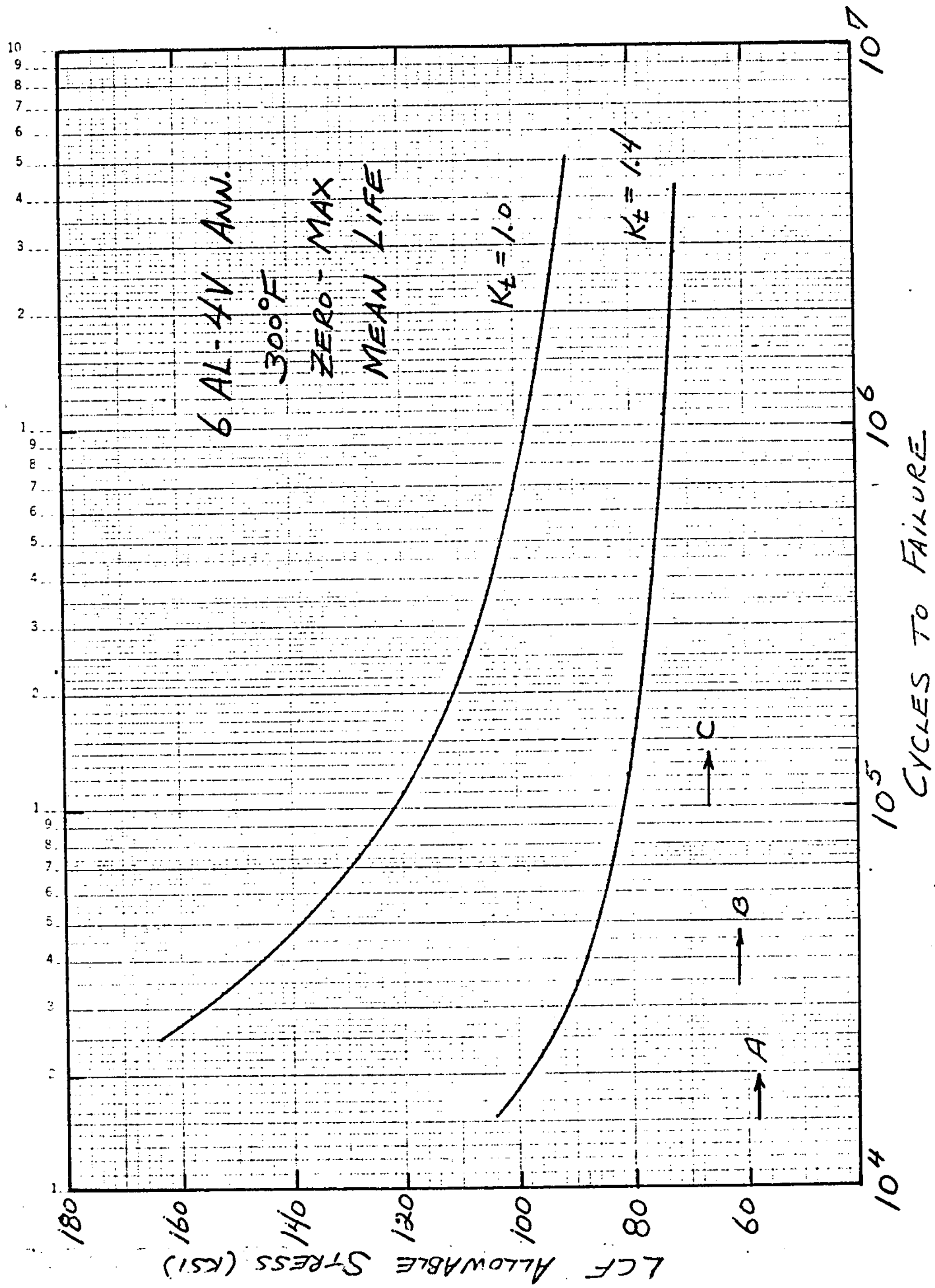

Figure 23. Low Cycle Fatigue Material Properties for Ti 6AL4V.

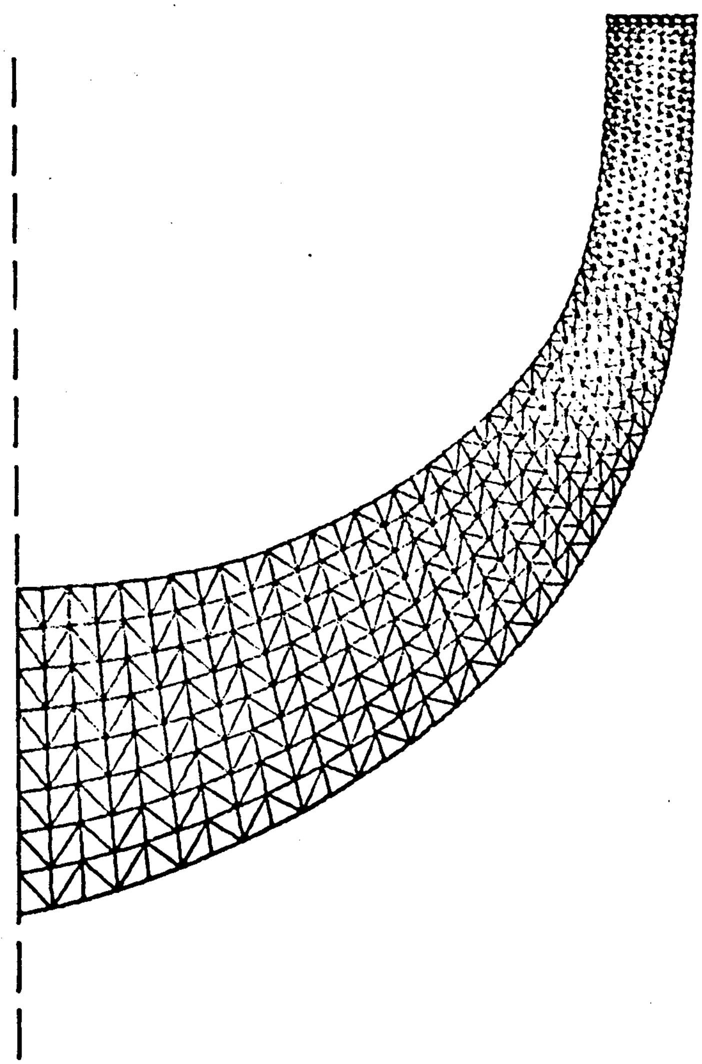

Figure 24. Triangular Plate Model for Scaled Impeller Full Blade.

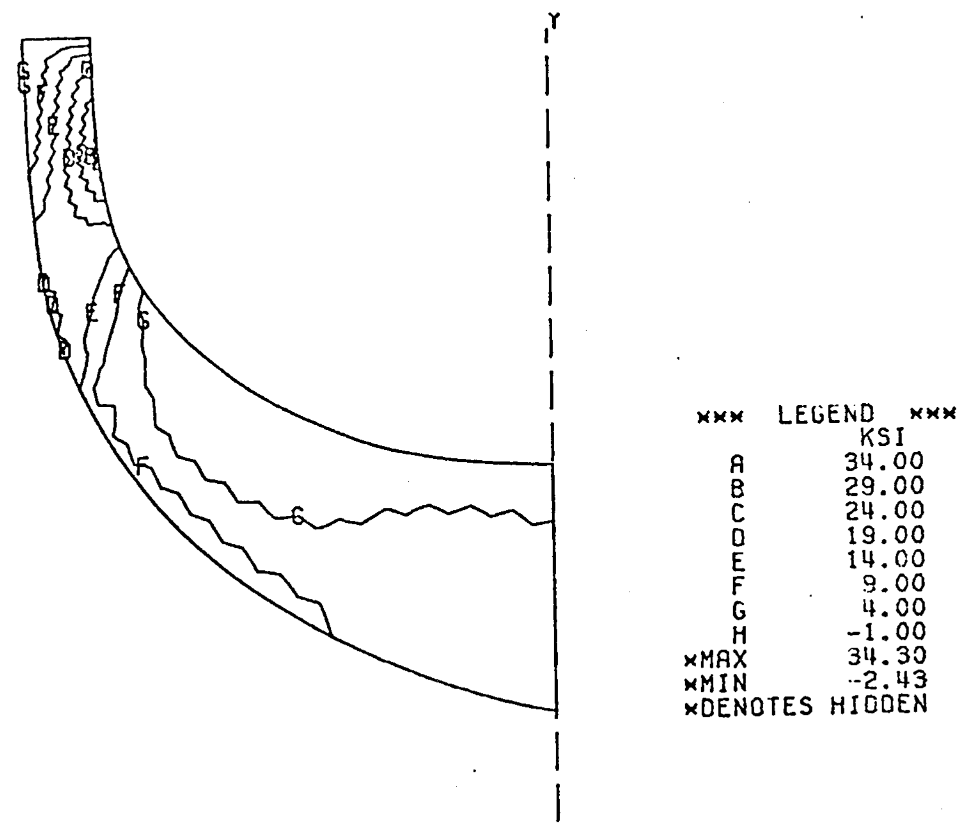

Figure 25. Pressure Surface ~ Maximum Principal Stress.

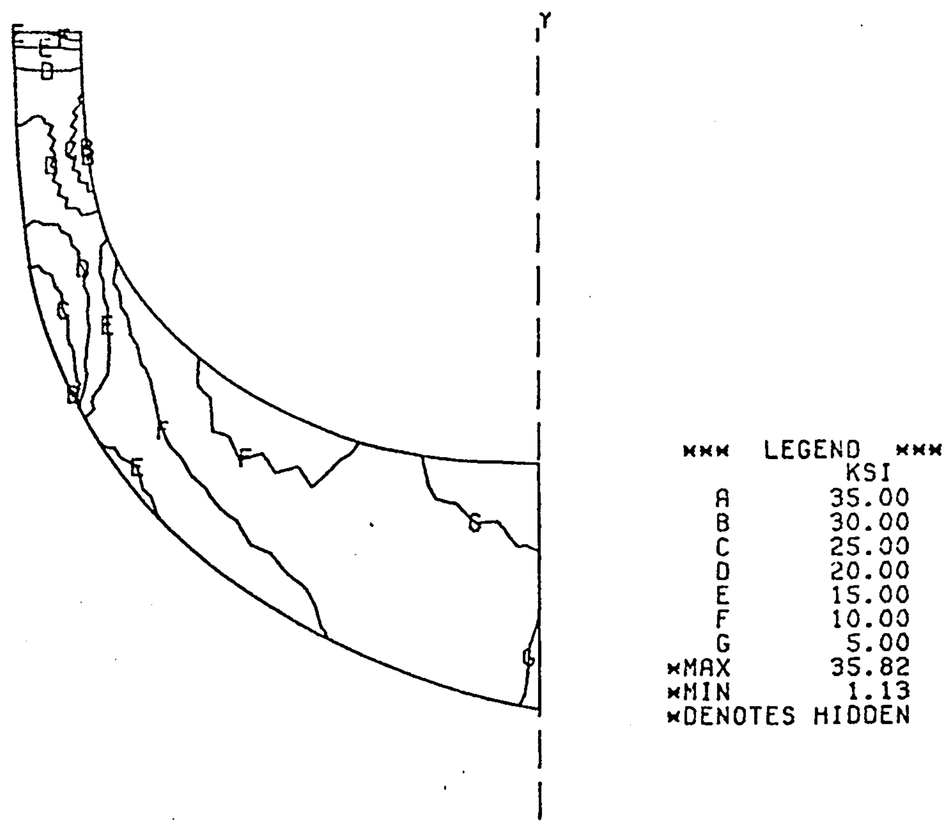

Figure 26. Pressure Surface ~ Equivalent Stress.

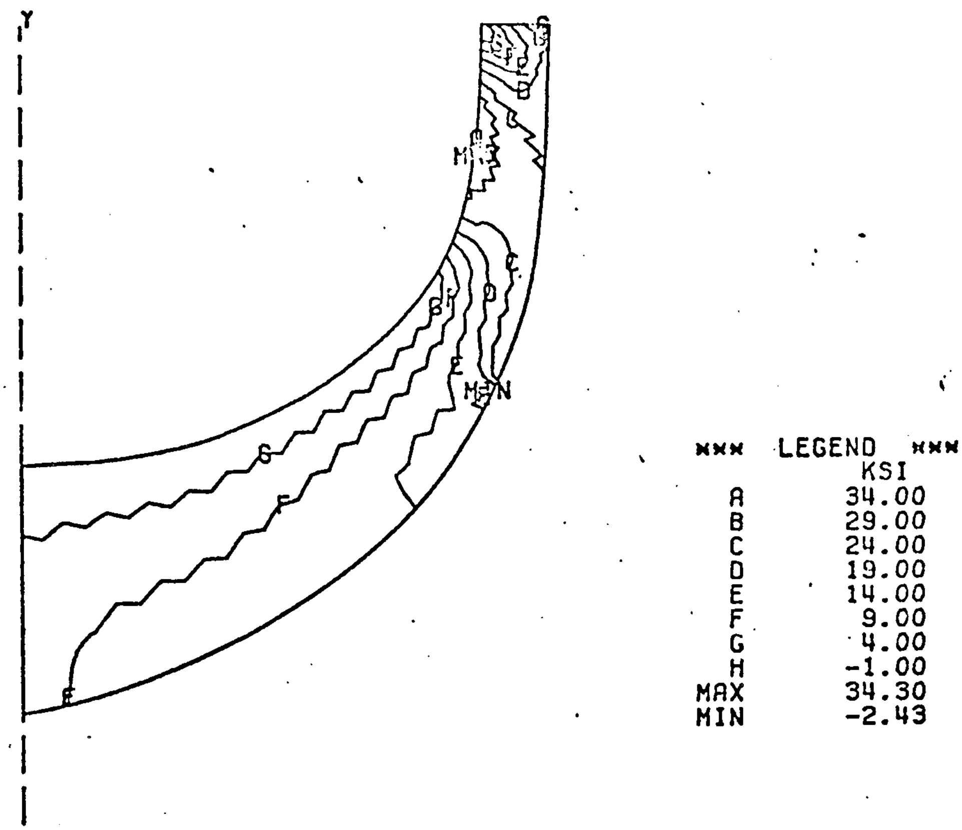

Figure 27. Suction Surface ~ Maximum Principal Stress.

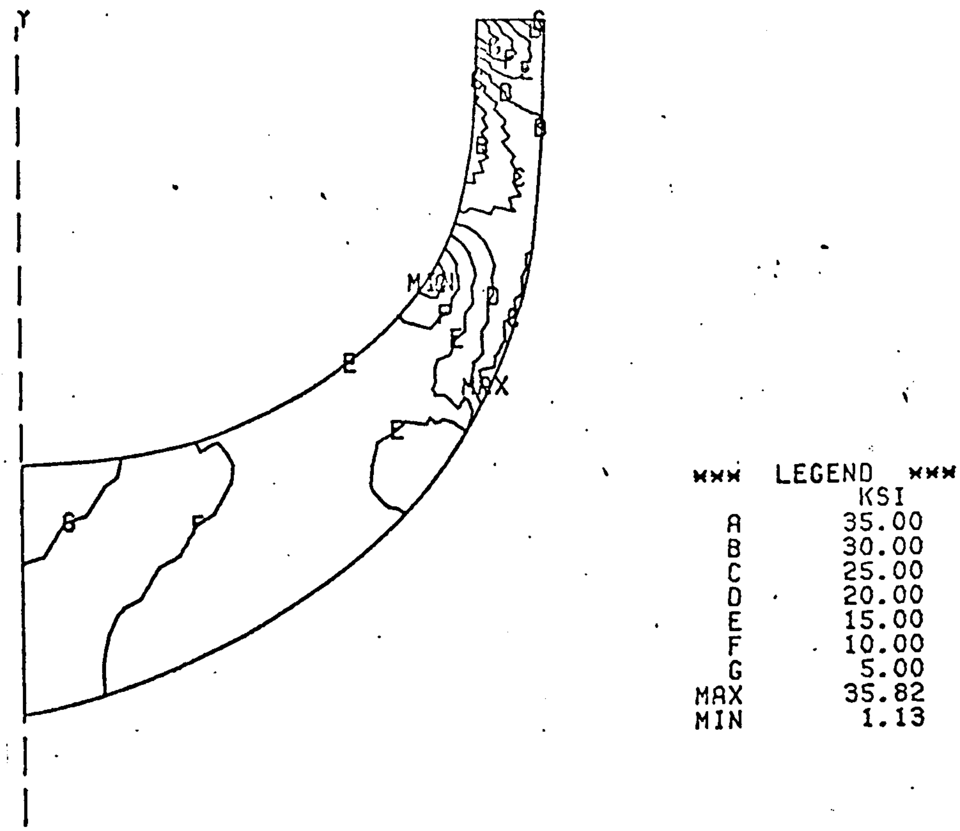

Figure 28. Suction Surface ~ Equivalent Stress.

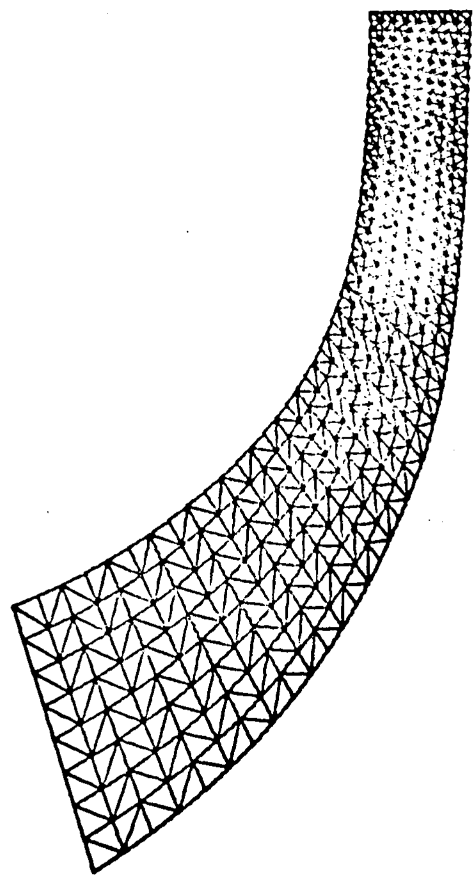

Figure 29. Triangular Plate Model for Scaled Impeller Splitter Blade.

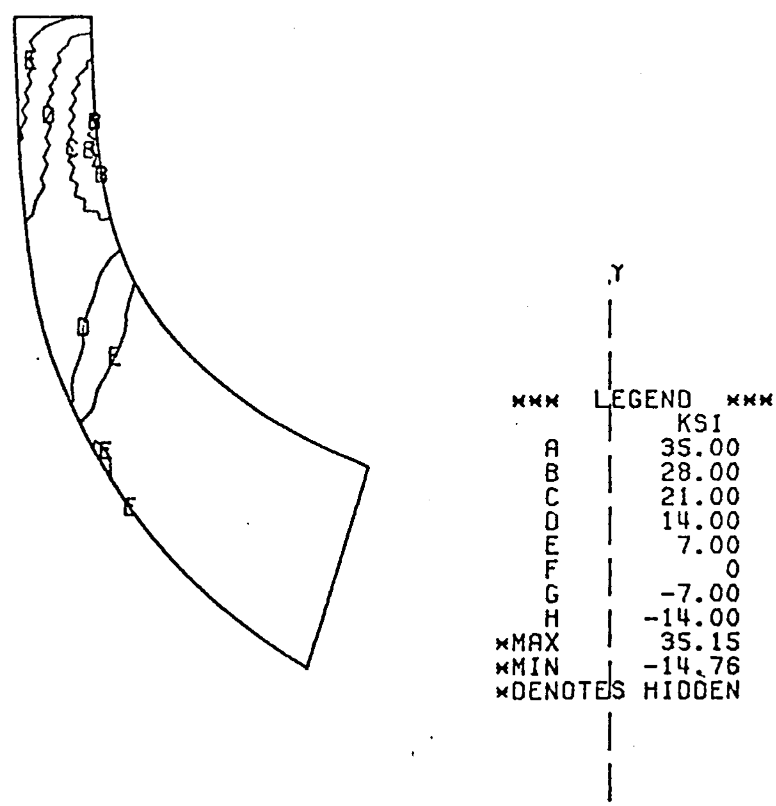

Figure 30. Pressure Surface ~ Maximum Principal Stress.

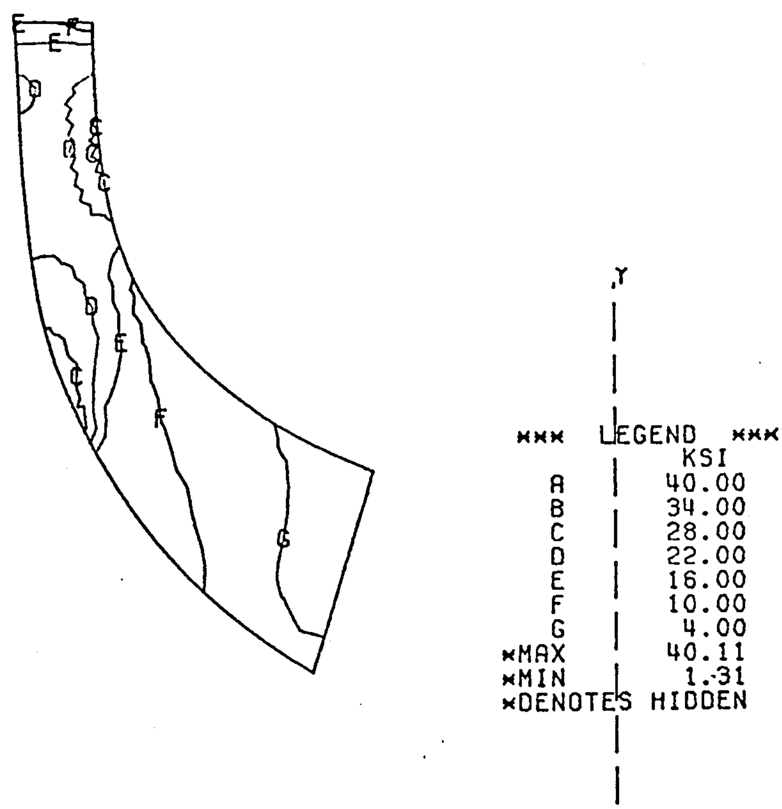

Figure 31. Pressure Surface ~ Equivalent Stress.

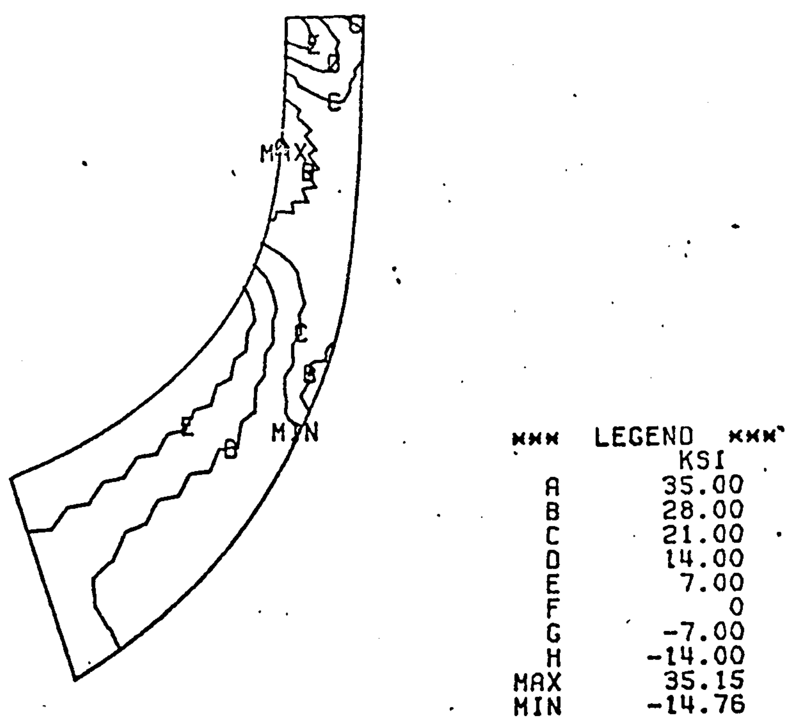

Figure 32. Suction Surface ~ Maximum Principal Stress.

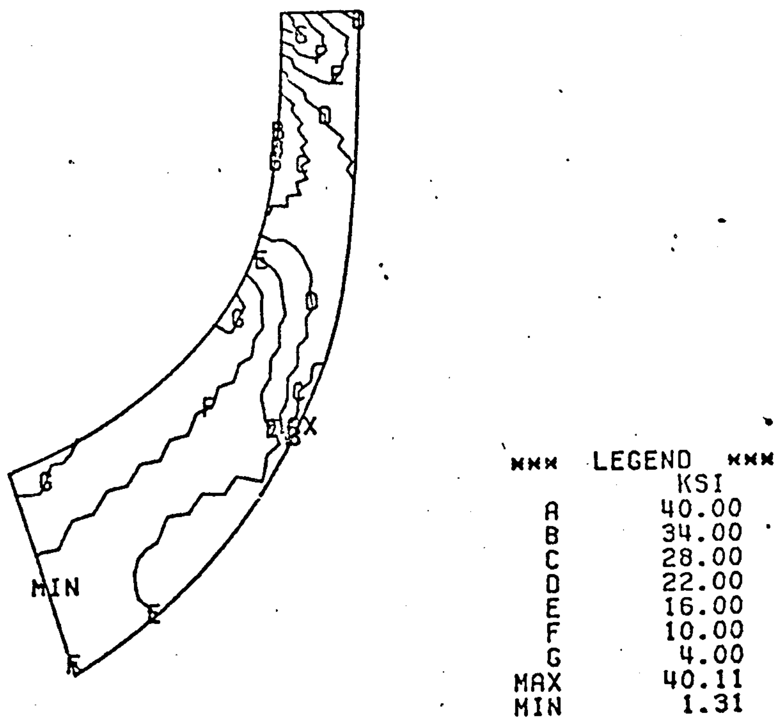

Figure 33. Suction Surface ~ Equivalent Stress.

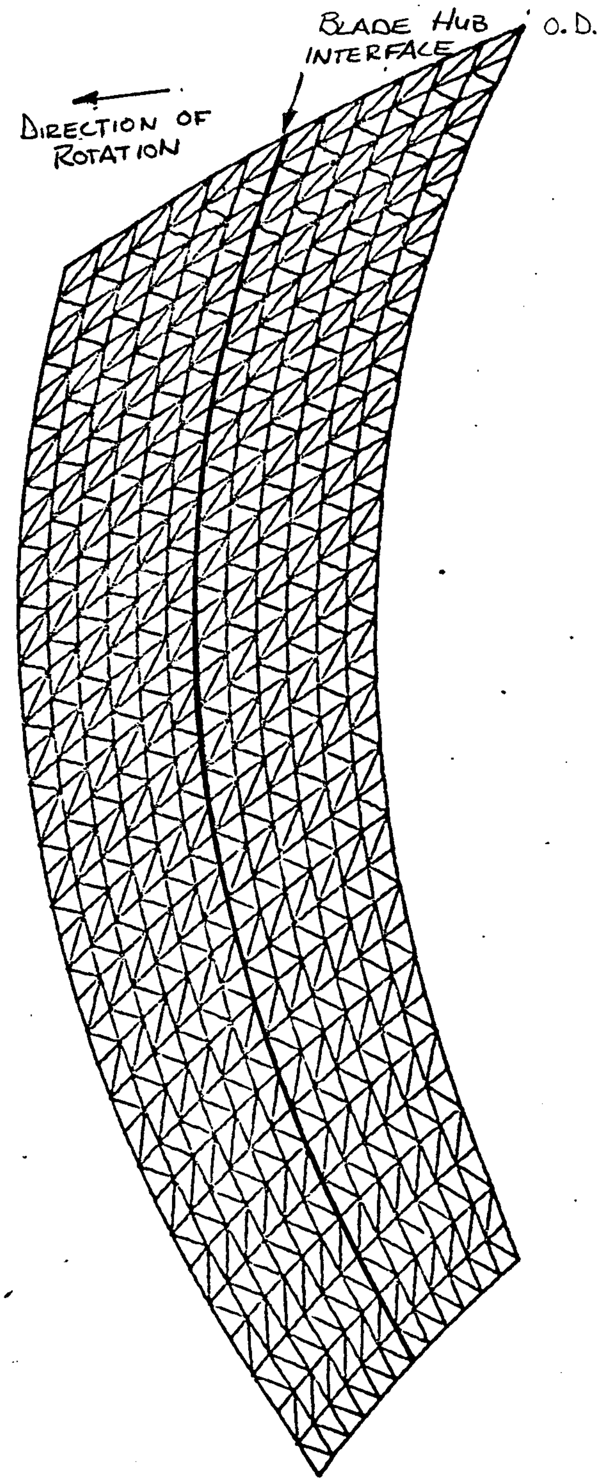

Figure 34. Triangular Plate Model for Impeller Backplate.

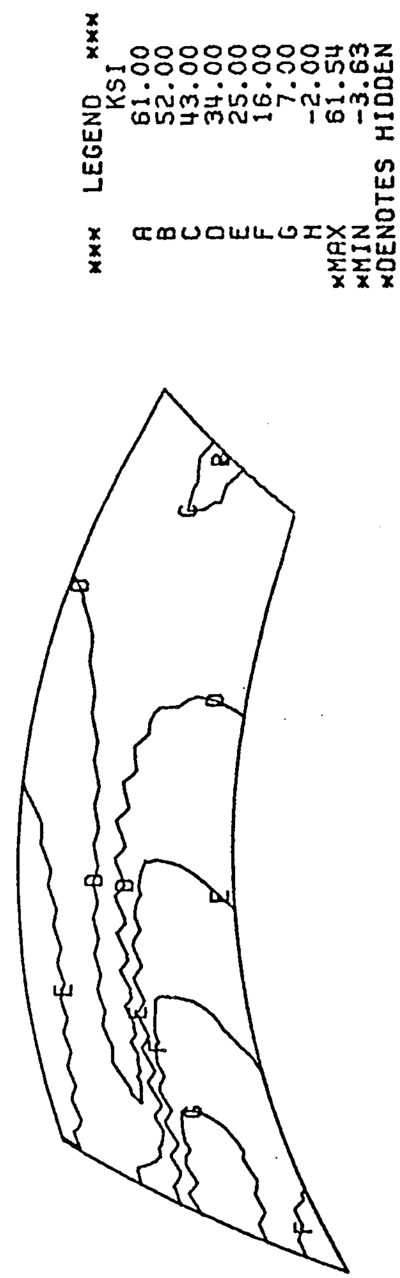

Figure 35. Maximum Principal Stress ~ Backface Surface.

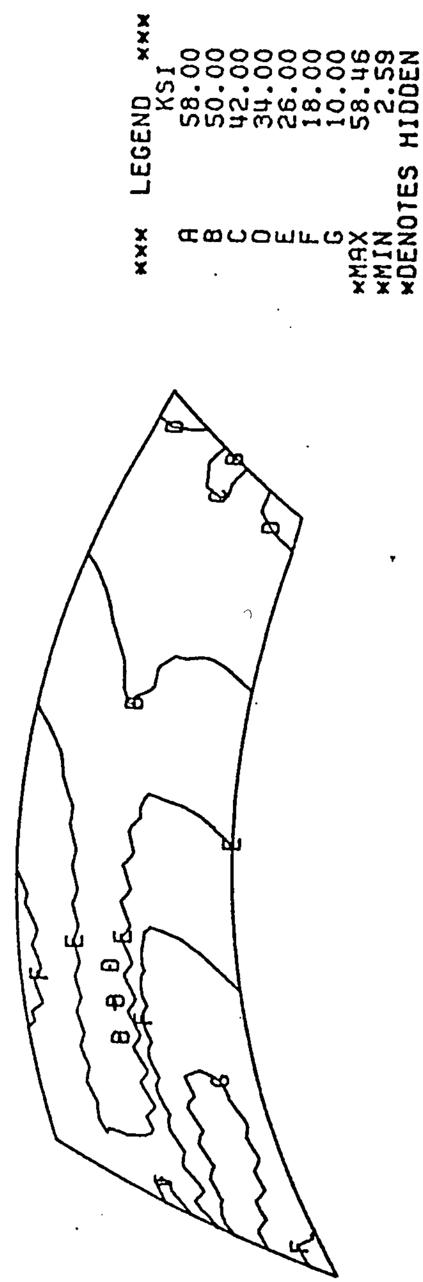

Figure 36. Equivalent Stress ~ Backface Surface.

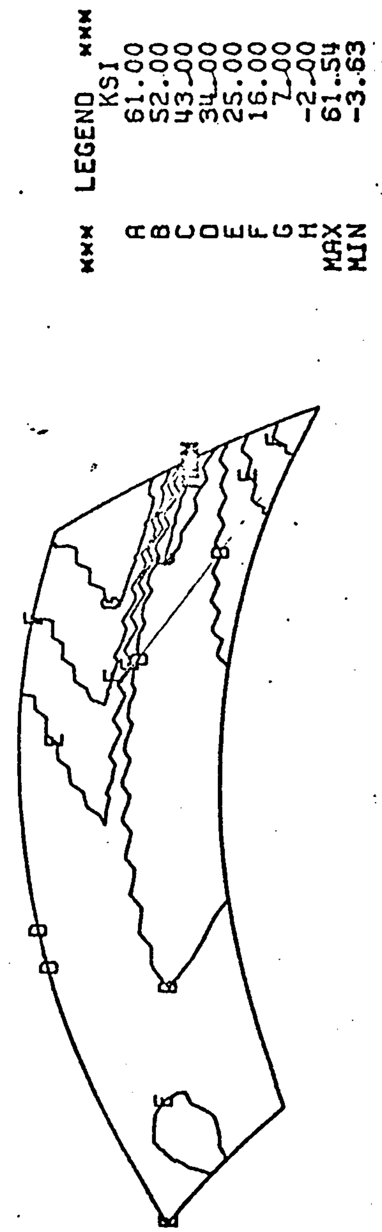

Figure 37. Maximum Principal Stress ~ Flowpath Hub Surface.

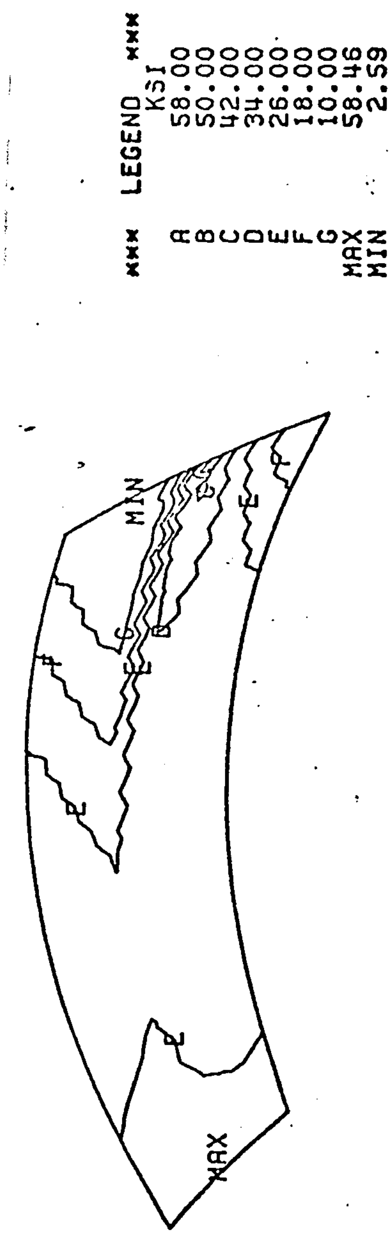

Figure 38. Equivalent Stress ~ Flowpath Hub Surface.

Maximum equivalent stresses from the triangular plate analysis are summarized in Figure 39. Locations A and B are on the full blade leading edge, C is on the splitter leading edge and D is at the maximum stress location on both the full blade and splitters. Based on the stresses and stress concentration factors defined in Figure 39 and the Goodman diagram presented in Figure 40, a high cycle fatigue analysis was performed. The maximum steady stress location on the splitter yielded the lowest vibratory allowable stress, 14.4 ksi.

The final output of the static stress analysis was a complete definition of the deflection characteristics of the wheel, backplate and blade geometry. This definition was used to convert the "hot running" aerodynamic geometry into an equivalent manufacturing, "cold", definition. Details of this conversion and the resulting manufacturing definition are presented in Section IV.

A summary of pertinent deflections is given in Figure 41. Of special interest are points 5 and 2. The calculated axial deflection at the impeller exit was 0.01463 inches with ground located near the impeller leading edge. This axial deflection must be accounted for in the establishment of cold build clearance. Point 2 is at the location of the curvic coupling. With point 1 grounded, the change in axial wheel length between points 1 and 2 is 0.00337 inches with the wheel length shortening due to Poisson's effect. This shortening must be accounted for by initial tie bolt stretch.

Finite element models similar to those used for static stress analysis were prepared for vibrational analysis. Resulting frequencies and mode shapes for the first 8 natural frequencies for the full blade and first 3 for the splitter are presented in Figures 42 through 52. A summary of these predicted frequencies is shown on a frequency-speed diagram for the full blade in Figure 53 and for the splitter in Figure 54. The first mode of the full blade is well above 4th harmonic of rotor speed and is, therefore, not susceptable to inlet distortion induced exitation that is often characterized by strong 2nd order

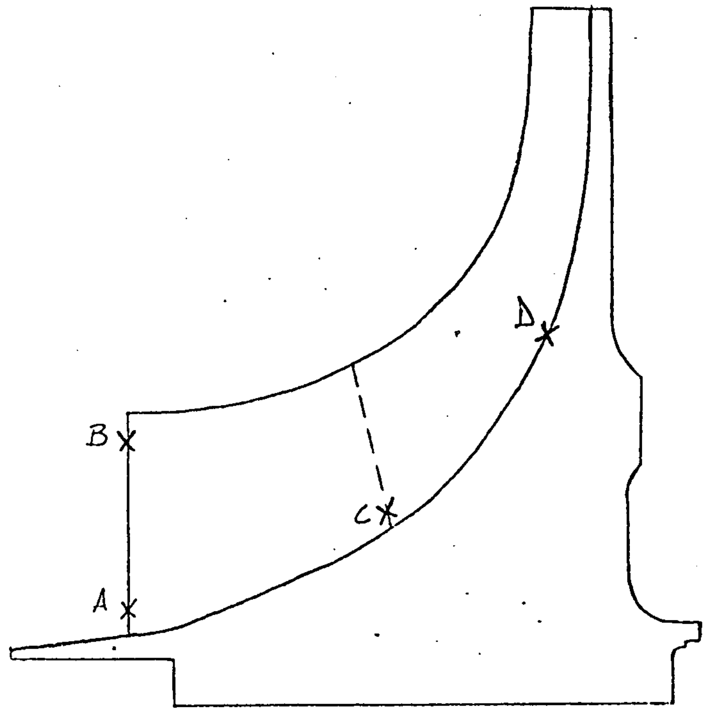

Location	K_t	Mean Stress (KSI)	-3σ Allow. Vib. (KSI)
A	3.0	7.4	15.7
B	3.0	4.8	16.1
C **	3.0	12.4	15.0
D *	1.35	35.8	15.1
D ***	1.35	40.11	14.4

* Blade Max. Stress
** Splitter Leading Edge
*** Splitter Max. Stress

Figure 39. Summary of High Cycle Fatigue Analysis.

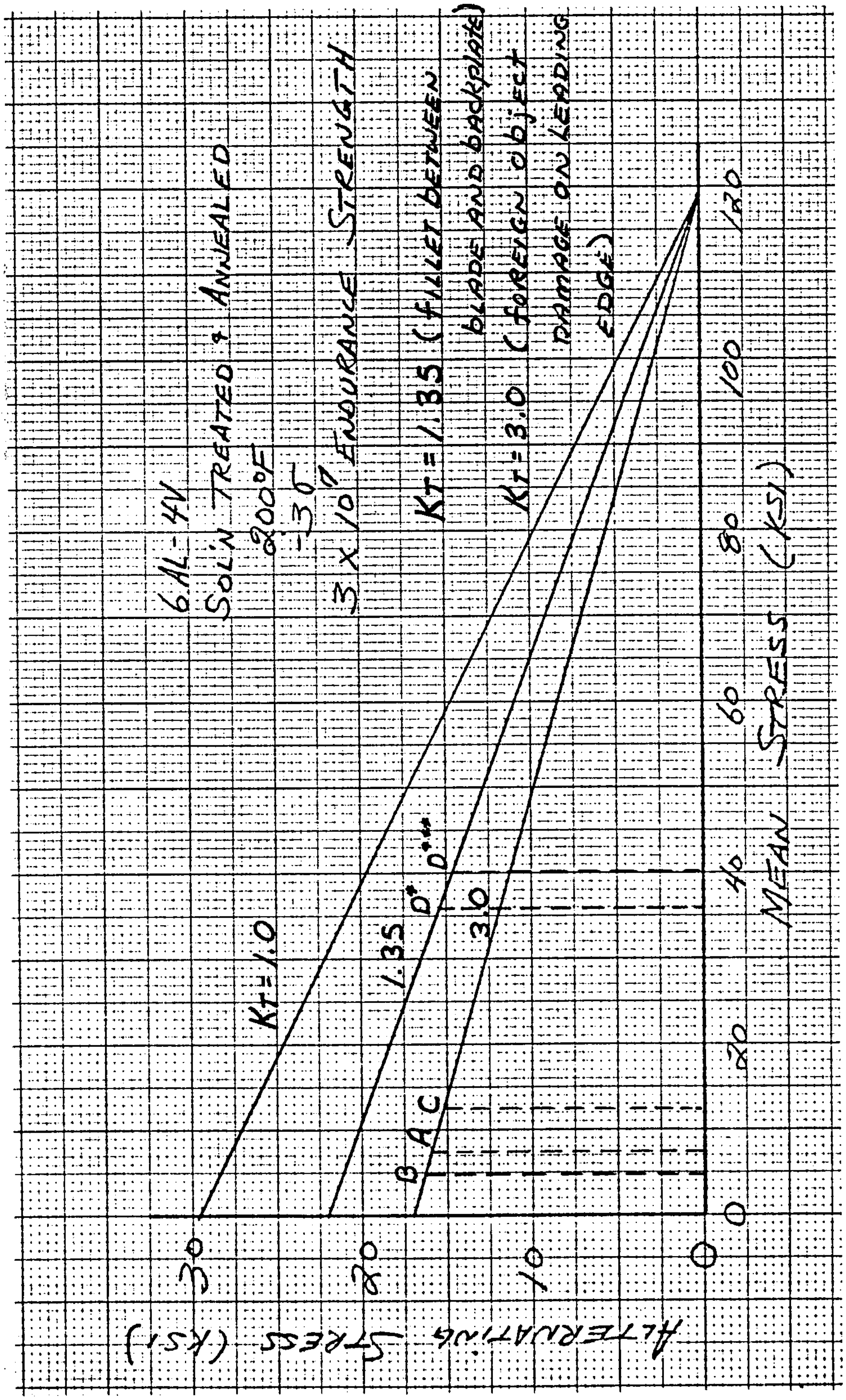

Figure 40. Goodman Diagram for Ti 6AL-4V Material.

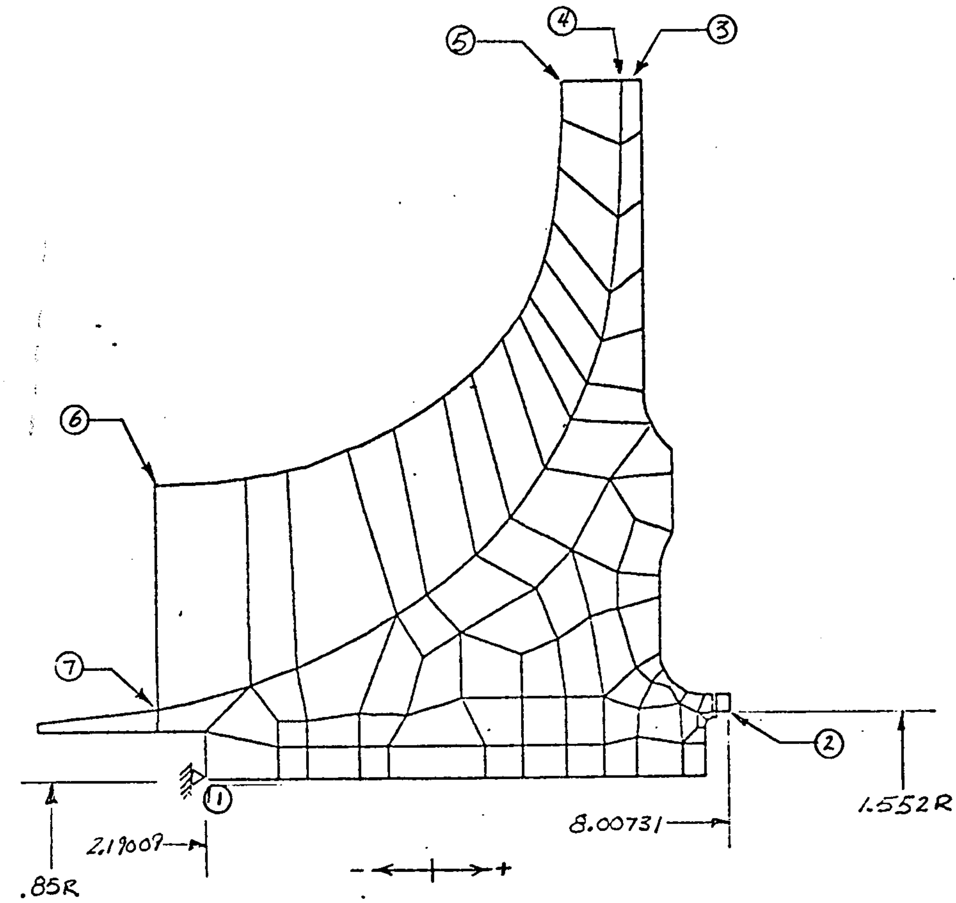

Location	Deflections: Radial	Tangential	Axial
1	.00021	-	0.0
2	.00204	-	-.00337
3	.01371	-.00162	-.01646
4	.01383	-.00191	-.01646
5	.01663	-.00529	-.01463
6	.00093	-.00171	-.00121
7	.00017	-	-.00053

Figure 41. Scaled Impeller Deflection Summary.

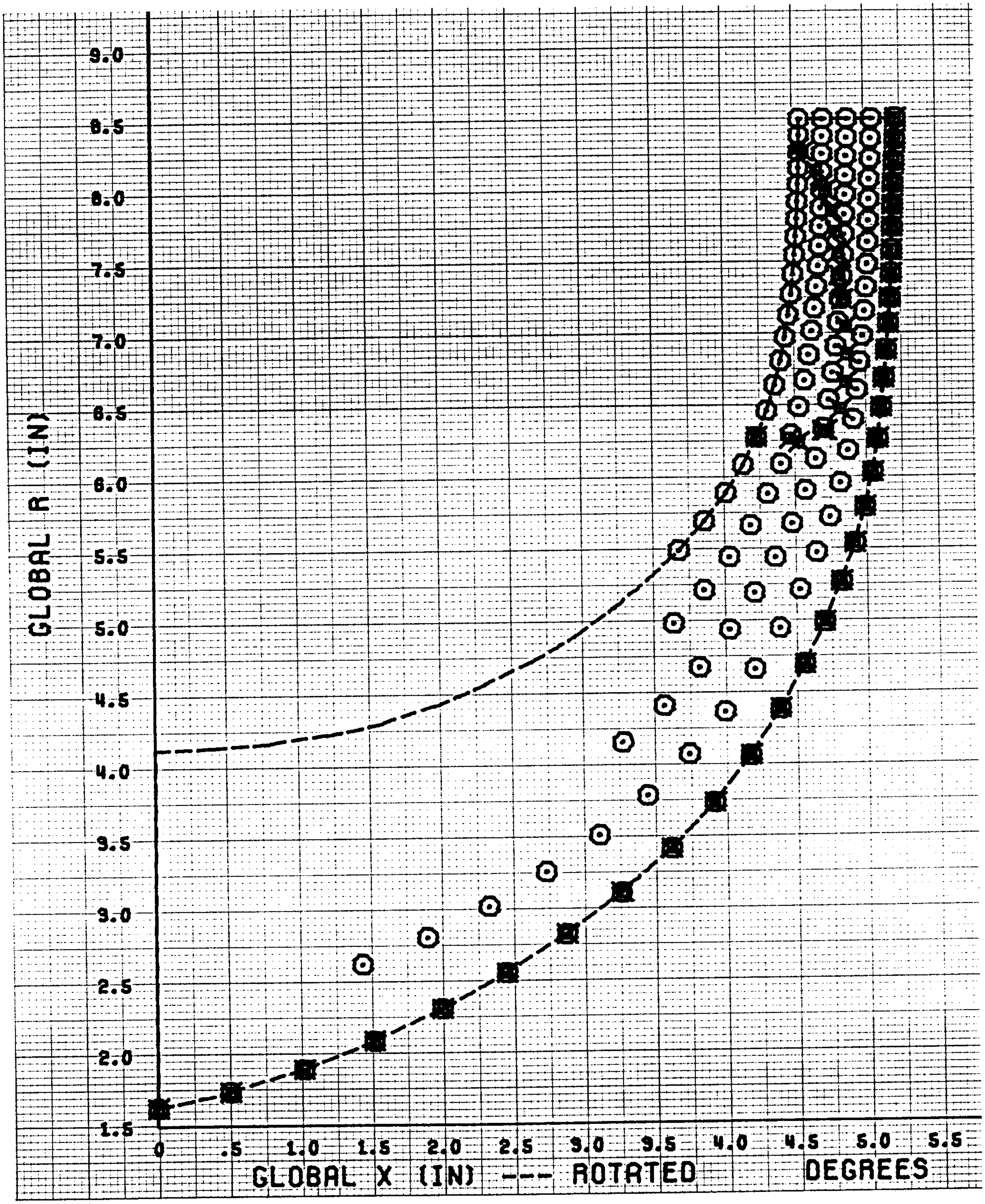

Figure 42. Full Blade ~ 1st Natural Frequency.

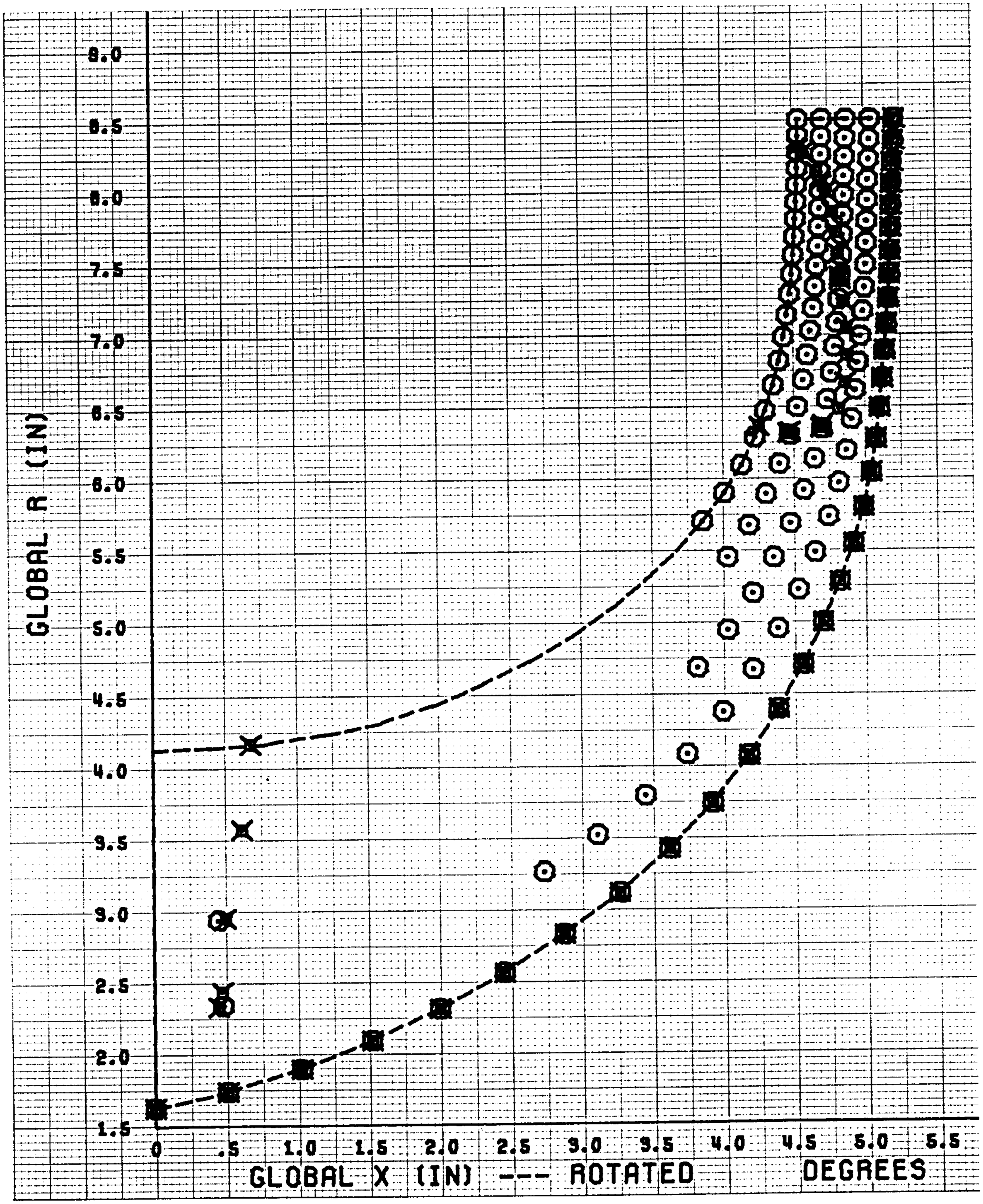

Figure 43. Full Blade ~ 2nd Natural Frequency.

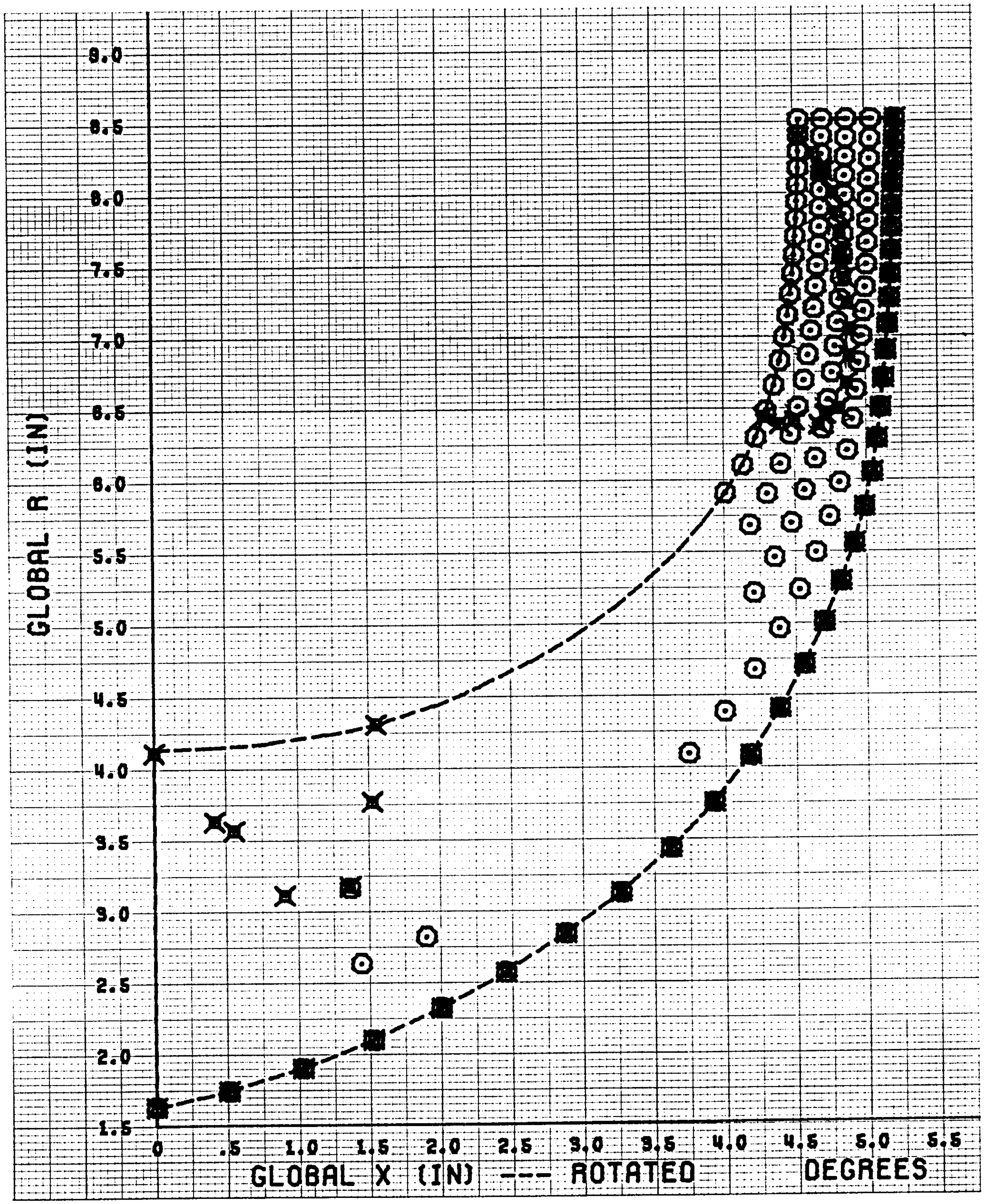

Figure 44. Full Blade ~ 3rd Natural Frequency.

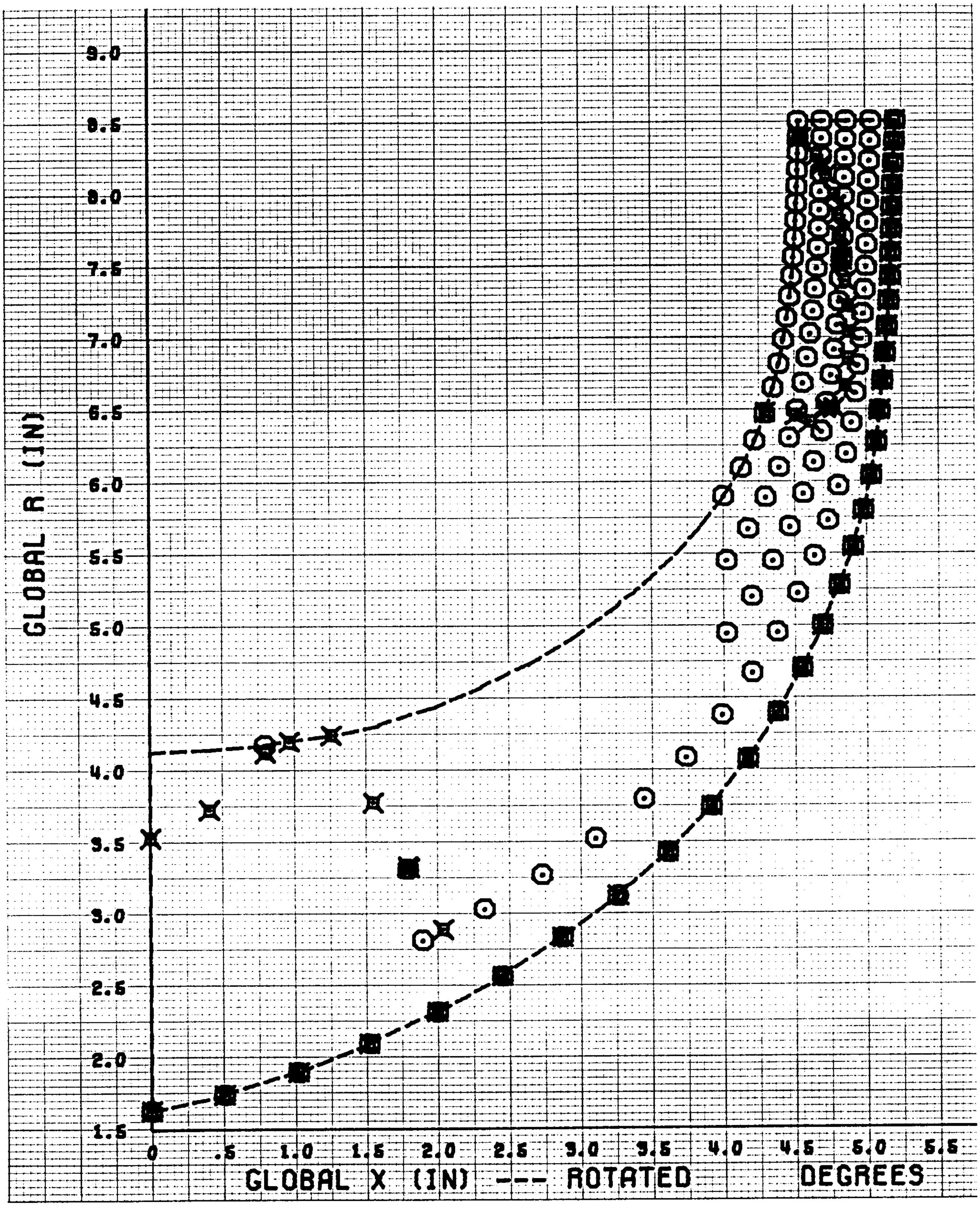

Figure 45. Full Blade ~ 4th Natural Frequency.

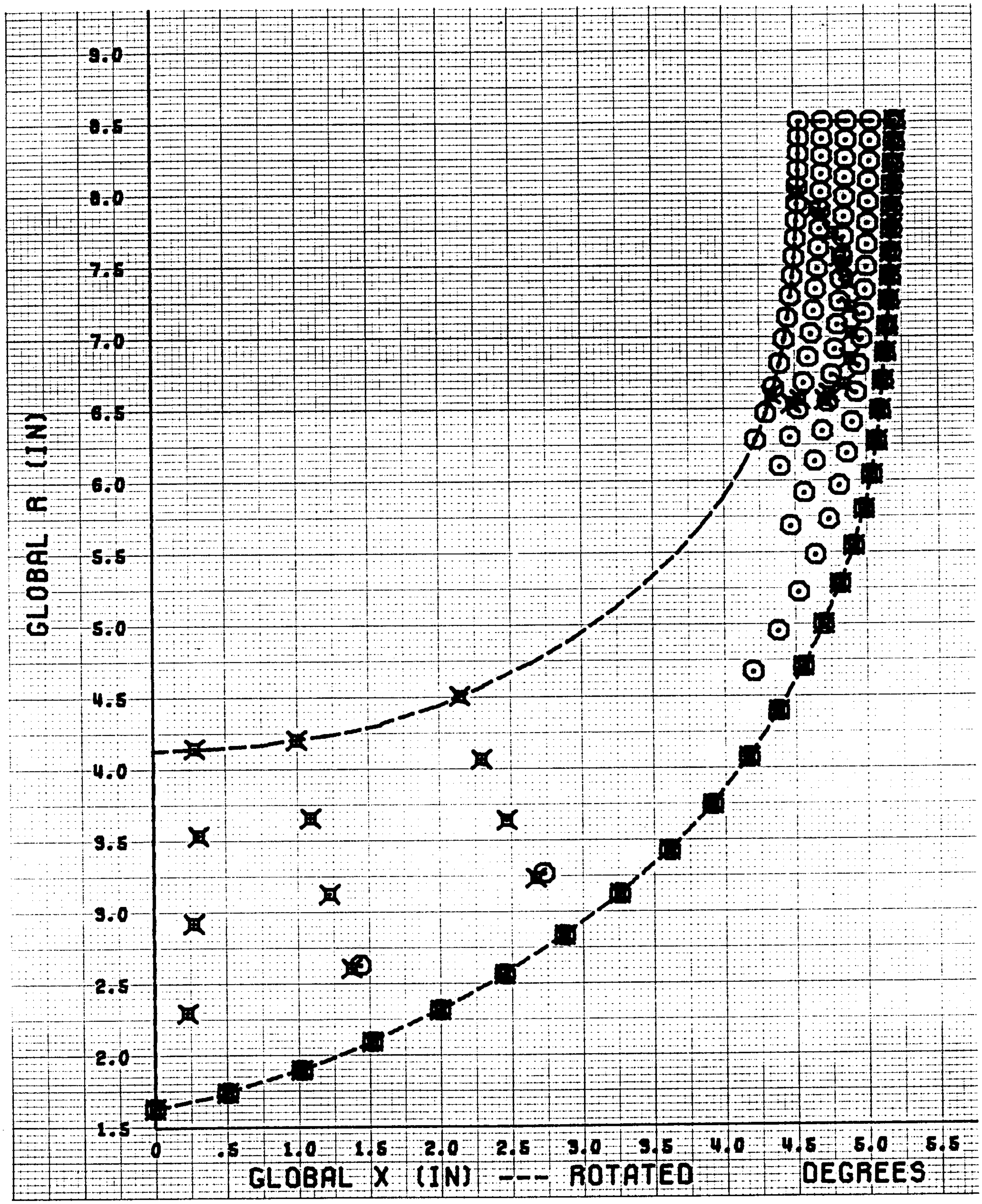

Figure 46. Full Blade ~ 5th Natural Frequency.

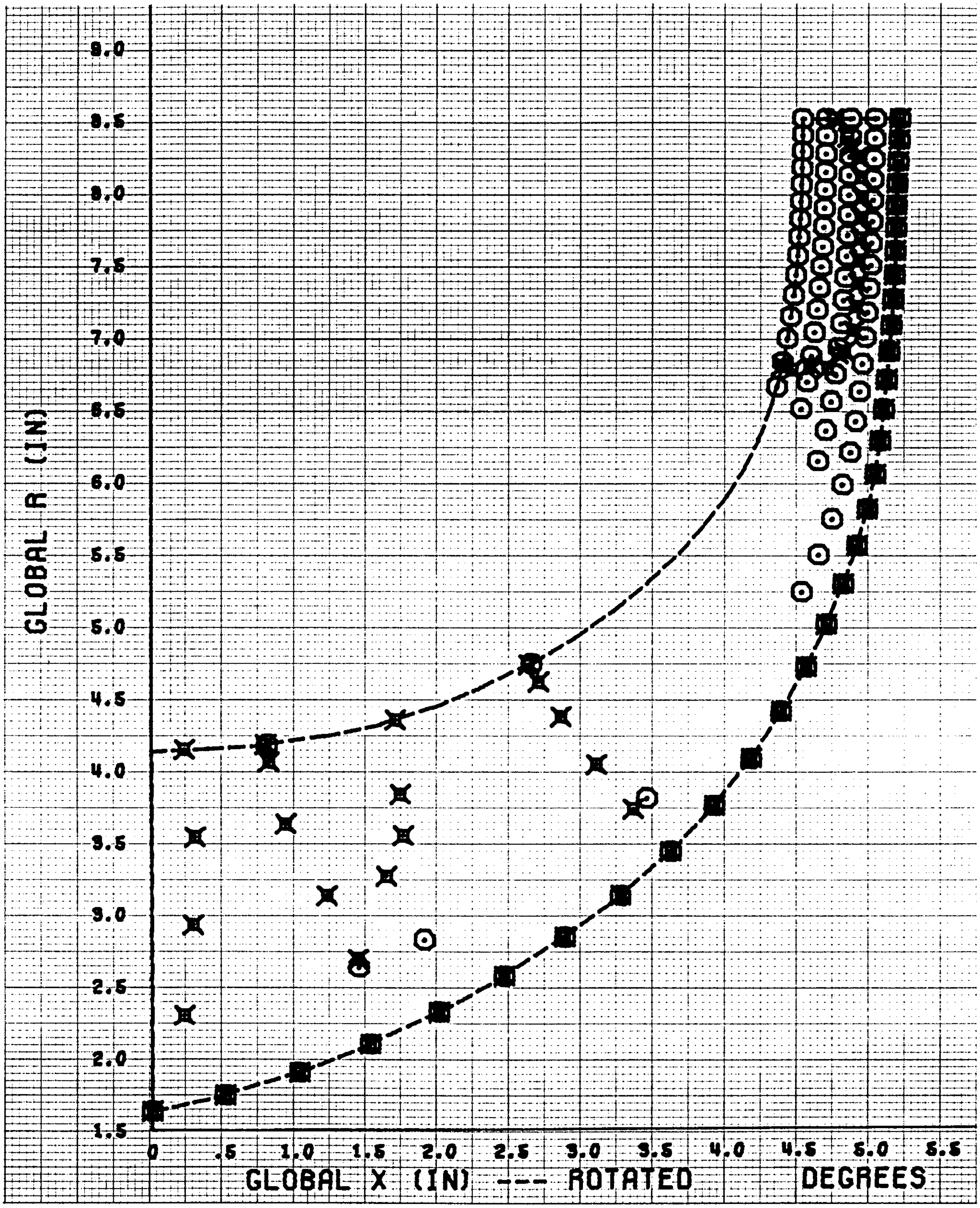

Figure 47. Full Blade ~ 6th Natural Frequency.

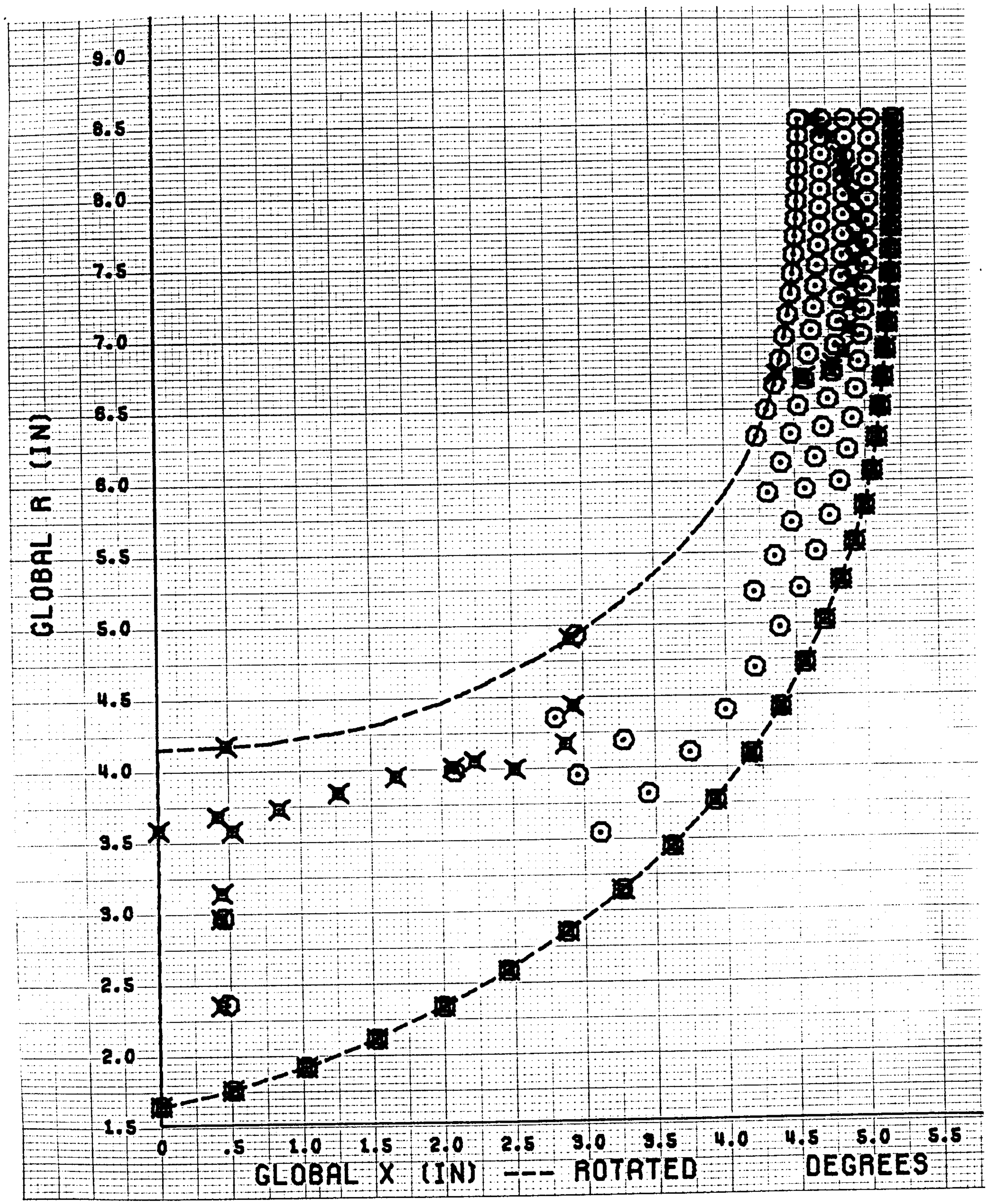

Figure 48. Full Blade ~ 7th Natural Frequency.

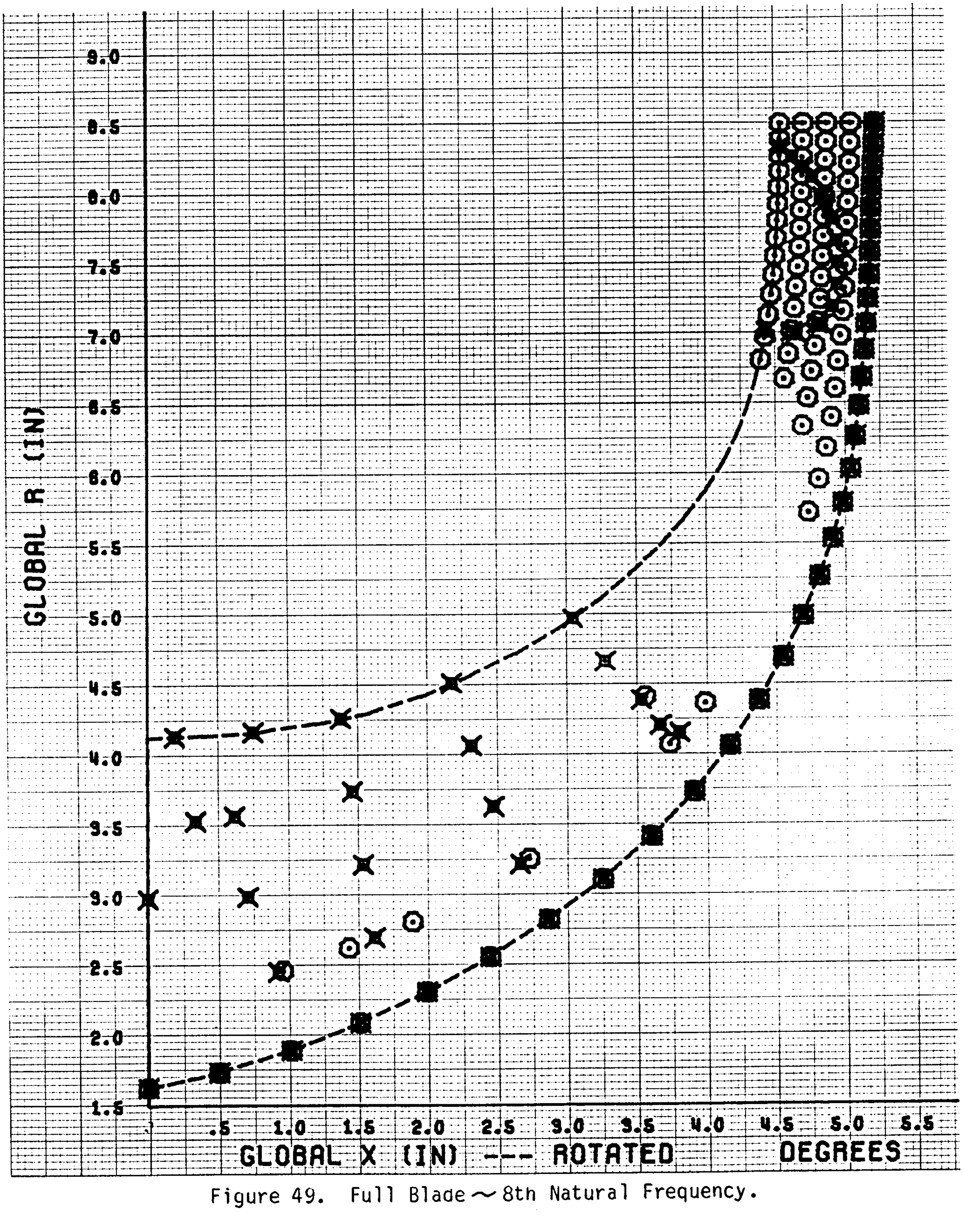

Figure 49. Full Blade ~ 8th Natural Frequency.

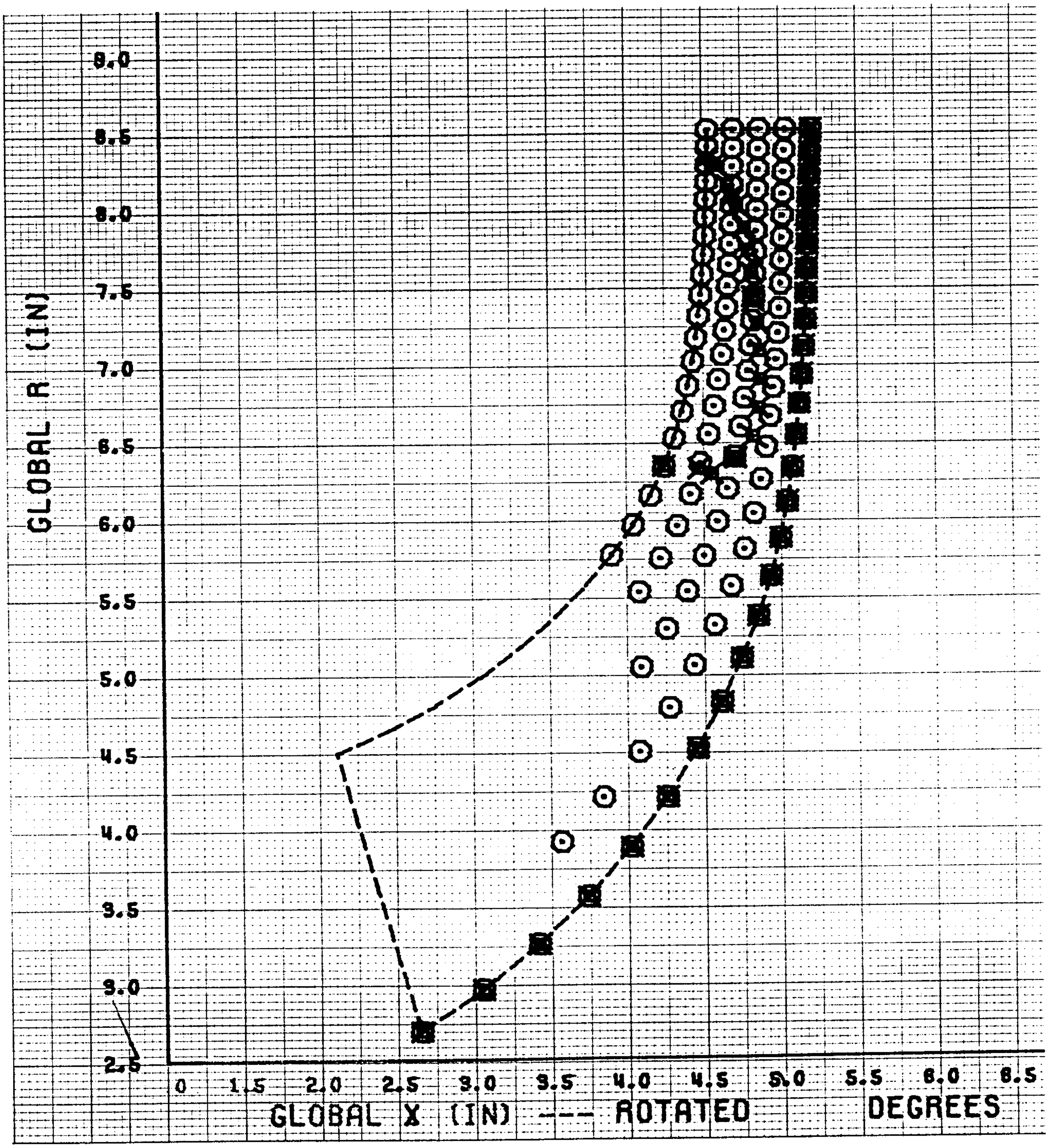

Figure 50. Splitter Blade ~1st Natural Frequency.

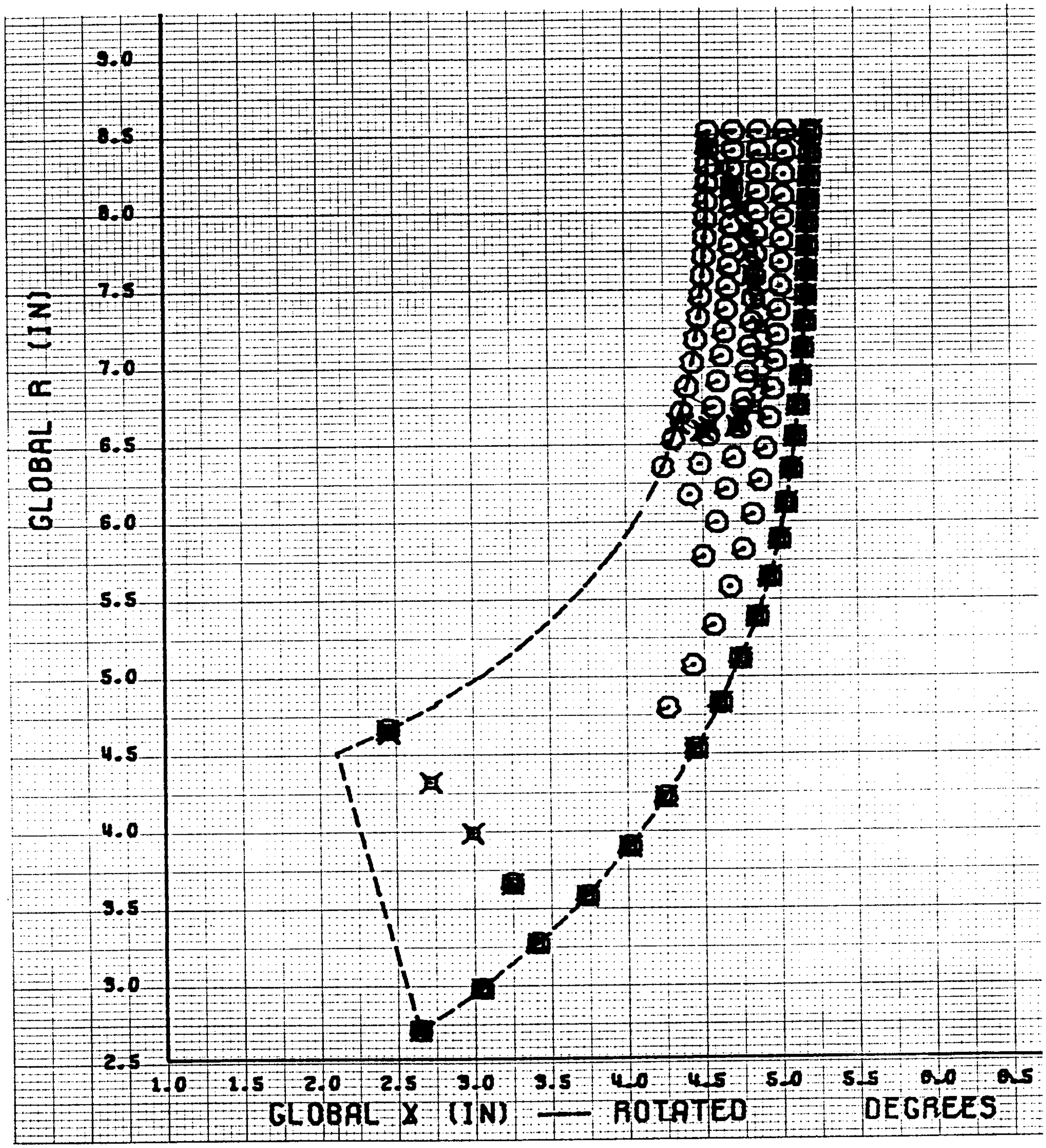

Figure 51. Splitter Blade ~ 2nd Natural Frequency.

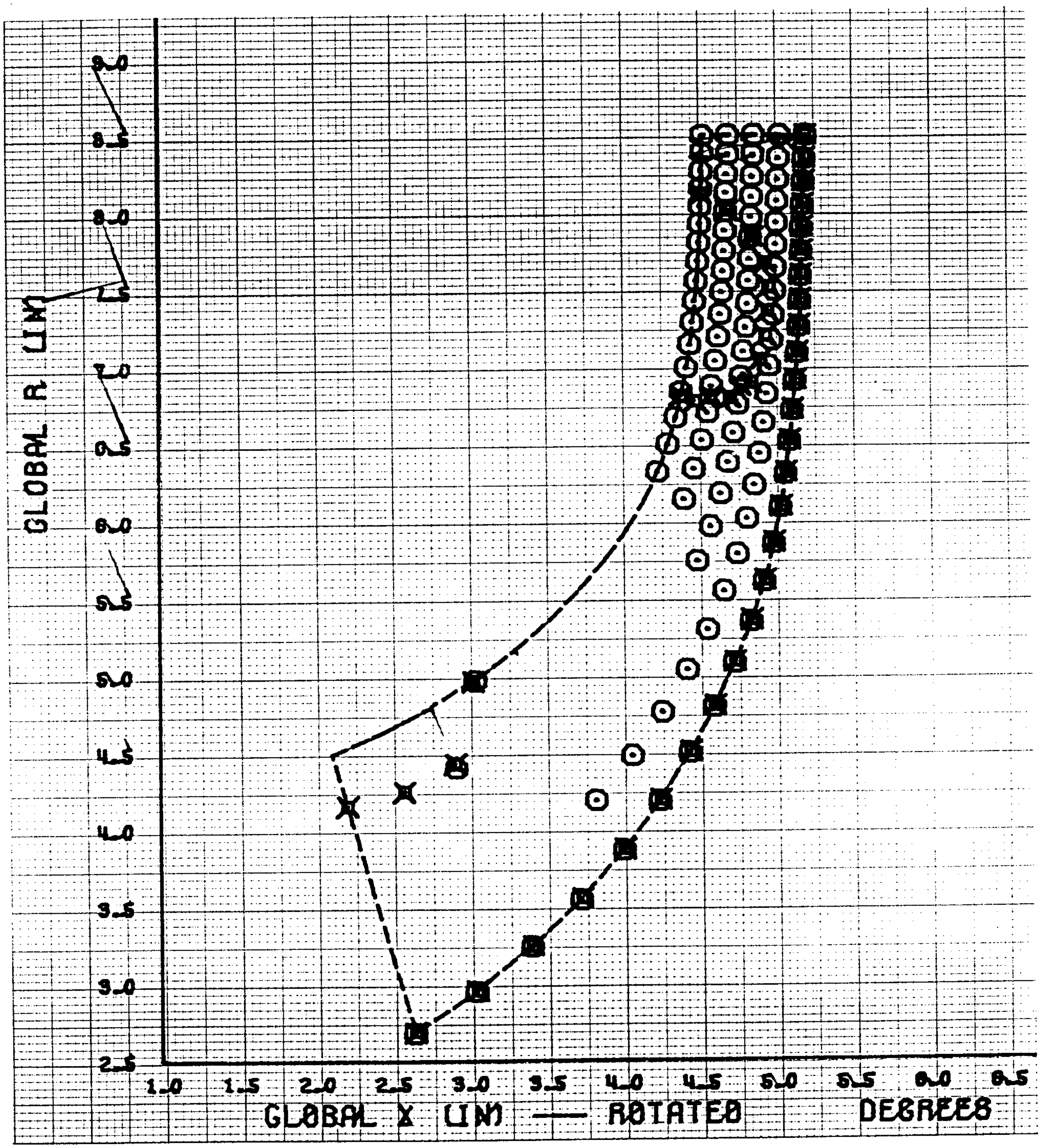

Figure 52. Splitter Blade ~ 3rd Natural Frequency.

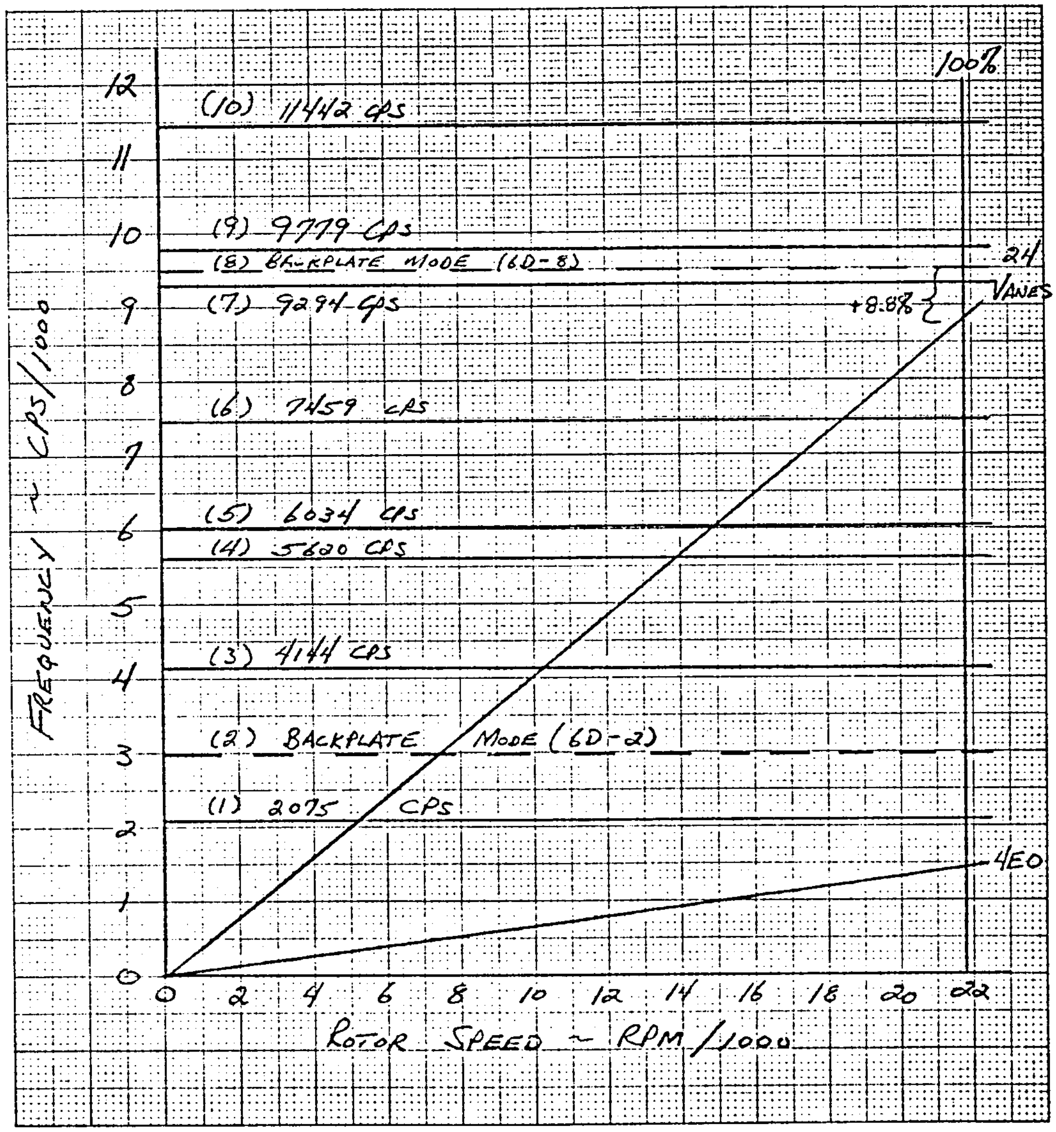

Figure 53. Frequency-Speed Diagram for Full Blade of Scaled Impeller.

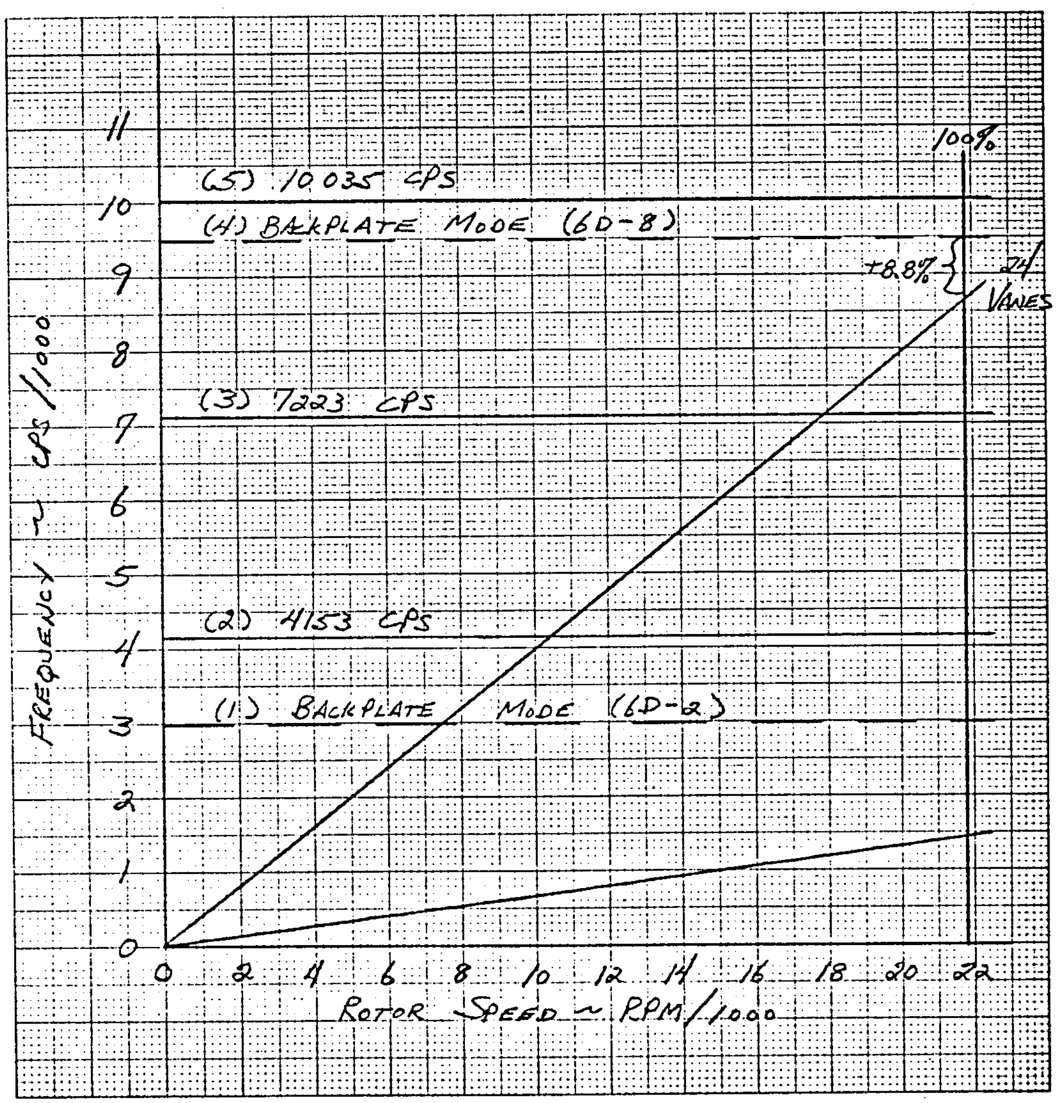

Figure 54. Frequency-Speed Diagram for Splitter Blade of Scaled Impeller.

(2EO) and its second harmonic, 4EO. The second and eighth modes shown in Figure 53 are backplate modes. The remaining modes are essentially blade modes with little or no coupling to the backplate structure.

The sixth diametral mode pattern (6D) was selected for analysis of the blade/backplate system because it is the only candidate mode which can be excited by the 24 engine order (diffuser vane number) when there are 30 airfoils on the rotating disk. The first backplate mode (6D-2), Figure 53, is acceptable because it is in resonance with 24EO at a very low speed and should be exposed to excitation only during transient operation. The second backplate mode (6D-8) should not be of concern unless steady state operation near 109% mechanical speed is anticipated.

In general, the natural frequencies are similar to those of the 404-III and, therefore, should be totally acceptable for anticipated rig operation.

IV. MANUFACTURING DEFINITION OF SCALED IMPELLER

This section describes the procedure by which the "hot running" impeller is converted into the "cold" or manufacturing definition. The initial portion of this process is to combine the "hot running" impeller geometry defined by aerodynamics with the deflection charactersitics calculated in the static stress analysis.

The "hot to cold" static stress analysis is performed by iteratively adjusting the impeller geometry and analytically "spinning" this geometry to design speed and temperature. Convergence is assumed when this "hot running" geometry matches that originally defined by the aerodynamics group. The final output of this analysis is a full 3-D cartesian definition which gives the X, Y, Z location of the desired "hot running" blade and the ∇X, ∇Y, ∇Z deflection required to convert this "hot running" blade to the manufacturing definition.

Blade generation programs, then, apply these deflections, reconstruct the "cold" blade, modify the shroud contour for the desired "hot running" clearance and, finally, define the cold blade on a series of planes passed both parallel and perpendicular to the engine axis.

Figure 55 indicates DDA practice for applying the "hot running" clearance. A constant clearance is first subtracted from the "hot" shroud line defined previously in Table II. The original 404-III had a constant 0.010 inches removed from the impeller hot shroud line. Using the 1.6529 linear scale factor, a clearance of .016529* was used for the scaled impeller. Since a static structure analysis was not performed, an absolute definition of the required "cold" build clearance is not possible. However, the change in clearance (relative to the originally defined "hot" shroud line) calculated for the impeller is provided in Figure 56 for reference.

* CHANGED TO .008" HOT CLEARANCE 7/12/83

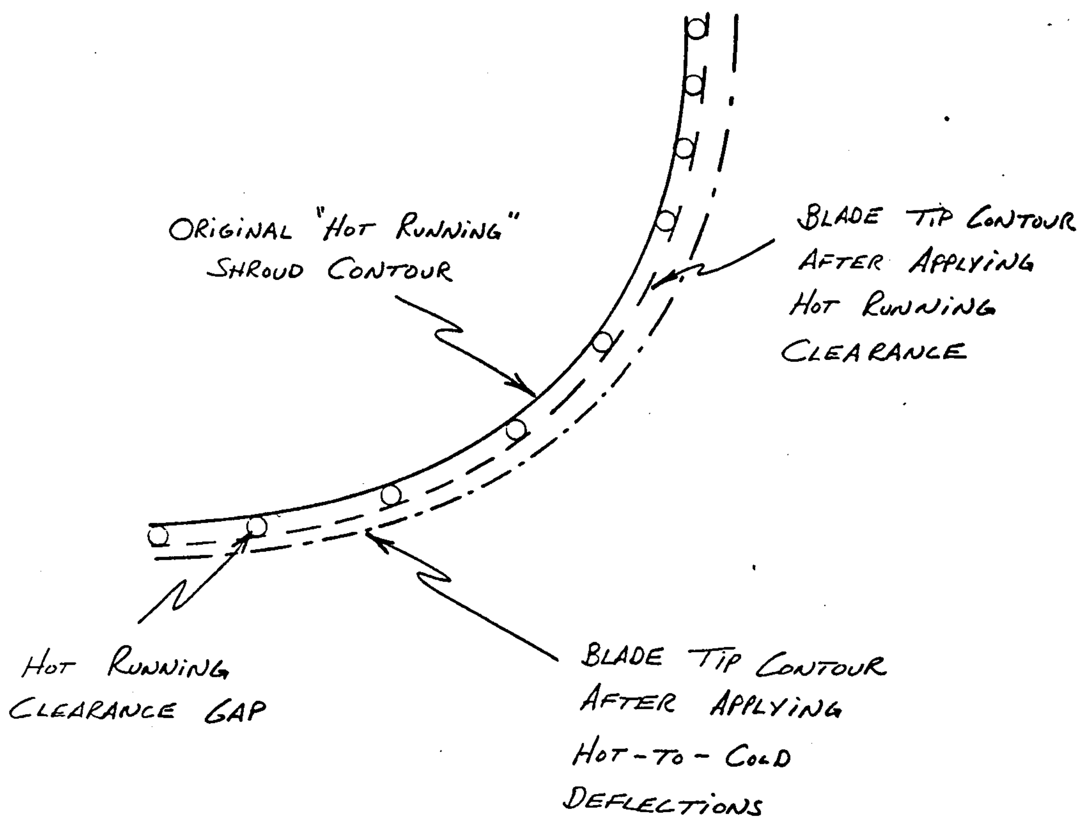

Figure 55. DDA Procedure for Clearance Allowance.

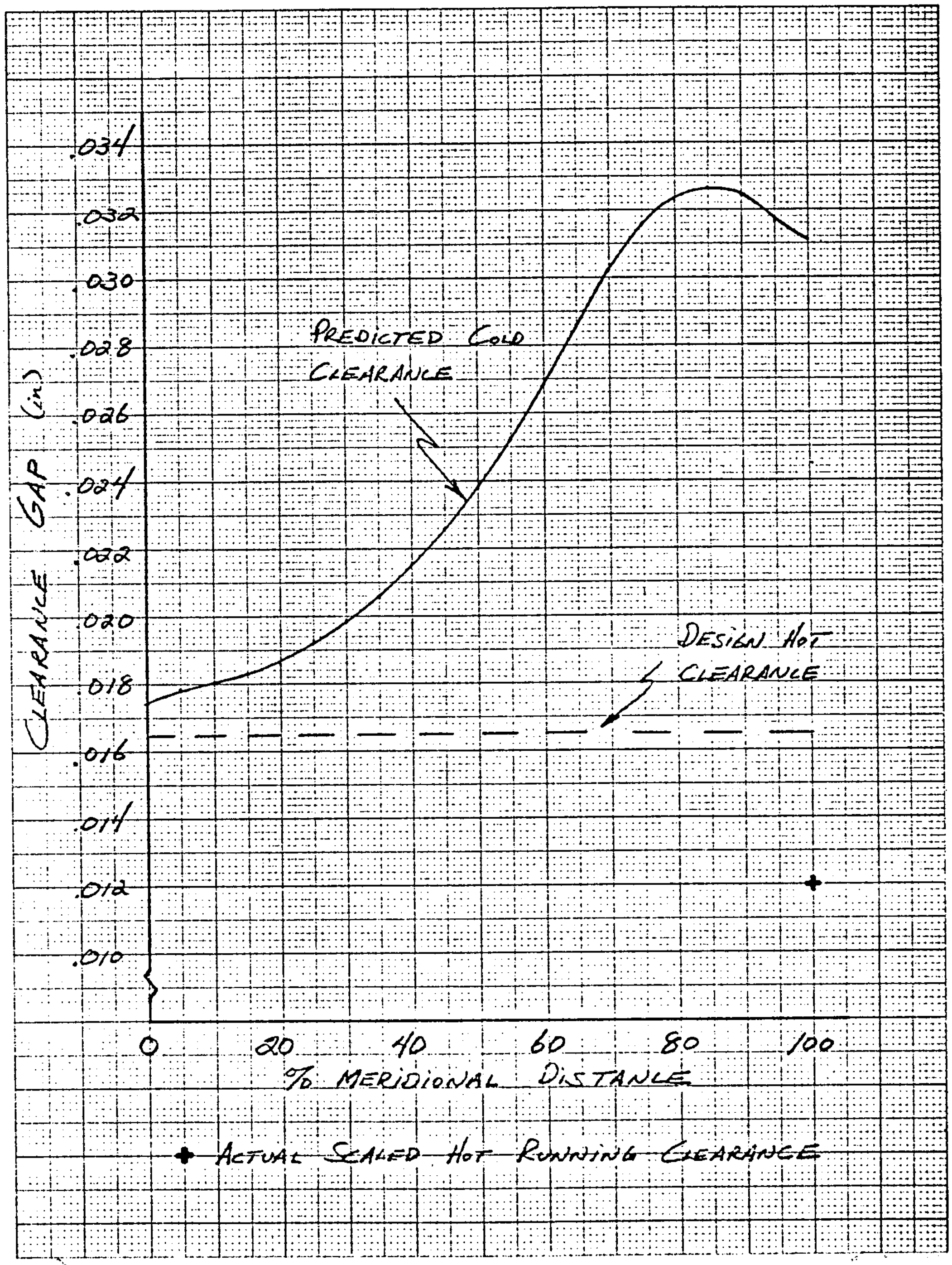

Figure 56. Scaled Impeller Clearance Change from "cold build" to "hot running" Condition.

The final "cold, manufacturing" definition of the impeller blade and splitter with the 0.016529 inch clearance removed is given in Tables V and VI, respectively. The "cold" blade surfaces are assumed to be constructed by straight lines from the hub to the shroud along the defined quasi-normals. The splitter blades are equally spaced between full blades at the impeller exit.

Planar sections were then passed through this "cold" geometry. The printed coordinate intersections of these planes with the quasi-normals is called a blade book and is included as Attachment A. Punched card definition of the hot and cold blade surfaces defined in Tables II, III, V and VI and the blade book coordinates are included as Attachment B. Milar plots of the planar intersections are know as Master Charts and are included as Attachment C. These plots are five times scale and can be used for final part inspection. Finally, a SK drawing was prepared to define the wheel geometry and locations of the planar Master Chart sections. This drawing is Attachment D.

TABLE 1. SCALED 4C4-III IMPELLER COORDINATES - COLD BLADE.

MEAN BLADE DEFINITION - FULL BLADE.

%M/MO	R HUB	Z HUB	R SHROUD	Z SHROUD	TTAN HUB	TTAN SHROUD	THETA HUB	THETA SHROUD
0.00	1.6312	0.0009	4.1148	0.0012	0.1328	0.0759	1.6331	0.0319
2.50	1.6763	0.2357	4.1225	0.1811	0.1940	0.0937	7.0300	3.5987
5.00	1.7306	0.4684	4.1309	0.3611	0.2174	0.1058	11.4915	6.9206
7.50	1.7545	0.6988	4.1375	0.5419	0.2323	0.1144	15.2587	9.9524
10.00	1.8668	0.9268	4.1500	0.7221	0.2413	0.1215	18.6542	12.8321
12.50	1.9469	1.1524	4.1693	0.9020	0.2490	0.1252	21.6394	15.5586
15.00	2.0332	1.3754	4.1934	1.0810	0.2541	0.1271	24.3302	18.1342
17.50	2.1256	1.5961	4.2220	1.2589	0.2593	0.1266	26.6931	20.5510
20.00	2.2240	1.8140	4.2564	1.4359	0.2642	0.1259	28.8285	22.8341
22.50	2.3276	2.0255	4.2947	1.6142	0.2691	0.1246	30.7135	25.0204
25.00	2.4389	2.2415	4.3429	1.7875	0.2733	0.1234	32.4163	27.0526
27.50	2.5591	2.4484	4.4040	1.9530	0.2762	0.1220	33.9167	28.9024
30.00	2.6843	2.6521	4.4695	2.1195	0.2794	0.1208	35.2751	30.6658
32.50	2.8125	2.8541	4.5407	2.2895	0.2829	0.1196	36.4730	32.3234
35.00	2.9497	3.0501	4.6155	2.4553	0.2861	0.1183	37.5653	33.8921
37.50	3.0946	3.2407	4.6940	2.6166	0.2890	0.1170	38.5328	35.3700
40.00	3.2476	3.4243	4.7788	2.7750	0.2917	0.1159	39.4325	36.7650
42.50	3.4082	3.6021	4.8697	2.9307	0.2942	0.1145	40.2456	38.0747
45.00	3.5772	3.7708	4.9685	3.0824	0.2966	0.1134	41.0284	39.3051
47.50	3.7552	3.9309	5.0783	3.2307	0.2984	0.1121	41.7665	40.4403
50.00	3.9407	4.0812	5.1916	3.3736	0.3006	0.1109	42.5027	41.5278
52.50	4.1347	4.2210	5.3060	3.5114	0.3034	0.1096	43.2269	42.5648
55.00	4.3343	4.3522	5.4286	3.6431	0.3057	0.1085	43.9686	43.5597
57.50	4.5397	4.4745	5.5616	3.7700	0.3069	0.1081	44.7215	44.4950
60.00	4.7498	4.5884	5.6985	3.8881	0.3086	0.1079	45.5048	45.4244
62.50	4.9653	4.6926	5.8365	3.9585	0.3107	0.1085	46.3134	46.3552
65.00	5.1845	4.7873	5.9845	4.0986	0.3132	0.1087	47.1628	47.2655
67.50	5.4075	4.8741	6.1444	4.1894	0.3161	0.1078	48.0519	48.1443
70.00	5.6342	4.9483	6.3104	4.2680	0.3195	0.1073	48.9834	49.0237
72.50	5.8650	5.0101	6.4853	4.3336	0.3231	0.1069	49.9455	49.8834
75.00	6.0584	5.0589	6.6604	4.3884	0.3283	0.1074	50.9733	50.7835
77.50	6.3354	5.0898	6.8353	4.4298	0.3359	0.1092	52.0663	51.7272
80.00	6.5727	5.1173	7.0124	4.4645	0.3436	0.1102	53.2253	52.7046
82.50	6.8102	5.1419	7.1917	4.4916	0.3501	0.1103	54.4505	53.7161
85.00	7.0480	5.1623	7.3727	4.5137	0.3589	0.1106	55.7408	54.7596
87.50	7.2862	5.1784	7.5564	4.5299	0.3698	0.1111	57.0842	55.8194
90.00	7.5246	5.1905	7.7401	4.5430	0.3828	0.1121	58.5167	56.9413
92.50	7.7633	5.1957	7.9240	4.5523	0.3970	0.1136	60.0275	58.1109
95.00	8.0021	5.2029	8.1079	4.5595	0.4150	0.1160	61.6489	59.3707
97.50	8.2410	5.2119	8.2920	4.5643	0.4370	0.1189	63.3811	60.7190
100.00	8.4801	5.2229	8.4759	4.5668	0.4629	0.1227	65.2241	62.1562

TABLE VI. SCALED 4C4-III IMPELLER COORDINATES - COLD BLADE.

MEAN BLADE DEFINITION - SPLITTER.

%M/MO	R HUB	Z HUB	R SHROUD	Z SHROUD	TTAN HUB	TTAN SHROUD	THETA HUB	THETA SHROUD
30.00	2.6844	2.6523	4.4685	2.1170	0.1118	0.0564	34.8684	30.2201
31.75	2.7736	2.7541	4.5181	2.2368	0.1401	0.0668	35.8399	31.4803
33.50	2.8667	2.9331	4.5695	2.3542	0.1634	0.0754	36.7345	32.6815
35.25	2.9637	3.0693	4.6222	2.4689	0.1802	0.0817	37.5435	33.8195
37.00	3.0647	3.2027	4.6768	2.5825	0.1945	0.0873	38.2932	34.9096
38.75	3.1701	3.3335	4.7345	2.6946	0.2068	0.0918	38.9734	35.9492
40.50	3.2791	3.4606	4.7956	2.8055	0.2178	0.0960	39.6146	36.9412
42.25	3.3917	3.5843	4.8594	2.9139	0.2280	0.1004	40.2088	37.8810
44.00	3.5080	3.7039	4.9274	3.0211	0.2372	0.1037	40.7798	38.7797
45.75	3.6293	3.8195	5.0005	3.1270	0.2452	0.1056	41.3225	39.6346
47.50	3.7547	3.9304	5.0776	3.2299	0.2527	0.1068	41.8520	40.4520
49.25	3.8844	4.0367	5.1568	3.3304	0.2597	0.1073	42.3604	41.2299
51.00	4.0179	4.1382	5.2364	3.4291	0.2662	0.1079	42.8711	41.9785
52.75	4.1544	4.2345	5.3177	3.5245	0.2721	0.1084	43.3815	42.6908
54.50	4.2939	4.3266	5.4035	3.6172	0.2777	0.1085	43.8991	43.3828
56.25	4.4359	4.4145	5.4948	3.7077	0.2829	0.1079	44.4209	44.0487
58.00	4.5807	4.4980	5.5884	3.7940	0.2880	0.1075	44.9559	44.7050
59.75	4.7284	4.5771	5.6835	3.8759	0.2928	0.1074	45.5020	45.3501
61.50	4.8783	4.6517	5.7800	3.9555	0.2974	0.1078	46.0653	45.9895
63.25	5.0308	4.7217	5.8795	4.0295	0.3019	0.1081	46.6450	46.6224
65.00	5.1847	4.7874	5.9848	4.0988	0.3062	0.1082	47.2438	47.2505
66.75	5.3397	4.8503	6.0958	4.1634	0.3105	0.1076	47.8615	47.8714
68.50	5.4970	4.9060	6.2100	4.2224	0.3144	0.1073	48.4987	48.4929
70.25	5.6572	4.9536	6.3287	4.2755	0.3178	0.1073	49.1529	49.1120
72.00	5.8189	4.9953	6.4501	4.3214	0.3215	0.1071	49.8320	49.7381
73.75	5.9825	5.0307	6.5725	4.3625	0.3256	0.1073	50.5345	50.3685
75.50	6.1469	5.0610	6.6956	4.3974	0.3298	0.1075	51.2650	51.0114
77.25	6.3123	5.0848	6.8184	4.4262	0.3337	0.1080	52.0232	51.6659
79.00	6.4780	5.1063	6.9418	4.4517	0.3382	0.1087	52.8103	52.3356
80.75	6.6440	5.1255	7.0664	4.4733	0.3432	0.1094	53.6230	53.0196
82.50	6.8103	5.1425	7.1923	4.4917	0.3489	0.1097	54.4708	53.7204
84.25	6.9767	5.1573	7.3190	4.5077	0.3557	0.1102	55.3513	54.4370
86.00	7.1433	5.1700	7.4467	4.5206	0.3631	0.1105	56.2713	55.1735
87.75	7.3101	5.1809	7.5752	4.5314	0.3712	0.1104	57.2297	55.9275
89.50	7.4770	5.1892	7.7037	4.5407	0.3801	0.1115	58.2296	56.7110
91.25	7.6440	5.1928	7.8323	4.5479	0.3896	0.1141	59.2678	57.5202
93.00	7.8111	5.1978	7.9612	4.5540	0.4007	0.1163	60.3538	58.3650
94.75	7.9781	5.2050	8.0911	4.5590	0.4129	0.1180	61.4826	59.2386
96.50	8.1453	5.2118	8.2200	4.5627	0.4274	0.1195	62.6701	60.1611
98.25	8.3127	5.2182	8.3480	4.5652	0.4440	0.1208	63.9166	61.1326
100.00	8.4805	5.2241	8.4751	4.5668	0.4628	0.1222	65.2218	62.1535

V. APPENDICIES

Attachment A Impeller Blade Book (not attached directly to this report)

Attachment B Punched Card Definition of "Hot" and "Cold" Blade Surfaces (not attached directly to this report)

Attachment C Milar Plots of Master Chart Sections (not attached directly to this report)

Attachment D Impeller Detail Drawing (page 73)

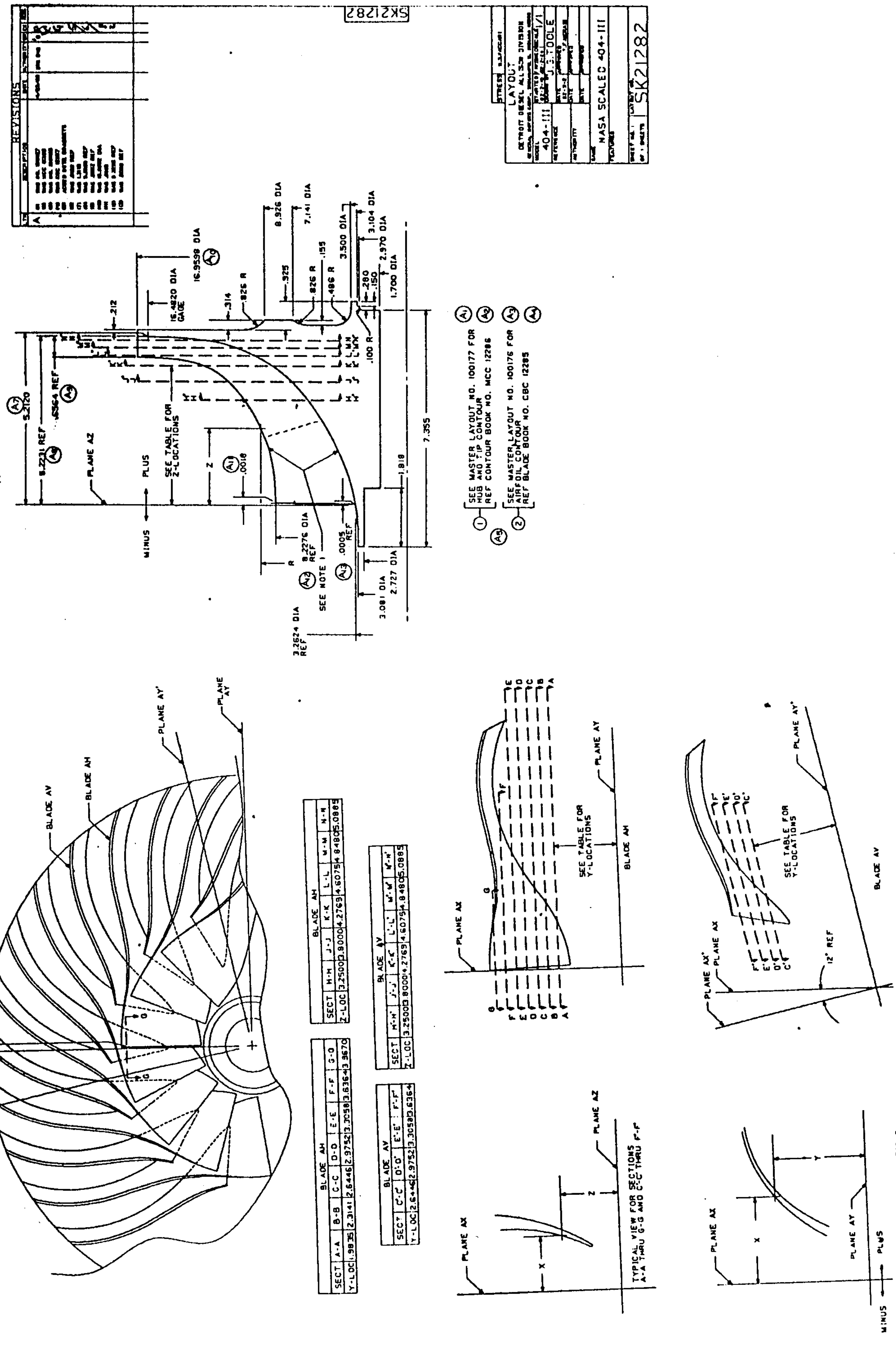

BLADE AH						
SECT	H-H	J-J	K-K	L-L	M-M	N-N
Z-LOC	3.2500	3.8000	4.2769	4.6075	4.8480	5.0885

BLADE AV						
SECT	H'-H'	J'-J'	K'-K'	L'-L'	M'-M'	N'-N'
Z-LOC	3.2500	3.8000	4.2769	4.6075	4.8480	5.0885

BLADE AH							
SECT	A-A	B-B	C-C	D-D	E-E	F-F	G-G
Y-LOC	1.9835	2.3141	2.6446	2.9752	3.3058	3.6364	3.9670

BLADE AV				
SECT	C'-C'	D'-D'	E'-E'	F'-F'
Y-LOC	2.6446	2.9752	3.3058	3.6364

REPORT DOCUMENTATION PAGE

Form Approved
OMB No. 0704-0188

1. AGENCY USE ONLY (*Leave blank*)	2. REPORT DATE	3. REPORT TYPE AND DATES COVERED
	July 1997	Final Contractor Report

4. TITLE AND SUBTITLE

Coordinates for a High Performance 4:1 Pressure Ratio Centrifugal Compressor

5. FUNDING NUMBERS

WU–523–26–13
C–NAS3–23268

6. AUTHOR(S)

Ted F. McKain and Greg J. Holbrook

7. PERFORMING ORGANIZATION NAME(S) AND ADDRESS(ES)

Detroit Diesel Allison
Division of General Motors Corporation
Indianapolis, Indiana 46206

8. PERFORMING ORGANIZATION REPORT NUMBER

E–10833

9. SPONSORING/MONITORING AGENCY NAME(S) AND ADDRESS(ES)

National Aeronautics and Space Administration
Lewis Research Center
Cleveland, Ohio 44135–3191

10. SPONSORING/MONITORING AGENCY REPORT NUMBER

NASA CR–204134

11. SUPPLEMENTARY NOTES

Project Manager, Jerry R. Wood, Turbomachinery and Propulsion Systems Division, NASA Lewis Research Center, organization code 5810, (216) 433–5880.

12a. DISTRIBUTION/AVAILABILITY STATEMENT

Unclassified - Unlimited
Subject Category 07

This publication is available from the NASA Center for AeroSpace Information, (301) 621–0390.

12b. DISTRIBUTION CODE

13. ABSTRACT ***(Maximum 200 words)***

The objective of this program was to define the aerodynamic design and manufacturing coordinates for an advanced 4:1 pressure ratio, single stage centrifugal compressor at a 10 lbm/sec flow size. The approach taken was to perform an exact scale of an existing DDA compressor originally designed at a flow size of 3.655 lbm/sec.

14. SUBJECT TERMS

Single stage centrifugal compressor; Scaled compressor

15. NUMBER OF PAGES

80

16. PRICE CODE

A05

17. SECURITY CLASSIFICATION OF REPORT	18. SECURITY CLASSIFICATION OF THIS PAGE	19. SECURITY CLASSIFICATION OF ABSTRACT	20. LIMITATION OF ABSTRACT
Unclassified	Unclassified	Unclassified	